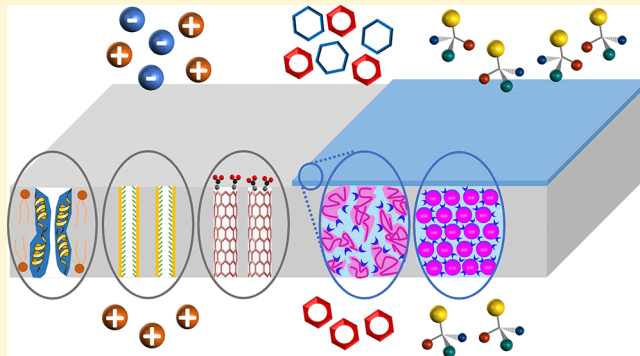


1 Controlling and Expanding the Selectivity of Filtration Membranes[†]

2 Ilin Sadeghi,^{ID} Papatya Kaner,^{ID} and Ayse Asatekin*^{ID}

3 Chemical and Biological Engineering Department, Tufts University, 4 Colby Street, Medford, Massachusetts 02155, United States

4 **ABSTRACT:** Chemical separations account for about 50% of
 5 costs and energy use associated with chemical and petrochemical
 6 manufacturing, corresponding to about 10%
 7 of all energy use in the U.S. Membrane separations are highly
 8 energy efficient, simple to operate, scalable, and portable.
 9 Broader use of membranes is limited by the selectivity of
 10 available membranes, mostly confined to the separation of
 11 species about an order of magnitude or more different in size
 12 in the liquid phase. This perspective focuses on new
 13 approaches for creating liquid filtration membranes that can
 14 perform more challenging separations. We first discuss the
 15 selectivity mechanisms of currently available membranes and
 16 compare them with the operation of biological systems that
 17 exhibit enhanced selectivity. Then, we review some approaches for creating isoporous membranes with narrow pore size
 18 distributions for enhanced size-based selectivity. We discuss biological systems that exhibit selectivity based on factors beyond
 19 size and how they can inspire the design of membranes capable of complex separations. After a review of approaches for creating
 20 membranes for separating similarly sized solutes, based on their charge, we discuss the development of membranes that can
 21 perform even more challenging separations, differentiating between solutes of similar size and charge based on other molecular
 22 criteria. This burgeoning area of research promises to transform chemical and pharmaceutical manufacturing if membranes with
 23 sufficient selectivity and permeability for realistic separations can be prepared using scalable manufacturing methods.



1. INTRODUCTION

24 Chemical separations account for approximately 50% of costs
 25 and energy use associated with chemical and petrochemical
 26 manufacturing. On the whole, this corresponds to about 10%
 27 of all energy use in the U.S.¹ Separating mixtures is also a
 28 critical challenge in pharmaceutical and biopharmaceutical
 29 manufacturing, which involves the separation of similar small
 30 molecules from each other. Most of these separations are
 31 performed by energy intensive unit operations such as
 32 distillation, extraction, and absorption. Extraction, absorption,
 33 and chromatography also require the use of an auxiliary solvent
 34 that can add to the costs and environmental impact of the
 35 process.

36 Membrane separations are extremely energy efficient
 37 compared with most other separation technologies.^{2,3} For
 38 instance, seawater desalination using membranes consumes up
 39 to 90% less energy than the thermal methods that previously
 40 dominated the field.⁴ Membrane systems are very simple to
 41 operate. They are modular and easily scalable, capable of
 42 addressing both small and large-scale separations. They have
 43 small footprints and are portable, exhibit reliable performance
 44 that is relatively insensitive to fluctuations in feed composition,
 45 and do not require any solvent addition. These advantages
 46 have made membrane systems the technology of choice in
 47 several separations where sufficiently selective and stable
 48 membranes exist. For example, current desalination mem-
 49 branes, designed to retain salt yet pass water, operate at energy

efficiencies close to the thermodynamic minimum with 50
 51 lifetimes measured in years in well-designed systems.⁴ The
 52 use of gas separation membranes in air separation, hydrogen
 53 recovery, and natural gas processing is also spreading.⁵³ Membranes are also widespread in water and wastewater
 54 treatment, food and beverage industries, lab and sterile water
 55 systems, and biomanufacturing for the concentration of 56
 56 biologic drugs.⁵⁷

57 Wider use of membrane systems is limited by the availability 58
 59 of membranes that can successfully separate the desired 59
 60 components from each other.³ Most filtration membranes on 61
 61 the market today are designed to remove all solutes above a 62
 62 given size from a feed stream (e.g., cell debris from a 63
 63 biomolecule solution, hydrated salts from water). Particularly 64
 64 when liquid separations are involved, it is difficult to separate 65
 65 solutes that differ in size by less than an order of magnitude.⁶⁶ Nonsize-based separations are rarely attempted using mem-⁶⁶
 67 branes, though many membrane materials exhibit at least some
 68 electrostatic contributions to their separation abilities. In other
 69 words, the range of separations that can be attempted using
 70 membranes is severely limited by membrane selectivity.⁷⁰

71 If membranes with more controlled selectivity can be 71
 72 designed and manufactured, they can potentially replace more 72
 73 energy-intensive processes such as distillation, extraction, or 73

Received: August 6, 2018

Revised: October 9, 2018

Published: October 11, 2018

[†]This Perspective is part of the *Up-and-Coming* series.

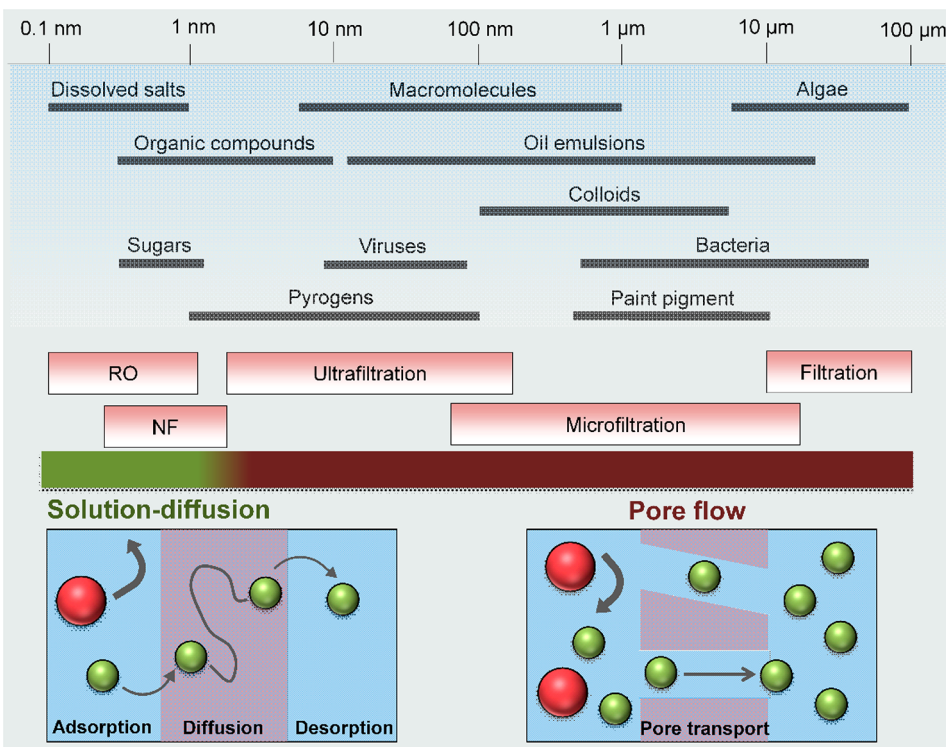


Figure 1. Current classification of filtration membranes according to effective pore size and corresponding transport mechanisms in effect. The axis at the top of the figure denotes the typical size scale of filtered materials and thus effective pore sizes of membranes capable of removing them.

74 chromatography. This would transform the manufacturing
 75 processes for many organic chemicals including active
 76 ingredients of pharmaceuticals, petroleum products, and
 77 bioderived chemicals. Yet, this is a challenging task. Creating
 78 isoporous membranes, or membranes with narrow pore size
 79 distribution, requires extreme precision in creating a high
 80 density of regular features only nanometers in size. This is
 81 difficult with scalable processes needed to reliably manufacture
 82 membrane rolls several feet in width, thousands of feet in
 83 length. Attempting more complex separations, such as the
 84 separation of solutes of similar size, requires further
 85 manipulating the membrane chemistry to emphasize differ-
 86 ences in solute–membrane interactions. These challenges
 87 make the search for highly selective membranes manufactured
 88 through scalable methods a growing membrane research area
 89 with much to explore.

90 This perspective focuses on novel approaches for designing
 91 and manufacturing polymeric membranes with controlled
 92 selectivity, with the ultimate objective of developing mem-
 93 branes that can address new separations. The main focus is on
 94 liquid separations, as most applications of complex chemical
 95 structure-based separations (e.g., pharmaceutical manufac-
 96 turing, extraction of biomolecules) occur in liquid solutions. We
 97 particularly emphasize small molecule separations, though
 98 some protein separations are also discussed. We first discuss
 99 selectivity mechanisms of membranes on the market today,
 100 and briefly discuss efforts to create membranes with improved
 101 size-based selectivity by creating narrow pore size distributions.
 102 Then, we overview some natural systems that can inspire the
 103 design of new membranes with more complex selectivity. The
 104 rest of this perspective focuses on approaches for creating
 105 membranes that separate solutes based on criteria other than
 106 size. A large portion of the literature in this field focuses on
 107 charge-based separation of solutes in water. Beyond direct

108 applications, this often serves as an initial proof-of-concept for
 109 novel approaches. We then present the relatively few reports of
 110 membranes that separate solutes, especially small organic
 111 molecules, based on other chemical criteria such as hydro-
 112 phobicity or chirality. Finally, we discuss our outlook on future
 113 directions and on key challenges that still need to be addressed. 114

2. MEMBRANE SELECTIVITY TODAY

Liquid filtration membranes today are typically classified based 114 on the size of solutes or particles they retain (Figure 1),^{5,6} 115 f1 though other classifications exist based on operation pressure. 116 Microfiltration (MF) membranes are those with pores 0.1–10 117 μm in diameter. They are typically used to remove bacteria and 118 particulates. Membranes with pores 2–100 nm in diameter are 119 classified as ultrafiltration (UF) membranes, though their 120 effective pore size is typically reported in terms of molecular 121 weight cutoff (MWCO), defined as the molecular weight of a 122 probe solute retained by 90%. UF membranes can retain 123 viruses, macromolecules, and emulsified oils. Both MF and UF 124 membranes have porous selective layers, and transport through 125 them follows the pore flow mechanism. This means 126 components that are smaller than the pore size pass through, 127 whereas larger solutes are retained. Separations based on this 128 sieving mechanism are sensitive to the distribution of pore 129 sizes. Commercial porous UF membranes made by traditional 130 fabrication methods usually do not have a narrow pore size 131 distribution or high pore density, especially as membrane pores 132 get smaller.⁷ This is why UF and MF are often used to retain 133 all components above a certain size (e.g., sterilization, removal 134 of organic macromolecules for wastewater treatment, concen- 135 tration of a protein drug), but rarely to separate components of 136 the same class (e.g., separating two proteins, even proteins and 137 viruses) from each other. Industry experts typically suggest it is 138 very challenging to separate liquid mixtures containing 139

140 components whose sizes differ by less than an order of
141 magnitude using membrane filtration processes.
142 Nanofiltration (NF) and reverse osmosis (RO) membranes
143 are typically included in the same membrane selectivity chart
144 that links removal with solute size. The 1996 IUPAC
145 nomenclature defines RO membranes as those through
146 which only solvent molecules pass through, whereas particles
147 and dissolved molecules smaller than 2 nm are rejected in NF.⁵
148 In practice, NF membranes typically retain doubly charged
149 ions and are designed for water softening, whereas RO
150 membranes retain all salts and can be used for desalination.
151 Yet, their selective layers are not porous. NF and RO
152 membranes typically feature a continuous, thin (~100 nm or
153 less) polymer layer supported by a porous layer that serves as
154 mechanical support. These layers were initially made of the
155 same material, with the asymmetric morphology, termed an
156 integrally skinned membrane, formed through the carefully
157 controlled manufacturing process utilizing nonsolvent induced
158 phase inversion (NIPS). The initial discovery of this process by
159 Loeb and Sourirajan⁸ enabled desalination membranes with
160 sufficiently high flux to be used for water treatment. The
161 formation of thin film composite (TFC) membranes, which
162 consist of a porous support coated by a very thin, nonporous
163 layer of another polymer, enabled independent optimization of
164 these two components and achieved better performance. The
165 process of interfacial polymerization (IP) to create cross-linked
166 polyamide selective layers⁹ led to the membrane chemistry that
167 most commercial NF and RO membranes utilize today.¹⁰
168 Transport through RO membranes is best described by the
169 solution-diffusion model, where components that permeate the
170 selective layer get solvated in the polymer, diffuse across, and
171 desorb into the permeate side. Selectivity arises from
172 differences in solubility and diffusivity in this polymer selective
173 layer.^{4,6,11} Transport through NF membranes is believed to be
174 in between, or a combination of, pore-flow and solution-
175 diffusion mechanisms, i.e., between UF and RO membranes.¹²
176 Most membranes on the market today are designed for the
177 filtration of aqueous solutions. However, the polymeric
178 materials used in most of these membranes dissolve, swell,
179 or degrade in many organic solvents. This makes them
180 unusable for the separation of organic mixtures or for the
181 removal or concentration of solutes in nonaqueous solvents.
182 There are extensive and highly demanding applications of such
183 separations including the concentration of products in
184 chemical and pharmaceutical manufacturing, solvent recovery
185 and exchange, catalyst recovery, and the separation and
186 purification of organic compounds such as drugs or consumer
187 chemicals. This has driven extensive research in developing
188 membrane materials that are robust and selective in organic
189 solvents, and membrane processes that utilize such membranes
190 for energy-efficient separations. In general, the goal has been to
191 translate membranes that operate well in aqueous media,
192 particularly NF and RO, to perform in the presence of organic
193 solvents. Organic solvent nanofiltration (OSN), also termed
194 solvent resistant nanofiltration (SRNF), is used to describe
195 membranes that perform NF-type separations in nonaqueous
196 solvents, with typical MWCO values in the 200–1000 Da
197 range.¹³ The selectivity of OSN has both size-based and
198 solubility-driven components.^{13–16} More recently, organic
199 solvent reverse osmosis (OSRO) membranes with even smaller
200 effective MWCO values have been reported, with the goal of
201 achieving solvent/solvent separations.¹⁴ OSN membranes have
202 been commercially available through several companies. They

have been demonstrated to successfully address critical
203 processes in many industries, including lube oil dewaxing,
204 biodiesel production, catalyst recovery, and product concen-
205 tration and solvent recovery in pharmaceutical and chemical
206 manufacturing.¹⁷ While OSN membranes can successfully
207 address many solvent/solute separations, their ability to
208 separate two solutes from each other is limited unless these
209 solutes exhibit large differences in size.¹⁶ This limits the
210 applications in which they can be used. While improving the
211 selectivity of OSN membranes is a highly active research area,
212 rational control of the selectivity of OSN membranes is, for
213 now, challenging given the complex separation mechanisms
214 involved in their use.
215

An overall trade-off between selectivity and either
216 permeance (defined as flux normalized by applied pressure)
217 or permeability (defined as permeance normalized by
218 membrane thickness)⁵ can be observed for the wide variety
219 of synthetic membranes, used in processes as different as gas
220 separation, desalination, and sterile filtration.¹⁸ Membranes
221 with high selectivity between desired components typically
222 have lower permeances or permeabilities, leading to higher
223 energy use. The permeability-selectivity trade-off is inherent
224 to the solution-diffusion mechanism in effect for gas separation
225 membranes with homogeneous polymer selective layers,
226 linking membrane selectivity to gas diffusivity.¹⁹ A similar
227 inherent trade-off exists for water/salt separation in desalina-
228 tion membranes, which also follow the solution-diffusion
229 model.^{4,11,20} Interestingly, similar behaviors are observed for
230 other synthetic membranes that operate on other transport
231 mechanisms, including protein separation in porous UF
232 membranes⁷ and ion transport in charged polymers for
233 electrically driven separations.²¹ This leads to an effective
234 “upper bound” of performance, describing maximum selectivity
235 achieved for a given permeability, for instance, reported for
236 various membrane processes. This upper bound has been used
237 to describe the state-of-the-art for each membrane process, and
238 as a benchmark for the success of new membrane technologies
239 under development. For instance, isoporous membranes with
240 very narrow pore size distributions, described below, can have
241 high selectivity combined with high permeance, enabling
242 researchers to overcome this upper bound through a radically
243 new approach.²²
244

3. ISOPOROUS MEMBRANES: BETTER SIZE-BASED SELECTIVITY

Essentially all UF and MF membranes on the market today are
246 manufactured using the nonsolvent induced phase separation
247 (NIPS) process. NIPS involves casting a polymer solution on a
248 solid substrate followed by immersion in a nonsolvent bath.²³
249 The solvent in the polymer solution mixes with the nonsolvent,
250 causing the polymer to precipitate on the substrate as a solid,
251 porous membrane. NIPS-prepared membranes with a meso-
252 porous skin display a fairly broad pore size distribution in their
253 selective layer. This likely leads to the permeance/selectivity
254 trade-off described above.^{7,18} It also limits their use in several
255 applications that require better size-based selectivity or the
256 capability to separate solutes closer in size, including the
257 removal of viruses from protein solutions^{24,25} and the
258 separation of two proteins from each other.^{26–28} Several
259 approaches that utilize self-assembly of biological pores and/or
260 block copolymers have targeted this gap, offering significant
261 benefits with their narrow pore size distributions, high
262 porosity, and adjustable chemical and physical properties.
263

Many of these “isoporous” membranes can also serve as platforms to implement new routes for creating selective and functional nanopores, as discussed below.

The most established techniques to fabricate isoporous UF and MF membranes today are track etching, anodization of aluminum films, and lithography.^{29–31} Figure 2 presents the

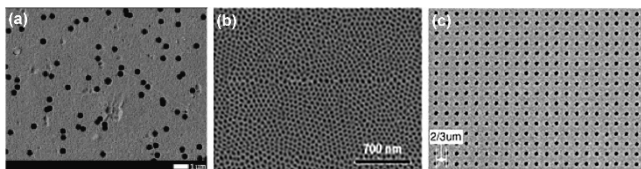


Figure 2. Surface SEM of membranes fabricated by track etching, anodic aluminum oxide (AAO), or lithography. (a) Track-etched poly(ethylene terephthalate) (PET) membrane with 423 ± 25 nm pores. Reprinted from ref 35. Copyright 2018, with permission from Elsevier. (b) Anodic aluminum oxide (AAO) film formed by mild anodization. Adapted with permission from ref 30. Copyright 2006, Springer Nature. (c) Polyimide microfiltration membranes with 200 nm pores fabricated by aperture array lithography. Reprinted from ref 33. Copyright 2004, with permission from Elsevier.

pore array and morphology of representative membranes fabricated by track etching, anodic aluminum oxide (AAO), or lithography. In track etching, a latent track of polymer is degraded by ion irradiation, and then chemically etched to transform the damaged area into pores.³² Membranes manufactured by track etching have a uniform pore size distribution; however, their porosity is limited to <10% due to potential pore superimposition of tracks creating double/triple pores. On the other hand, anodic aluminum oxide (AAO) membranes comprise tightly packed pores of hexagonal geometry in the 10–200 nm diameter range, but their lack of flexibility and brittleness limit their use. Lastly, lithography techniques have emerged as a fairly inexpensive alternative to prepare MF membranes with periodically spaced, uniform cylindrical pores.^{33,34} However, lithography is a multistage, laborious process, and it is challenging to attain smaller pores in UF range.

Self-assembly broadly stands for autonomous arrangement of pre-existing components into organized structures or patterns without external guidance.³⁵ Self-assembly is ever-present in nature, from protein folding to the formation of the cell membrane and other functional biological nanostructures. It is also a convenient avenue for forming membranes with well-controlled nanostructure (e.g., pores) and surface chemistry without the need for complex manufacturing techniques.^{37,38} Some of the earliest records of self-assembled membrane selective layers with narrow pore size distribution directly utilized biological materials. The outermost cell envelopes of many eubacteria, and archaeabacteria have crystalline surface layers (“S-layers”)^{39–42} that possess 2–8 nm pores,^{43,44} in the UF working range. These S-layers were incorporated into UF membranes as selective layers to leverage these attractive features. In one of the first examples of UF membranes with S-layers, recrystallized S-layer self-assembly products were applied as selective layer on a support membrane.⁴⁵ The isolated and purified cell wall protein of bacteria was reconstituted as an ultrathin layer on a porous MF membrane. This layer was then fixed by cross-linking with glutaraldehyde. The resultant UF membranes showed a precisely ordered S-layer protein structure with 5 nm pore

size and a sharp molecular weight cutoff (MWCO), with the rejection rising from 0 to 100% within the 30 to 40 kg/mol range. In addition, glutaraldehyde-treated S-layers were shown to have a net negative surface charge owing to free carboxyl groups of the amino acids. In a follow-up study, these carboxyl groups were chemically activated with carbodiimide, and macromolecules with different sizes and structures were immobilized on the membrane surface through the reaction between their amino groups and the carbodiimide.⁴⁶ These modified S-layer ultrafiltration membranes showed strong resistance against protein adsorption. Overall, S-layer ultrafiltration membranes had significantly improved size-based selectivity compared to UF membranes manufactured by NIPS. Yet, scale-up of this system was deemed not feasible due to challenges in biopolymer isolation, purification, reconstitution and reproducibility of defect-free films at large-scale.

Block copolymer (BCP) self-assembly has emerged as a promising alternative that can bypass these challenges while achieving narrow pore size distribution and high porosity. BCPs consist of incompatible blocks that microphase-separate into distinct domains with an equilibrium domain size of 3–100 nm. The equilibrium domain size and geometry are determined by the Flory–Huggins interaction parameter between blocks and degree of polymerization. Diblock copolymers may self-assemble into spheres, cylinders, gyroid (a periodic bicontinuous cubic structure), and lamellae.^{47–49} Triblock polymers may lead to even more complex geometries. Among these nanostructures, the cylinder and gyroid phases attract great attention from membrane scientists because they can be tailored to form membranes with densely packed nanopores of uniform size.

Porosity can be imparted to self-assembled BCP structures following their formation and stabilization/fixation to create membranes by, for example, selective etching of one of the blocks.^{50,51} Another strategy is the addition of a component that interacts with and swells one of the domains during membrane formation, followed by its removal by leaching to leave behind void spaces.^{24,52} For instance, thin films were spin-coated from blends of poly(styrene)-block-poly(methyl methacrylate) (PS-*b*-PMMA) BCP with PMMA homopolymer.²⁴ Cylindrical PMMA domains were aligned perpendicular to the surface after high temperature annealing under vacuum. The thin film was removed from the silicon wafer by immersion into HF, and then immersed into acetic acid to extract the PMMA homopolymer. A composite membrane was prepared by carefully transferring the thin film on a porous PS support. The membrane had high flux and could efficiently remove viruses from the feed, and the nanopore size could be adjusted by varying the blend composition.⁵² However, scale-up of this approach would be challenging because manufacturing steps used are not readily implemented in industrial systems.

To achieve isoporous membranes using highly scalable approaches, BCP self-assembly has been integrated into the NIPS process to establish a single-step membrane manufacturing method called self-assembly/nonsolvent induced phase separation (SNIPS) (Figure 3).^{53–57} SNIPS involves the formation of membranes from BCPs using a carefully controlled NIPS process that utilizes a mixture of two cosolvents with different volatility and polarity. The supramolecular assembly of the block copolymers into micelles, followed by ordering and merging of these micelles as one of the cosolvents evaporates and the system is exposed to water,

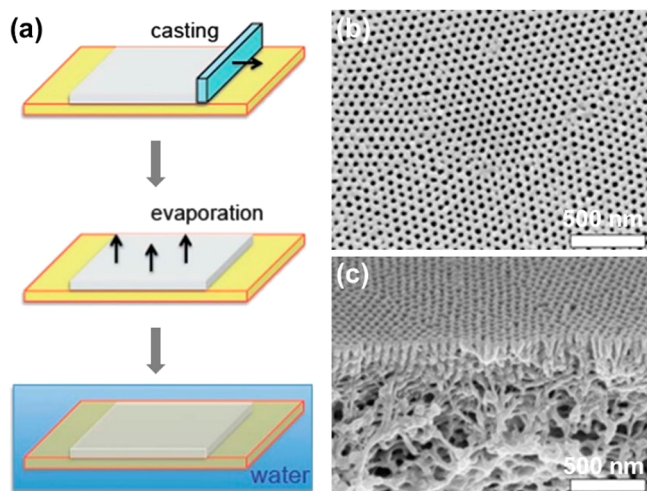


Figure 3. (a) Schematic of the SNIPS membrane fabrication technique and resulting membrane morphology. A polymer solution is prepared by dissolving a block polymer in a solvent or mixture of solvents. The solution is then drawn into a thin film through simple casting techniques (e.g., using a doctor blade). Solvent is allowed to evaporate from the thin film in a controlled manner for a predetermined period of time. Then, the thin film is plunged into a nonsolvent bath (e.g., water). The nonsolvent causes the polymer to precipitate, which kinetically traps the nanostructure of the membrane. The result is a nanoporous membrane with an asymmetric structure that comprises a highly selective active layer situated on top of a gutter layer with a high porosity. Republished with permission of Royal Society of Chemistry, from ref 61. (b and c) SEM micrographs of the top layer and cross section of membranes made using the SNIPS process, showing the regular order of membrane pores prepared by SNIPS. Reprinted by permission from ref 62. Copyright 2007, Nature Publishing Group.

373 has been demonstrated to drive pore formation (Figure 3).⁵⁸
 374 This leads to a very narrow pore size distribution and high
 375 porosity.^{59,60} However, combining the right selective solvents
 376 and process conditions is crucial. Cryo-scanning electron
 377 microscopy and other advanced imaging technologies have
 378 proven useful in tracking the effect of solvent composition and
 379 additives on supramolecular assembly in solution, and also on
 380 the ultimate membrane morphology.⁴⁷

381 The first example of an isoporous SNIPS membrane was
 382 developed using the diblock copolymer polystyrene-block-
 383 poly(4-vinylpyridine) (PS-*b*-P4VP) with ~15 wt % P4VP.⁵⁵
 384 The morphology of PS-*b*-P4VP membranes produced by
 385 SNIPS showed a fairly thin, ~100–200 nm layer of isoporous
 386 channels on top of a sponge-like macroporous support (Figure
 387 3).²⁶ Pore size typically ranged between 3 to 20
 388 nm.^{26,53–55,59,61} The pore size of SNIPS membranes can be
 389 controlled by mixing BCPs with different additives. Additives
 390 that preferentially interact with one of the BCP blocks through
 391 coordination or hydrogen bonding can alter domain size
 392 during self-assembly.⁶³ For instance, bivalent cations present in
 393 the casting dope complex with pyridine and assist the
 394 formation of isoporous membranes.⁶⁴ In addition, hydrogen-
 395 bonding compounds of –OH/–COOH functionalized organic
 396 molecules⁶⁵ and ionic liquids⁶⁶ were proven effective in tuning
 397 the morphology of PS-*b*-P4VP asymmetric nanoporous
 398 membranes. Addition of carbon nanotubes in small amounts
 399 has been shown to stimulate a stronger network between
 400 micelles and result in more stable membranes.⁶⁰ Additives used
 401 in other BCP membranes span organic materials such as

homopolymers,⁶⁷ carbohydrates,⁶⁸ and small organic molecules,⁶⁵ as well as inorganic materials such as metal salts^{59,64,69} and TiO₂ nanoparticles.⁶³ Overall, use of additives served as an efficient strategy to achieve membranes with highly uniform pores, improved permeance and selectivity, depending on the system of interest. The narrowest domain size attained with BCP self-assembly is ~3 nm.⁷⁰ Thus, membranes prepared by BCP self-assembly are excellent for separations in the UF size range. However, accessible pore sizes are still substantially larger than required for small molecule separations, RO and NF applications. SNIPS process has been modified to access these small pore sizes by modifying BCP self-assembly. In this vein, using mixtures of different block copolymers were found to yield membranes with an effective pore size of ~1.5 nm.⁷¹ Custom-designed triblock copolymers can also yield membranes whose pore size can be modified by exposing them to particular reactants after manufacture to reduce the effective pore size down to ~1 nm.^{56,72} These membranes, however, all comprise charged polymer chains lining their pores. Thus, while they perform size-based separation of neutral solutes, their selectivity for charged compounds is heavily influenced by electrostatic interactions. Nonetheless, this approach constitutes a very promising method for creating membranes with charged, functionalizable nanopores for many applications.

To create <3 nm nanopores without charged groups, polymers with random and comb-shaped architectures have been exploited. The microphase separation of amphiphilic comb-shaped copolymers with hydrophobic backbones and hydrophilic poly(ethylene oxide) (PEO) side-chains were studied as membrane selective layers.^{73–78} These copolymers microphase separate to form bicontinuous nanodomains of PEO and the hydrophobic backbone, with domain size controlled by side-chain length. PEO domains can absorb water and act as effective nanochannels with an effective size of ~1 nm in diameter,^{74,75} allowing permeation of water and solutes sufficiently small to pass through the channels. These membranes not only displayed size-based separation of dye molecules, but also exceptional fouling resistance. As the pores are partially filled with the PEO chains, the effective pore size of the membrane was responsive to parameters that changed the solvent quality of the feed for PEO, including temperature,⁴⁴² pressure,⁴⁴³ ionic strength,⁴⁴³ and the presence of an alcohol.⁷⁶ While these responsive properties are intriguing for some applications, they can also lead to changes in selectivity during operation due to fluctuations in feed properties. It should also be pointed out that these membrane chemistries have the potential to be further functionalized through the inclusion of a third monomer during synthesis, to create functional pores with different rejection properties.^{79,80}

Random copolymers that combine hydrophilic and zwitterionic repeat units have also been shown to self-assemble into similar water-permeable nanochannel networks (Figure 4a,b).⁸¹ When coated onto a porous support, these membranes form isoporous membranes with ~1 nm effective pore size, exhibiting a sharp rejection curve independent of solute charge (Figure 4c).^{81,82} These membranes can be formed of copolymers with a variety of hydrophobic⁸¹ and zwitterionic⁸² groups. For a specific subset of zwitterionic repeat units, membranes exhibit unprecedented degrees of fouling resistance, with little to no flux decline even during the filtration of high fouling solutions and no measurable flux decline that cannot be recovered by a simple water rinse (Figure 4d).^{81–83} The effective pore size of these membranes is particularly

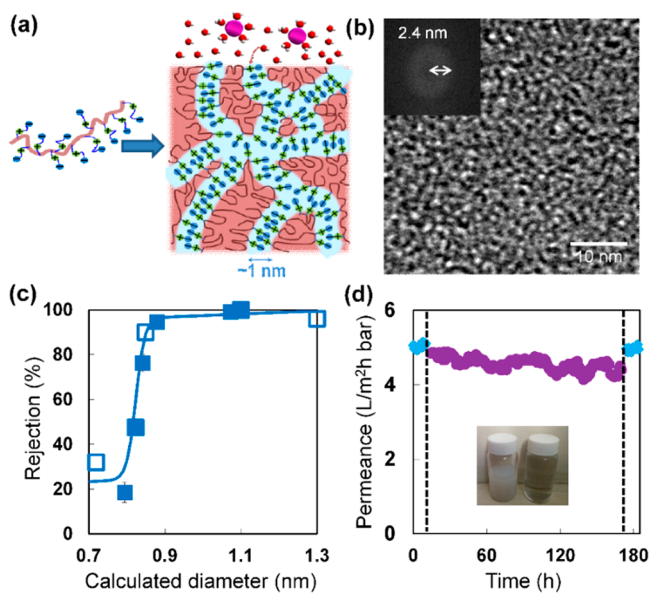


Figure 4. Formation of isoporous, highly fouling resistant membranes through the self-assembly of zwitterionic random copolymers. (a) Schematic showing the self-assembly of zwitterionic groups into bicontinuous networks of zwitterionic (indicated by green and blue charged groups) and hydrophobic (pink) domains. The zwitterionic domains act as a network of hydrophilic nanochannels ~ 1 nm in diameter, held together by the glassy hydrophobic domains. Water molecules and solutes smaller than or equal to the domain size (red) can enter these channels and permeate through the membrane, while larger solutes (fuchsia) are retained. Reproduced from ref 81 with permission from Elsevier. (b) Transmission electron microscopy (TEM) brightfield image of the self-assembled nanostructure of a zwitterionic copolymer, poly(trifluoroethyl methacrylate-random-sulfobetaine methacrylate) (PTFEMA-*r*-SBMA), exhibiting bicontinuous networks of zwitterionic (dark) and TFEMA (light) microphases. The inset shows fast Fourier transform (FFT) of the images with the characteristic period of 2.4 nm shown on the arrow, corresponding to a channel size of ~ 1.2 nm. Reprinted with permission from ref 82. Copyright 2017 American Chemical Society. (c) Rejections of charged (filled symbols) and neutral (empty symbols) dyes by a PTFEMA-*r*-SBMA TFC membrane. Charged and neutral dyes roughly fit onto a single rejection curve, demonstrating the selectivity is size-based, and not charge-based. The sharp rejection curve demonstrates narrow pore size distribution. Reproduced from ref 81 with permission from Elsevier. (d) Dead-end filtration of an oil emulsions through PTFEMA-*r*-SBMA TFC membrane. Plot shows the initial permeance of water (blue), followed by the permeance of a 1500 mg/L oil-in-water emulsion (purple). Then, the membrane is rinsed with water several times, and water permeance is measured again (blue). The membrane exhibits no measurable irreversible flux loss. Inset shows a photo of the feed (left) and permeate (right), showing high oil removal. Adapted from ref 83. Copyright 2017, with permission from Elsevier.

promising for small molecule separations based on size, difficult to achieve by existing membranes. Their manufacture is simple, involving only the coating of a porous support with the copolymer. If the selective layer is thin, membrane permeances much higher than commercial membranes with similar nominal MWCO, but broader pore size distribution. However, to date, it has been difficult to tune the pore size of these membranes.

In addition to self-assembling polymers, lyotropic liquid crystals (LLCs) have been proposed as a class of materials for designing membranes with very small pores.^{84–90} In a selective

solvent, amphiphilic LLCs can self-assemble into various ordered structures, including lamellar, cylindrical, hexagonal, and 3D bicontinuous cubic phases with interconnected channels (Figure 5).^{91,92} To form stable selective layers for

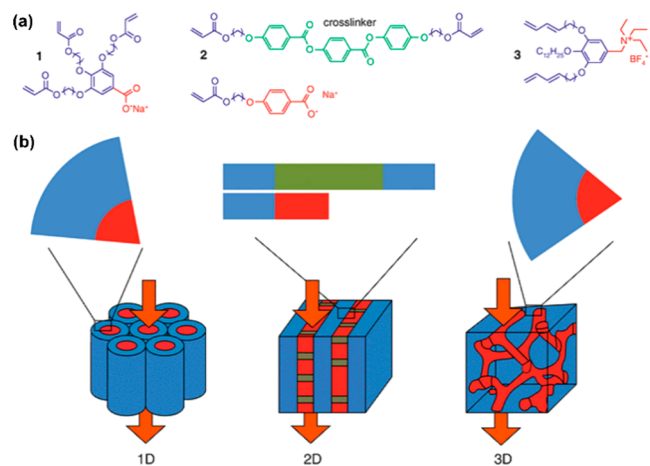


Figure 5. Liquid crystal membranes. (a) Examples of chemical structures of the LCs used in the construction of nanoporous membranes. One columnar or hexagonal LC, two smectic or lamellar LCs, and three bicontinuous cubic LCs. (b) The self-assembly of these materials to form nanostructured materials, with respectively one, two, or three-dimensional pores. The red part represents the pore while the blue fraction is the molecular region. Adapted from ref 91. Copyright 2010, John Wiley and Sons. Reprinted from ref 92. Copyright 2016, Springer-Verlag Berlin Heidelberg.

filtration membranes, self-assembly of polymerizable LLCs into one of these geometries is induced by appropriate selection of a solvent system and amphiphilic monomers.^{84,86} The self-assembled structure is then fixed by photo-cross-linking.⁸³ Membranes with effective pore size between ~ 0.29 – 1.2 nm have been achieved using polymerizable LLCs.^{87–90} To manufacture the early LLC membranes for small molecule separations, a self-assembling inverse hexagonal LLC containing ionizable carboxylic acid groups was coated as a thin film on porous support by solution casting, followed by solvent evaporation and photo-cross-linking.⁸⁷ The amphiphilic self-assembly process localizes the ionic headgroups exclusively at the hydrophilic/hydrophobic interface, resulting a membrane with negatively charged pores of ~ 1.2 nm. The membrane exhibited size-based separation for small organic anionic solutes, but very low flux as many of the cylindrical domains were not aligned vertically to the surface. In a more recent approach, a cubic phase forming LLC was hot-pressed onto a porous fabric and then cross-linked to form a supported membrane with a bicontinuous 3D network of channels.^{88,90} The effective pore size of the membranes was estimated between ~ 0.29 – 0.75 nm depending on the pore model used, and salt ions as well as organic solutes with diameters above 9 Å were rejected. The bicontinuous cubic structure eliminated the need for vertical alignment of the channels, but the high thickness of the membrane again resulted in low flux.

Thermotropic liquid crystals (TLCs) undergo temperature-driven self-assembly because of phase separation between the ionic and nonionic units of the monomer.^{93–99} This leads to bicontinuous cubic structures with a 3D network of narrow channels, which allow passage of smaller molecules. In this vein, TLC membranes were manufactured by coating the

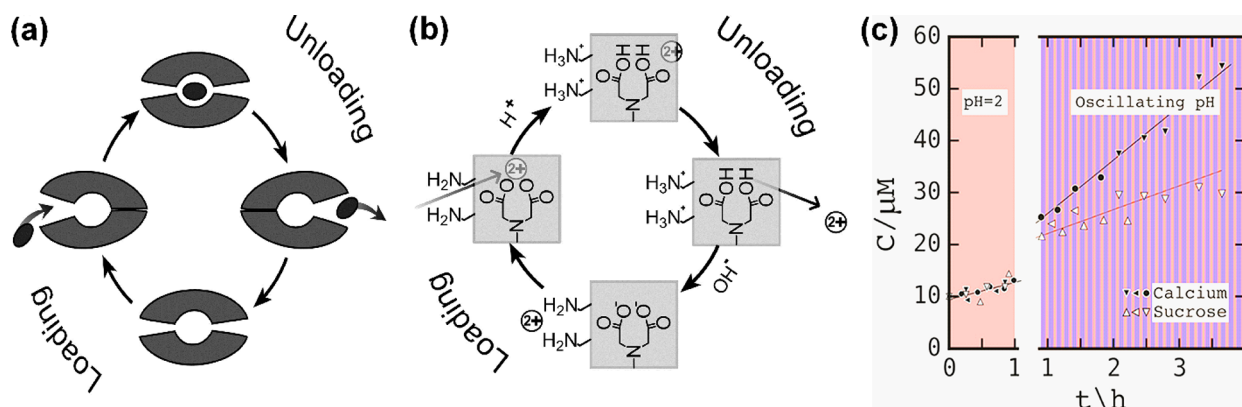


Figure 6. Selective transport of Ca^{2+} ions over sucrose through a biomimetic membrane modeled after ion pumps. Reprinted with permission from ref 106. Copyright 2018 American Chemical Society.

bicontinuous cubic TLC phase on a layered base.⁹⁹ The membranes showed 0.6 nm pore size, and the flux and salt rejection were found approximately in the nanofiltration range. One drawback in this composite system is the multistage process, which renders scalability challenging. Despite that the bicontinuous organization in TLCs are promising for membrane applications, TLCs have not been widely studied by membrane researchers.

More recently, more scalable methods to create thin film composite (TFC) membranes with a polymerized LLC selective layer have been developed.⁸⁴ The use of glycerol instead of more volatile solvents and a specially designed polymerizable surfactant enabled the formation of LLCs that remained stable during a coating process. The resultant membranes exhibit rejection properties between NF and RO membranes.¹⁰⁰ Due to their uniform pore size, charge, and subnanometer pores, cross-linked LLCs are very promising for treatment of complex, highly saline wastewaters.^{89,101} The effective pore size of LLC-based membranes can be further modified through postprocessing methods, such as by cross-linking the bicontinuous cubic LLC phase with butyl rubber¹⁰² or conducting alumina atomic layer deposition (ALD) inside the pores.¹⁰³ The cross-linking method could yield a pore diameter as small as 0.57 nm, tight enough to reject water-miscible nerve agent stimulant by over 99%. The ALD coating could bring the pore size below 0.55 nm, and these membranes could be utilized for light gas separations. As the technology stands today, the pores of these membranes are likely too small to enable the formation of membranes that separate most small organic molecules, even upon functionalization. Expanding the library of functionalizable amphiphiles that can self-assemble to create different domain sizes can further broaden the use of this family of materials to a wide range of selective membranes.¹⁰⁴ Nonetheless, polymerizable LLCs comprise a promising approach for the rational design of highly selective membranes.

diffusion mechanism, but large and/or hydrophilic molecules and ions cannot. Thus, cell walls and membranes feature a variety of transport structures that control permeation of various species. These include transport proteins that perform active transport of solutes against a concentration gradient, compounds that bind and carry specific solutes across the lipid bilayer membrane, and transmembrane proteins that form biological pores that synergistically use size, charge, and intermolecular interactions to only allow a specific solute through. The high selectivity and permeability of these biological systems has inspired many researchers to either incorporate biological materials such as transport proteins into membranes, or mimic these structures using synthetic means. An example of this, the incorporation of S-layer proteins into membranes, was described in the previous section. Many others are described in an excellent recent review.¹⁰⁵ Here, we briefly discuss some of these systems with a focus on controlling selectivity with the goal of accessing novel separations.

Some transport proteins pump specific solutes from one side of the cell membrane to the other, capturing a molecule outside the cell and releasing it inside by changing its conformation. These fascinating features were recently mimicked by a two-layer membrane to selectively transport Ca^{2+} ions over sugar molecules.¹⁰⁶ These membranes feature two pH-responsive layers: an amine-functionalized gating layer that allows permeation of solutes only at high pH, and a matrix rich in imidoacetic acid groups that bind Ca^{2+} ions at high pH but release them in low pH (Figure 6). When an oscillating pH is applied to the feed, the membrane acts as an ion pump. At low pH, Ca^{2+} ions pass through the gate layer and bind the imidoacetic acid groups. At low pH, the gate is closed, and Ca^{2+} ions in the matrix are released. Ca^{2+} and sucrose permeate through the membrane at similar rates at constant pH. When an oscillating pH is used, Ca^{2+} permeation rate is about four times that of sucrose. The oscillating pH process needed for the ion pumping effect by this membrane is challenging to execute in a large-scale membrane system. Nonetheless, this study demonstrates that we can mimic complex biological systems using relatively simple materials through thoughtful design of not only a novel functional membrane but also a novel process to leverage its unique responsive properties.

Another interesting feature of cell membranes is the presence of compounds that act as carriers of specific ions or molecules. These hydrophobic molecules, called ionophores, bind their target ion outside the cell, making it soluble in the

4. BIOMIMETIC APPROACHES TO MEMBRANE DESIGN

Unlike the synthetic membranes today, biological transport systems have extremely high selectivity–permeability combinations, enabling the regulation of the transport of a huge array of molecules and ions into and out of cells.¹⁰⁵ The cell membrane is a lipid bilayer. Hydrophobic small molecules can partition into this bilayer and permeate following the solution-

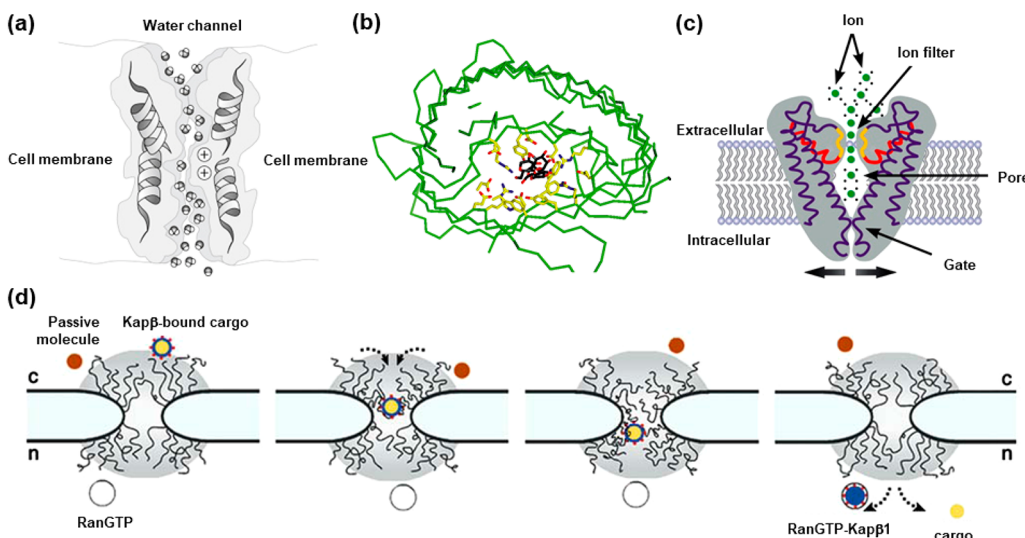


Figure 7. Some biological structures that inspired biomimetic approaches for creating membranes with controlled selectivity. (a) Aquaporin, showing single file diffusion of water molecules through its pore. Reproduced from ref 124 with permission from Elsevier. (b) Cross-section through a maltoporin monomer bound to maltotriose (depicted black), showing the interaction between the sugar molecule and the pore walls. Reproduced from ref 114 with permission from Elsevier. (c) Schematic diagram of the basic structural elements of an ion channel including the ion selectivity filter, the water-filled pore, and the channel gate. Ions are depicted as circles moving through the filter in a single-file manner. Reproduced from ref 125 with permission from Elsevier. (d) Schematic of a proposed model of operation for the NPC, regulated by binding and unbinding interactions between phenylalanine-glycine domains and the carrier proteins. From ref 126. Reprinted with permission from AAAS.

601 cell membrane. They then release it into the cytoplasm, 602 allowing permeation following the concentration gradient. This 603 mechanism, called facilitated or carrier mediated transport,^{6,107} 604 exhibits exceptional selectivity, as only the target compound 605 can interact with the carrier. This is often combined with high 606 permeability for the target compound, making facilitated 607 transport an ideal mode of operation for highly selective 608 membranes.^{108,109} This has led researchers to incorporate 609 ionophores into membrane selective layers to create ion- 610 selective membranes, particularly for sensors and ion-selective 611 electrodes.¹¹⁰ However, most membranes that use this 612 mechanism involve a liquid carrier phase, which limits their 613 application in large scale, pressure-driven separations.^{6,108}

614 Finally, cells have several types of biological pores that 615 regulate transport following a concentration gradient. These 616 pores include aquaporin and other water channels, ion 617 channels, porins that selectively pass specific solutes such as 618 sugars, and the nuclear pore complex (NPC), which regulates 619 permeation between the cytoplasm and the cell nucleus 620 (Figure 7).¹¹¹ These biological pores frequently feature a 621 constricted pore similar in diameter to the target compound 622 (<1 nm for ion channels and porins^{112–114}) and functional 623 groups lining the pore that interact with the target during 624 passage (e.g., anionic or hydrogen bonding groups^{112–114}). 625 This is an exquisite example of how nature uses nanostructure 626 and chemical functionality synergistically. The nanostructure 627 constricts flow and confines all components passing through, 628 forcing them to interact with the chemically functional walls. 629 Solutes that interact favorably with the functional groups are 630 shuttled through by carrier-mediated or facilitated transport, 631 whereas those that do not are excluded.¹⁰⁷ They have the 632 highest transport rates among transport proteins, predicting 633 high flux and selectivity in membrane applications. This has led 634 the majority of researchers pursuing biomimetic approaches to 635 model this family of transport systems in their work.

A significant portion of this research has focused on permeating water while retaining all else with the ultimate goal of water desalination and purification. These studies have heavily focused on aquaporins (Figure 7a), biological water channels that selectively permeate water while preventing the permeation of ions through size exclusion and electrostatic repulsion mechanisms. Their selectivity and flux is enhanced due to the single file transport of water molecules.¹¹⁵ Researchers have utilized these features either by incorporating biological water channels such as aquaporin into membranes,^{116,117} or by mimicking these using artificial water channels embedded in membranes.^{115,118,119} This highly active research direction led to the commercialization of aquaporin-containing membranes for water treatment by forward osmosis (FO) and other processes.^{115,117} Systems utilizing aquaporin or its mimics can remove salts with extremely high water fluxes, mimicking the selectivity of RO and NF membranes. It also has potential applications in wastewater treatment of reuse,¹²⁰ though this is highly dependent on the matrix the water channels are embedded in.¹²¹ Their selectivity is hard to tune,¹²² though with the advent of synthetic water channels,^{122,123} the potential exists for tuning their separation capabilities.

There are also numerous biological channels that transport other solutes with great selectivity. For instance, porins that bridge bacterial cell walls can selectively allow the passage of specific biomolecules such as sugars (Figure 7b). Ion channels allow the permeation of select ions and often also feature gating/responsive properties (Figure 7c). The nuclear pore complex (NPC) controls the passage of a variety of biomacromolecules through the membrane that separates the cell nucleus from the cytoplasm; only solutes that are bound to carrier molecules are ferried through (Figure 7d). These intriguing nanostructures have inspired the design of nanostructured materials that modulate the transport of solutes with selectivity based on factors other than size, several of which are described below. Similar to aquaporins, these biological

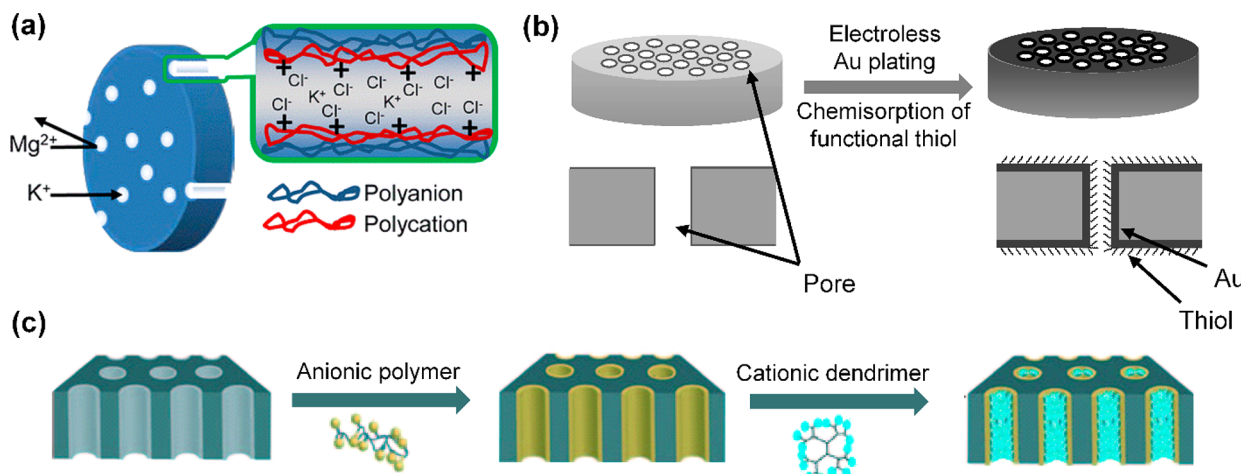


Figure 8. Template methods for the fabrication of membranes with charge-based selectivity. (a) LBL assembly within the pores of TE membranes showing transport selectivity between monovalent and multivalent ions. Reprinted with permission from ref 153. Copyright 2013 American Chemical Society. (b) Formation of gold nanotube membranes by electroless gold plating within the pores of a TE membrane followed by the functionalization of pore walls with self-assembled thiol monolayers. Reprinted from ref 182. Copyright 2008, with permission from Elsevier. (c) Tethering self-assembled anionic polymers within the pores of a TE membrane followed by vacuum filtration of a high generation cationic dendrimer. Reprinted with permission from ref 167. Copyright 2008, John Wiley and Sons.

systems also feature pores only slightly larger than their target, lined with functional groups that interact with their target exclusively and reversibly. A key challenge to mimicking these functional nanochannels, however, is the creating nanoscale, functionalizable pores through scalable manufacturing techniques.

5. ELECTROSTATIC INTERACTIONS: CHARGE-BASED SELECTIVITY

A very large portion of the current literature on controlling membrane selectivity focuses on separating solutes based on their charge. Such separations have a range of practical applications including water softening, heavy metal removal, recovery of valuable ions, and desalination.¹²⁷ Ion transport also has implications on areas such as energy conversion, nanofluidic transistors, drug delivery, medical analytics, and sensing.^{128–130} Membranes that can separate small organic molecules of similar size but differing charges also have several applications, especially in the extraction and purification of small pharmaceutical molecules such as amino acids^{131–133} and antibiotics.^{134,135} Separation of large biomolecules (e.g., proteins) based on their charge is also of interest in areas such as biotechnology and biopharmaceuticals.¹³⁶

It should be pointed out that essentially all membranes with charged surfaces are capable of exhibiting some charge-based selectivity due to electrostatic interactions between the membrane surface and ionic species that permeate through the membrane.^{137–140} Furthermore, most commercial membranes have at least mildly charged surfaces by design, though this is not necessarily aimed at achieving charge-based separations. Membranes are typically made of hydrophobic materials as these remain mechanically stable in water. Hydrophobic surfaces, however, are prone to the adsorption of organic compounds, oil, and microorganisms from the feed. This phenomenon, termed fouling, leads to pore clogging and is a major issue in the operation of membrane systems that causes increased energy use, frequent need for maintenance, and shorter membrane lives.^{141–143} To limit fouling, most MF and UF membranes are manufactured using methods that will

improve their surface hydrophilicity. Most of these methods result in negatively charged surfaces that electrostatically repel negatively charged solutes that make up a large fraction of common foulants (e.g., bacteria, alginate, natural organic matter, proteins). NF and RO membranes typically have residual negative charges on their surface that arise from the synthesis method. These charges not only prevent fouling, but also enhance salt rejection through Donnan exclusion.¹⁴⁴ Intermolecular interactions (e.g., hydrogen bonding, polarity, hydrophobic interactions), which affect the solubility of solutes in the dense selective layer, also play a role in solute rejection and membrane selectivity.^{145–148} As a result, the selectivity of NF and RO membranes for organic molecules is complex, affected by not only solute size but also charge and a combination of other molecular features, while size exclusion is the main separation mechanism.^{140,148,149}

Nonetheless, the preparation of membranes that exhibit varying rejections of solutes (salt ions or organic molecules) based on charge through electrostatic and other interactions has attracted extensive attention. Beyond the applications discussed above, many novel membrane materials designed for this purpose result in structures with promise for more complex separations such as nanoscale channels that can be further functionalized to control their selectivity. Thus, beyond their performance as charge selective membranes, these technologies are promising starting points for filtration systems with more complex selectivity.

5.1. Charged Nanopores through Template Methods.

Ion channels (Figure 7c) are exquisite examples of charged nanopores that control transport of ions.¹⁵⁰ Highly efficient transport selectivity of these channels is due to their narrow diameter, slightly larger than solute being transferred, and the high density functional groups lining the pores. Their efficient ion transport and high ion selectivity has inspired several researchers to mimic these structures and create ion selective membranes that feature nanopores with charged pore surfaces.¹⁴⁴ However, the preparation of membranes with a high density of well-defined, uniform, and small (1–2 nm) pores with charged surfaces needed to get effective separation of ions and small

748 molecules is a major challenge. To create these structures, 749 many researchers have used commercial membranes with 750 evenly sized but larger pores as “templates”, narrowing down 751 and functionalizing the pores by various means (Figure 8). 752 **5.1.1. Layer by Layer Deposition and Polyelectrolyte 753 Adsorption.** One relatively straightforward approach to 754 creating charged nanopores involves the modification of 755 membranes with cylindrical through-pores with a polyelec- 756 trolyte multilayer (PEM) built by layer-by-layer (LBL) 757 deposition of oppositely charged polyelectrolytes. These 758 systems use track-etched (TE) or anodized aluminum oxide 759 (AAO) membranes, described earlier, as templates. To deposit 760 the PEM inside the membrane pores as opposed to just the top 761 surface of the membrane, polyelectrolyte solutions are filtered 762 through the template membrane in the desired order.¹⁵¹ This 763 creates narrower, charged pores that can exclude divalent ions 764 more than monovalent ions, leading to moderate selectivity 765 between monovalent and divalent ions at low ionic strength. 766 For example, the deposition of 1–2 bilayer(s) of polyelec- 767 trolytes within TE membranes with 200 nm pores reduces the 768 pore size to 60–100 nm and leads to some selectivity between 769 Cl[−] and SO₄^{2−} ions.¹⁵² LBL deposition inside smaller pores 770 (<50 nm) can yield narrower pore size (Figure 8a),¹⁵³ but is 771 particularly challenging and difficult to control. Adsorption 772 near the pore entrance can result in a nonuniform layer within 773 the pores, with the majority of pore modification occurring 774 near the pore entrance.^{153,154} The addition of more bilayers 775 leads to smaller pores, but also causes a dramatic decrease in 776 surface charge density due to structural reorganization and ion 777 pairing, reducing ion selectivity.¹⁵⁵ LBL deposition into 778 membrane pores is not very scalable, because it requires 779 multiple steps of adsorption for each polyelectrolyte and 780 subsequent rinsing. Furthermore, PEM coatings often have low 781 stability during prolonged use, extreme pH levels, ionic 782 strengths, or temperatures.¹⁵⁶

783 The LBL method has also been utilized to build PEM 784 nanotubes with charged cores on a template (AAO or TE) that 785 are then removed and integrated into a new membrane 786 selective layer.^{157,158} This approach allows the packing of a 787 higher number of nanotubes within the membrane, leading to 788 higher pore density. Furthermore, it can be used for the 789 fabrication of charge mosaic membranes, which possess 790 discrete oppositely charged domains that traverse through 791 the membrane thickness.¹⁵⁹ This structure allows for higher 792 ionic flux in comparison to similarly sized neutral molecules, 793 resulting in enrichment of ions in the permeate solution. 794 Charge mosaic membranes can be used for the recovery of 795 valued ions and removing dilute ionic contaminants. In 796 addition to LBL deposition to build PEM nanotubes, charged 797 mosaic membranes have been fabricated by several methods 798 including the self-assembly of multiblock polymers,¹⁶⁰ ion 799 exchange resins embedded in permeable matrices,¹⁶¹ and 800 conjugate electrospinning.¹⁶² All these approaches require the 801 orientation of the ionic domains perpendicular to the 802 membrane surface. Recently, inkjet printing, a rapid and 803 precise technique for the deposition of functional materials,¹⁶³ 804 has been used for the fabrication of charge mosaic membranes 805 on both porous membranes formed by functional copolymer 806 self-assembly¹⁶⁴ and on templated TE membranes.¹⁶⁵ These 807 studies combine functional polymers with the ease of 808 manufacturing provided by inkjet printing to prepare 809 membranes with unusual selectivity.

5.1.2. *Adsorption of Self-Assembling Polyelectrolytes.* An 810 alternative method for simultaneously narrowing down and 811 functionalizing the pores of TE membranes is to tether a 812 charged polymer that has already self-assembled into supra- 813 molecular structures in solution (vesicles, micelles, etc.)⁸¹⁴ through ionic interactions (Figure 8c). In comparison with 815 the adsorption of a polyelectrolyte, this approach will lead to a 816 more significant decrease in pore size with just one layer unless 817 these structures completely disassemble during the process. In 818 this method, Sn²⁺ ions are adsorbed into the pores of a TE 819 membrane, followed by the vacuum filtration of a solution of a 820 self-assembling anionic polymer. This approach can be 821 continued further by consecutive filtration of oppositely 822 charged polymers, similar to LBL assembly, to further narrow 823 down the pores down to ~6 nm and to control pore surface 824 charge.¹⁶⁶ This method is simple and fast, though it still suffers 825 from the low porosity of the TE membranes used as templates. 826 The pore size achieved by this technique is suitable for protein 827 separations, but too large for separating small molecules.⁸²⁸

To reach smaller pore size and higher functional group 829 density, a positively charged dendrimer can be similarly 830 deposited into the pores following the deposition of an 831 anionic polymer (Figure 8c). Small pores and high functional 832 group density upon tethering high generation dendrimers 833 results in very high separation selectivity between small organic 834 molecules of opposite charge.¹⁶⁷ However, the low resultant 835 porosity and flux of these membranes, the high cost of high 836 generation dendrimers and the limited stability of coatings held 837 together by Coulombic interactions limit the broader use of 838 this approach for industrial separations.⁸³⁹

5.1.3. *Gold Nanotube Membranes through Electroless 840 Deposition.* Electroless gold plating is likely the most versatile 841 and well-controlled template-based method for creating 842 membranes with controlled pore size and surface chemistry.⁸⁴³ This method involves sensitizing a modified-TE membrane 844 with SnCl₂, followed by immersing the membrane in an 845 AgNO₃ solution and finally a gold plating solution. This leads 846 to the conformal coating of the membrane pores with a layer of 847 gold, creating gold nanotubes (Figure 8b).¹⁶⁸ Pore size can 848 be controlled by varying the plating time, making it possible to 849 reach down to molecular dimensions (<1 nm) suitable for size- 850 based separation of small molecules.¹⁶⁹ The chemical 851 functionality of the pore walls of these membranes can be 852 controlled through the formation of a self-assembled 853 monolayer (SAM) upon exposure to functional thiols.¹⁷⁰ Ion 854 permselectivity can be introduced by two different routes. The 855 first involves imparting excess charge on the membrane by 856 applying an electrical potential in an electrolyte solution. This 857 enables the permselectivity to be switched reversibly. Ideal 858 cation permselectivity similar to Nafion can be obtained when 859 the pore radius is small relative to the thickness of the electrical 860 double layer within the pores.¹⁶⁸ However, obtaining switch- 861 able ion transport is only possible in electrolytes containing 862 nonadsorbing anions such as F[−]. Anions such as Cl[−] or Br[−] 863 adsorb at positive applied potentials, resulting in a cation 864 permselective membrane independent of applied potential.⁸⁶⁵ This can be prevented by the formation of an alkanethiol SAM 866 on the membrane.¹⁷¹ The second approach for creating 867 membranes with ion transport selectivity utilizes the 868 chemisorption of an ionizable thiol onto gold nanotubes.⁸⁶⁹ For example, chemisorption of carboxyl and amino functional 870 thiols yield cation- and anion- permselective membranes,⁸⁷¹ respectively.¹⁷² Switchable ion permselectivity can be obtained⁸⁷²

873 by the chemisorption of the amino acid cysteine. Varying 874 solution pH affects the ionization of the amine and carboxylic 875 acid groups on cysteine.¹⁷³ At small nanotube diameters (1.4 876 nm) and pH 12, a charged-based selectivity of 15 is reported 877 between two small organic molecules of opposite charge in 878 single-ion diffusion experiments. The selectivity was further 879 enhanced to ~110 in a competitive diffusion experiment.

880 This electroless gold plating technique provides exquisite 881 control over pore size and surface chemistry. This has led to 882 some of the most selective membranes reported to date, not 883 only based on charge but also based on other molecular 884 parameters, as discussed below.^{174,175} Nonetheless, its 885 complicated and lengthy manufacturing process limits its 886 commercial use. The electroless gold deposition contains 887 multiple steps and involves use of toxic chemicals and heavy/ 888 precious metal ions (Sn, Ag, Au). The plating step takes over 889 20 h to generate small pores. Furthermore, controlling the 890 uniformity of the gold layer within the nanotubes during the 891 gold deposition process is difficult, especially given the 892 curvature of the track-etched pores.¹⁶⁹ Also, chemisorption 893 of self-assembled monolayers within the narrow pores is very 894 slow.

895 An important drawback of all these template methods is the 896 very low porosities of the resultant membranes, down to <0.1% 897 (compared with 70–90% for a typical filtration membrane¹⁷⁶). 898 This leads to very low permeability and severely limits the use 899 of these gold nanotubule membranes for large scale 900 separations. Another inherent challenge is the difficulty in 901 obtaining a uniform coating layer along the pores. Uneven 902 coatings create bottleneck shaped pores that limit the 903 nanoconfinement effects and pore–solute interactions to the 904 pore entrance, resulting in lower selectivity.^{169,177–179} This 905 approach, however, has led to novel and powerful approaches 906 to create a wide variety of template nanomaterials for other 907 applications, including but not limited to drug delivery,
908 sensors, and electrode arrays.^{180,181}

909 **5.2. Aligned, Functionalized Carbon Nanotubes**
910 (**CNTs**). Inner cores of carbon nanotubes (CNTs) can act as 911 nanopores for filtration applications. CNTs exhibit extraordi- 912 nary transport properties arising from their exquisite, highly 913 defined structure. The graphitic pore walls of CNTs are 914 atomically smooth and hydrophobic. This leads to the 915 conduction of water molecules at speeds orders of magnitude 916 higher than that observed in bulk water, leading to high 917 permeability per pore.¹⁸³ If CNTs are vertically aligned and 918 processed to form the pores of a membrane selective layer, 919 they can be used to create membranes with uniform pore sizes 920 (6–7 nm for multiwalled carbon nanotubes (MWNTs) or 921 1.3–2 nm for double-walled nanotubes). These features have 922 led to the exploration of CNT-based membranes for 923 desalination and gas separation.^{184–186}

924 Several researchers have attempted to incorporate prema- 925 nufactured CNTs into membrane selective layers. For CNTs 926 to act as membrane pores, they have to be vertically aligned 927 across the membrane thickness, surrounded by an imperme- 928 able matrix. This has been attempted by a wide range of 929 methods that include the use of lyotropic liquid crystals 930 (LLCs),¹⁸⁷ strong magnetic fields,^{188,189} gel extrusion,¹⁹⁰ 931 mechanical shear,¹⁹¹ melt stretching,¹⁹² and anisotropic 932 flow.¹⁹³ Many of these methods are limited in their 933 effectiveness for achieving vertical orientation and/or their 934 scalability. They also require a supply of large quantities of 935 high quality CNTs of even length and with open ends. Despite

936 these challenges, a new start-up company, Mattershift, is 937 currently attempting the scale-up of a technology for the 938 manufacture of membranes featuring aligned CNTs. These 939 membranes exhibit charge-based selectivity,¹⁹⁴ but their 940 potential for functionalizability for more complex separations 941 is unknown due to the proprietary nature of the technology.
941

942 As opposed to aligning CNTs after manufacture, a template 943 method has been utilized to grow CNTs *in situ* within the 943 pores of an AAO support.^{195,196} The nanotubes were 944 subsequently uncapped by etching. The underlying AAO 945 template can be dissolved away in concentrated HF solution 946 and the gaps between CNTs can be filled with an impermeable 947 matrix. However, the inner diameter of CNTs obtained by this 948 method depends on the membrane pore size, ranging from 949 20–200 nm. The large pore size limits their application in 950 chemical and biological separation applications. Furthermore, 951 low areal tube density resulting from low porosity of AAO 952 supports further limits their application.
953

954 Alternatively, highly dense arrays of CNTs can be can be 955 grown on silicon or quartz substrates using catalytic CVD, 955 followed by conformal encapsulation of nanotubes in an 956 impermeable matrix (polymer,¹⁹⁷ silicon nitride^{198,199}) to 957 confine the flow within the CNT lumina. Subsequently, excess 958 matrix is removed from both sides of membrane and CNTs are 959 uncapped by reactive ion etching (Figure 9). Yet, producing 960

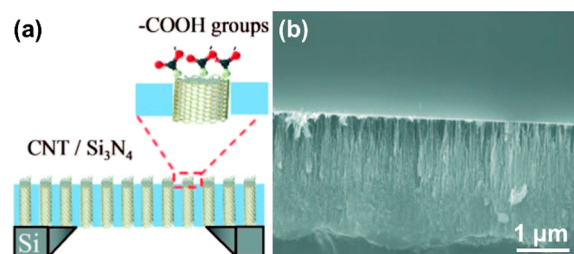


Figure 9. Membranes with CNT nanopores formed by growing vertically aligned CNTs, followed by the deposition of silicon nitride to fill gaps between the CNTs and etching to expose lumina. (a) Cross-section schematic of a CNT membrane representing the silicon support chip, aligned CNTs, the filling silicon nitride matrix, and the CNT tip functionalized with carboxylic acid groups. (b) Cross-section SEM image of the CNT/silicon nitride composite membrane showing the gap-free coating of silicon nitride. Reproduced with permission from ref 199. Copyright 2008 National Academy of Sciences.

membranes composed of densely packed, well-aligned CNTs is 961 not simple, because several steps needs to be conducted in a 962 clean room environment. In addition, these very thin 963 membranes are brittle and fragile, which limits the use of 964 these free-standing or silicon chip supported CNT membranes 965 to subcm² areas. As such, this approach is not amenable for 966 large scale separation applications, though it may be interesting 967 for drug delivery, microfluidic devices, and sensing.
968

An important feature of CNTs is the functionalizability of 969 the pore entrance, creating pores reminiscent of ion channels.
970 The oxidation process to uncap CNTs during manufacturing 971 results in charged pore entrances. Thus, resultant membranes 972 exhibit ion exclusion properties and charge-based selectivity of 973 solutes in dilute aqueous electrolyte solutions.^{194,199,202} The 974 pore entrances of CNTs can also be further functionalized 975 using carbodiimide mediated chemistry to control selectivity 976 and to narrow down the pore size at the entrance, including 977 tuning and enhancing charge-based selectivity. However,
978

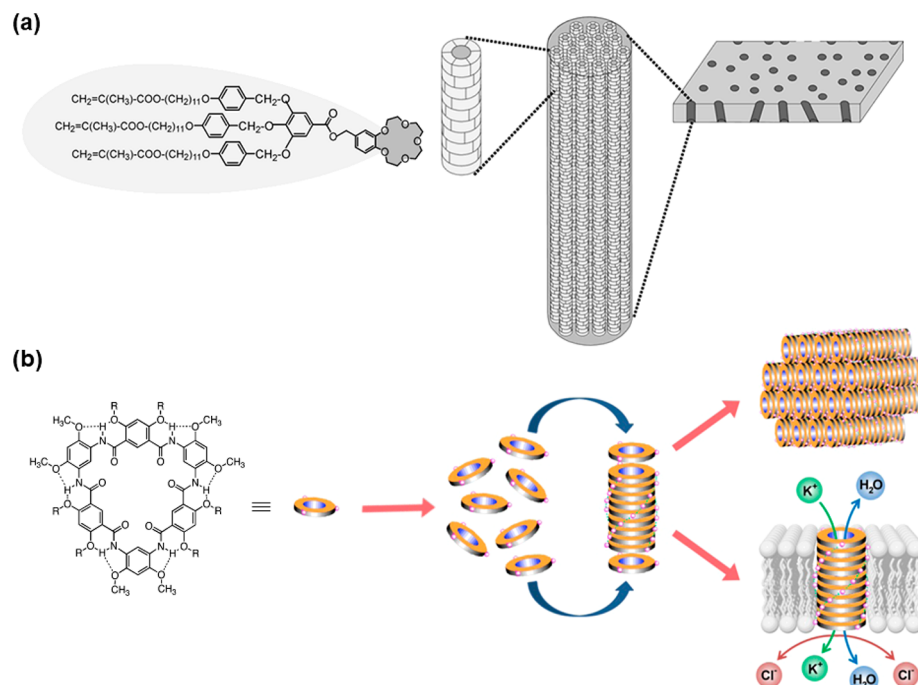


Figure 10. Formation of ion-selective nanopores by self-assembly of small molecules. (a) Self-assembly of a wedge-shaped monomer containing crown ether within the pores of TE membrane. Reprinted with permission from ref 223. Copyright 2000, John Wiley and Sons. (b) Self-assembly of macrocyclic peptides inside the hydrophobic core of lipid bilayers. Both show preferential cation transport. Reproduced with permission from ref 234. Copyright 2013 American Chemical Society.

979 separation efficiencies obtained have been lower than observed
 980 in pores that are functionalized throughout their length,
 981 because the interactions between solute and pore wall is
 982 limited to near tip entrance (only a distance of 7% of the
 983 nanotube length). Furthermore, the number of carboxylic acid
 984 groups at the CNT tips is relatively low, further contributing to
 985 the low selectivity.²⁰³

To increase the density of carboxyl groups on the pore surfaces and enhance the molecular interactions, the entire core of CNTs have been modified by electrochemical grafting.²⁰⁴ The pores were further narrowed down using a polypeptide spacer and a tetravalent sulfonated anionic molecule. Although the pores are not covered by grafting, the core-grafted CNT membrane showed a dramatic flux decline and almost no detectable pressure driven flow. This is because grafting the CNTs core compromises the smoothness and inertness nature of CNTs, required criteria for achieving high flux.^{205,206} Severe flux decline has also been reported for tip-functionalized MWNTs,^{205,206} and predicted for tip-functionalized SWNTs.^{207,208} There is ongoing research directed toward effective functionalization of CNTs to impart chemical selectivity while maintaining ultrafast permeation properties. Nevertheless, the current chemical modification techniques would likely adversely affect the permeation properties and raise a challenging question regarding their broader use.

1005 Current fabrication procedures for membranes with aligned
1006 CNTs are often prohibitive for the manufacture of filtration
1007 membranes at large scale.^{209–211} This is particularly true if the
1008 manufacturing process involves growing vertically aligned
1009 CNTs by CVD followed by the filling of interstices, the
1010 most well-studied approach for chemically functionalized CNT
1011 membranes.^{209–211} The production of these membranes
1012 involves many complex steps, often performed in a micro-

fabrication facility. It is also difficult to manufacture high purity CNTs without defects over large areas.²¹² Filling the interstices between CNTs to force permeation to the CNT lumina without disrupting the alignment or creating defects also remains a challenge.^{197,213} After this step, the membrane needs to be selectively etched to open up a high number of CNTs without creating voids in the matrix.^{202,203} All these complex manufacturing steps severely limit the applicability of aligned CNT membranes prepared by this method in filtration and separation applications, where hundreds of m² of membrane are needed. The exceptional properties of these functional CNT membranes have shown great promise in other applications that do not require low cost, large area manufacturing. For instance, functional aligned CNT films have been used for controlled drug delivery and in sensing utilizing their gating properties.^{197,200,201}

5.3. Functional Nanopores through Small Molecule 1029

Self-Assembly. Self-assembly of soft matter is a particularly powerful approach to forming functional nanostructures using scalable processes. Many natural materials form subnanometer organic nanotubes by self-assembly, including small molecule amphiphiles, dendrimers, peptides, peptidomimetics, DNAs, foldamers, and J-type rosettes.^{214–219} These self-assembled nanotubes could potentially serve as nanopores of membranes with controlled selectivity (Figure 10). However, forming large-area membranes with aligned nanochannels is, again, a crucial challenge. Below, we describe some studies where self-assembled nanotubes have been incorporated in membranes of sufficient area and integrity to study their transport properties and discuss their potential for scale-up.

5.3.1. Thermotropic Liquid Crystals with Functional 1043

Pores. Crown ethers are known for their selective binding to alkali metal cations through complexation.²²⁰ They can also stack and form effective nanopores with high cation selectivity

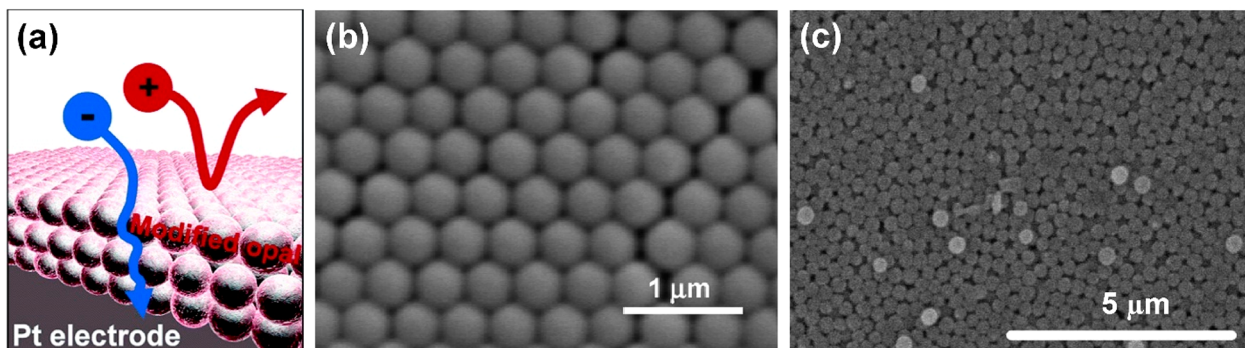


Figure 11. Layers and membranes formed by the self-assembly of silica nanoparticles into packed arrays. (a) Schematic of thin opal film comprising three layers of amine-modified silica spheres on a Pt electrode. Reprinted with permission from ref 236. Copyright 2005 American Chemical Society. (b) SEM image of the surface morphology of the opal film showing nanoparticles arranged in a hexagonal close packed array. Reprinted with permission from ref 235. Copyright 2006 American Chemical Society. (c) SEM image of the surface morphology of amine-modified, sintered free-standing membrane showing partial fusion of silica nanoparticles. Reprinted with permission from ref 241. Copyright 2009 American Chemical Society.

1047 (Figure 10a). Unlike previously described approaches that rely
 1048 on electrostatic interactions to exclude ions, crown ether
 1049 nanochannel membranes would retain their selectivity
 1050 independent of feed ionic strength. One approach to
 1051 incorporate stacked crown ethers into membranes involves
 1052 vertical stacking of cylindrical thermotropic liquid crystals
 1053 (TLCs) from amphiphiles containing crown ether moieties
 1054 and polymerizable, hydrophobic methacrylate end groups, held
 1055 together by a cross-linked methacrylate resin.²²¹ This was
 1056 obtained by casting a solution containing the wedge-shaped
 1057 amphiphilic monomer containing the crown ether groups, a
 1058 methacrylate, a cross-linker and a photoinitiator onto a
 1059 support. Subsequent cooling to -50°C results in the
 1060 formation of cylindrical aggregates containing stacked crown
 1061 ether units and causes thermo-reversible gelation. The layer is
 1062 then polymerized, fixing the supramolecular stacks into the
 1063 membrane selective layer. These membranes exhibit prefer-
 1064 ential transport of $\text{Li}^+ > \text{Na}^+ > \text{K}^+$ with Li^+/K^+ selectivity of
 1065 about 3. They also show very low water permeation rate due to
 1066 poorly aligned channels within a highly cross-linked, nonpolar
 1067 matrix polymer, which limits the probability of ions to transfer
 1068 and enter the next channel and permeate through.²²²

1069 To improve permeability, a TE membrane was used as a
 1070 template to grow vertically aligned crown ether stacks within
 1071 the through-pores.²²³ For this purpose, the TE membrane was
 1072 soaked in a hot methacrylate solution containing polymerizable
 1073 crown ether amphiphiles and a photoinitiator and then cooled
 1074 to grow supramolecular aggregates and cross-linked to arrest
 1075 the supramolecular structure. While this led to the formation of
 1076 some supramolecular channels perpendicular to the membrane
 1077 surface and subsequently some enhancement in ion transport
 1078 rate, a significant fraction of assemblies was still not aligned,
 1079 leading to low flux. Nonetheless, this directed assembly of
 1080 nanopores in a template demonstrates another promising
 1081 approach for creating narrow, functionalizable nanochannels
 1082 that can be utilized in future studies.

1083 **5.3.2. Macrocyclic Peptides.** Cyclic peptides with flat, rigid
 1084 conformation and the correct number and placement of the
 1085 amino acids can stack atop one another through intermolecular
 1086 hydrogen bonding and form tubular assemblies called cyclic
 1087 peptide nanotubes (CPNs) (Figure 10b). The diameter of
 1088 these nanotubes can be tailored by controlling the cyclic
 1089 peptide chemistry, from a few angstroms to a few nanome-
 1090 ters.²²⁴ It is also possible to place specific functional groups

1091 within the interior of nanotubes by varying the amino acids 1092 forming the ring. These properties make CPNs highly 1093 promising for the creation of biomimetic membranes with 1094 controlled selectivity. When embedded across the lipid bilayer, 1095 these nanotubes can serve as efficient cation-selective channels 1096 with high conductance and water flux.^{225,226} Functional groups 1097 in the peptides can also be altered to potentially control ion 1098 selectivity,²²⁷ though results remain hard to predict, as 1099 demonstrated by a study showing similar cation transport 1099 selectivity for channels of varying peptide length, polarity, 1100 charge, and ring size.²²⁸ Such changes also require complex 1101 synthesis procedures and may disrupt self-assembly.^{229,230}

1102 As with other functional nanotubes, the true challenge lies in 1103 integrating these nanotubes into membrane selective layers. 1104 Difficulty in aligning these highly aggregate-prone nanotubes 1105 vertical to the surface of a thin membrane selective layer makes 1106 their use in filtration applications hard to realize. Directed 1107 coassembly of polymer-conjugated macrocyclic peptides and a 1108 BCP was used to circumvent the need for the fabrication and 1109 alignment of nanotubes of uniform length and size.²³¹ CPN 1110 growth was confined to one BCP domain, aligned vertical to 1111 the surface of a thin film by annealing. When this membrane 1112 was used as the cover of a PDMS mold separating acidic and 1113 basic solutions containing a pH-indicator dye, a change in 1114 solution pH indicating cation transport selectivity was 1115 observed. This method results in some alignment of CPNs 1116 within the very thin, ~ 30 nm film. Nonetheless, ensuring a 1117 high density of CPNs that span the membrane thickness 1118 remains difficult, as does creating films that are mechanically 1119 stable enough to perform as a filtration membrane.²³²

1120 **5.4. Charged Nanopores through Self-Assembly of**
Inorganic Nanoparticles. While most of this perspective 1122 focuses on polymeric membranes, inorganic membranes are 1123 particularly attractive for specific applications that include high 1124 temperature gas separation, water treatment, and membrane 1125 reactors due to their high mechanical, chemical, and thermal 1126 stability. Inorganic nanoporous membranes are most com- 1127 monly prepared by anodization of aluminum, sol-gel methods, 1128 lithography, dip-coating, and chemical vapor deposition.²³³ 1129 More recently, highly porous membranes have been formed by 1130 the self-assembly of inorganic nanoparticles (NPs), the 1131 interstices between which form permeation pathways. This 1132 approach is attractive due to the ability to control pore size and 1133 functionality through straightforward methods. In this section,
 1134

1135 we describe the nanoporous membranes formed by self-
1136 assembly of inorganic and hybrid NPs.

1137 **5.4.1. Close-Packed Arrays of Colloidal Silica Nano-
1138 particles.** Colloidal silica NPs can self-assemble into well-
1139 ordered, close-packed arrays, or opals, of nanospheres that act
1140 as porous membranes (Figure 11). The interstitial space
1141 between the spheres serves as the pores whose size can be
1142 controlled in the 10–100 nm range by changing the size of
1143 silica nanospheres. The NP surfaces can then be functionalized
1144 using well-established silanol chemistry, creating a bicontin-
1145 uous network of functionalizable nanopores.

1146 Initial studies on this approach focused on thin opal films
1147 (~three layers) coated onto a Pt microelectrode and
1148 characterized the selectivity of these layers by measuring the
1149 permeation of redox-active molecules by voltammetry (Figure
1150 11a). These opal films were formed simply by dipping an
1151 electrode vertically in a colloidal alcohol solution followed by
1152 solvent evaporation (Figure 11b). The resultant silica opal film
1153 is negatively charged at high pH due to deprotonated hydroxyl
1154 groups on the surface, but minimal charge-based selectivity was
1155 observed.²³⁵ When the silica surfaces were functionalized with
1156 cationic amine moieties, a significant decrease was observed in
1157 the permeation of the cationic molecule $\text{Ru}(\text{NH}_3)_6^{3+}$ while the
1158 flux of neutral and negatively charged molecules of similar size
1159 remained unchanged.^{235,236} To narrow down the pores, the NP
1160 surface can be modified by attaching macrocycles such as
1161 calix[n]arenes or thiocalix[n]arenes that can selectively bind
1162 ions, resulting in charged nanopores²³⁷ that exhibit transport
1163 selectivity between neutral and positively charged solutes of
1164 similar size.²³⁸ Pores can be further narrowed down to about
1165 10 nm by grafting polyelectrolyte brushes inside the pores
1166 using surface-initiated ATRP.²³⁹ Grafting a weak cationic
1167 polyelectrolyte brush, poly(2-(dimethylamino)ethyl methacry-
1168 late), results in a 30–40% decrease in the limiting current for
1169 the cationic molecule $\text{Ru}(\text{NH}_3)_6^{3+}$ in voltammetry experi-
1170 ments, whereas the limiting current for the neutral molecule
1171 $\text{Fc}(\text{CH}_2\text{OH})_2$ decreases by only 10%. Polymer brush length
1172 can also be altered to tune the final pore size without
1173 perturbing the colloidal crystal lattice.²⁴⁰

1174 These initial electrochemical experiments suggest that these
1175 mesoporous silica colloidal materials can also be promising for
1176 membrane filtration applications. To test this premise, free-
1177 standing membranes with larger surface area were prepared by
1178 calcinating the silica nanospheres, forming a layer of nano-
1179 spheres on a glass slide by solvent evaporation, and then
1180 sintering the colloidal film at temperatures above 1000 °C.
1181 This causes the silica spheres to partially fuse with one another
1182 (Figure 11c), forming a more mechanically robust membrane.
1183 Further functionalization of these so-called nanofrit mem-
1184 branes has proven difficult due to the loss of silanol groups at
1185 high temperatures.^{241,242} To achieve more effective function-
1186 alization, free-standing sintered membranes were prepared
1187 using gold coated nanospheres. The surface was then modified
1188 with a SAM of thiol-containing molecules (e.g., cysteine),
1189 though this did not lead to significant pH response due to low
1190 surface coverage. When the pores were modified by grafting a
1191 brush of poly(methacrylic acid) (PMAA), a weak polyelec-
1192 trolyte, the permeation rate of a neutral molecule,
1193 ferrocenecarboxaldehyde, was 13 times higher in acidic
1194 solutions where the PMMA chains were protonated and
1195 collapsed onto the pore walls.²⁴³

1196 Opals formed by colloidal silica NPs exemplify a relatively
1197 simple approach to creating membranes with highly

1198 functionalizable nanopores. This is reflected in the studies 1199 described in the next section, where the silica surfaces are 1200 modified to achieve more complex separations. Due to the size 1201 of colloidal NPs and the packing geometry, the membrane 1202 pores formed by Si NPs are an order of magnitude larger than 1203 small molecule solutes. Yet, significant selectivity is achieved, 1204 likely due to the tortuous permeation pathway and high surface 1205 area that enforces a large number of solute–pore wall 1206 contacts.²⁴⁴ This phenomenon demonstrates the need for 1207 more detailed studies, both theoretical and experimental, to 1208 understand the effect of solute–wall interactions in complex 1209 geometries.

1210 **5.4.2. Co-Assembly of Gold Nanoparticles and Den-
1211 drimers.** An alternative approach to building functional 1212 membranes that leverage inorganic nanoparticles to confine 1213 flow involves the coassembly of gold nanoparticles (AuNP) 1214 and dendrimers. These membranes are prepared by immersing 1215 an amine-functionalized glass substrate in a solution of AuNPs 1216 functionalized with ammonium-terminated ligands, polydop- 1217 amine dendrimers, and carbon disulfide. As the dendrimers are 1218 cross-linked by carbon disulfide, the mixture precipitates onto 1219 the substrate and forms a selective coating layer (Figure 12). 1219 f12

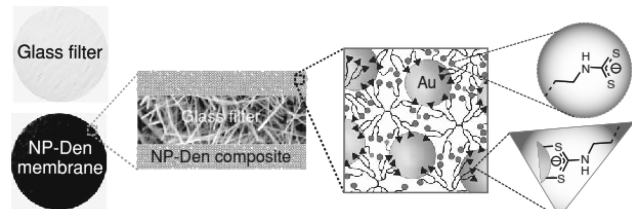


Figure 12. Schematic illustration of the fabrication and postfunctionalization of NP-Den composite membrane formed by dithiocarbamate cross-linking on a glass filter. Reproduced with permission from ref 246. Copyright 2012, John Wiley and Sons.

1220 The spaces between the AuNPs act as effective pores whose 1221 size can be altered by the dendrimer generation in the 7–12 1222 nm range, with lower generation dendrimers yielding smaller 1223 pores. Unreacted amine groups of the dendrimers can be 1224 further utilized for the functionalization of the membrane to 1225 create quaternary amine or carboxylate groups. These 1226 membranes exhibit modest charge-based selectivity between 1227 small organic molecules, likely because even the smallest pore 1228 size is quite large in comparison with small molecules.²⁴⁵ 1228

1229 **5.5. Polymer Self-Assembly To Create Charged
1230 Nanopores.** Polymer self-assembly is a promising approach 1231 for addressing some of the key manufacturing challenges 1232 described above for template methods and often simpler than 1233 the multistep manufacturing schemes required for small 1234 molecule and nanoparticle self-assembly. Polymer self- 1235 assembly has already been shown to enable the fabrication of 1236 highly porous membranes with narrow pore-size distributions, 1237 mostly investigated as size-selective membranes for aqueous 1238 filtration.^{56–58,74,75,81,83,247–249} Many of these self-assembled 1239 structures can be modified to address chemical structure-based 1240 separations by the incorporation of additional functionalities 1241 into their nanopores. By careful design of polymer chemistry 1242 and architecture, the final structure and functionality of 1243 membranes can be engineered to achieve separation selectivity 1244 that goes beyond size-screening.^{250,251} 1244

1245 **5.5.1. BCP Self-Assembly and SNIPS.** SNIPS, a highly 1245 scalable approach for creating isoporous UF membranes 1246

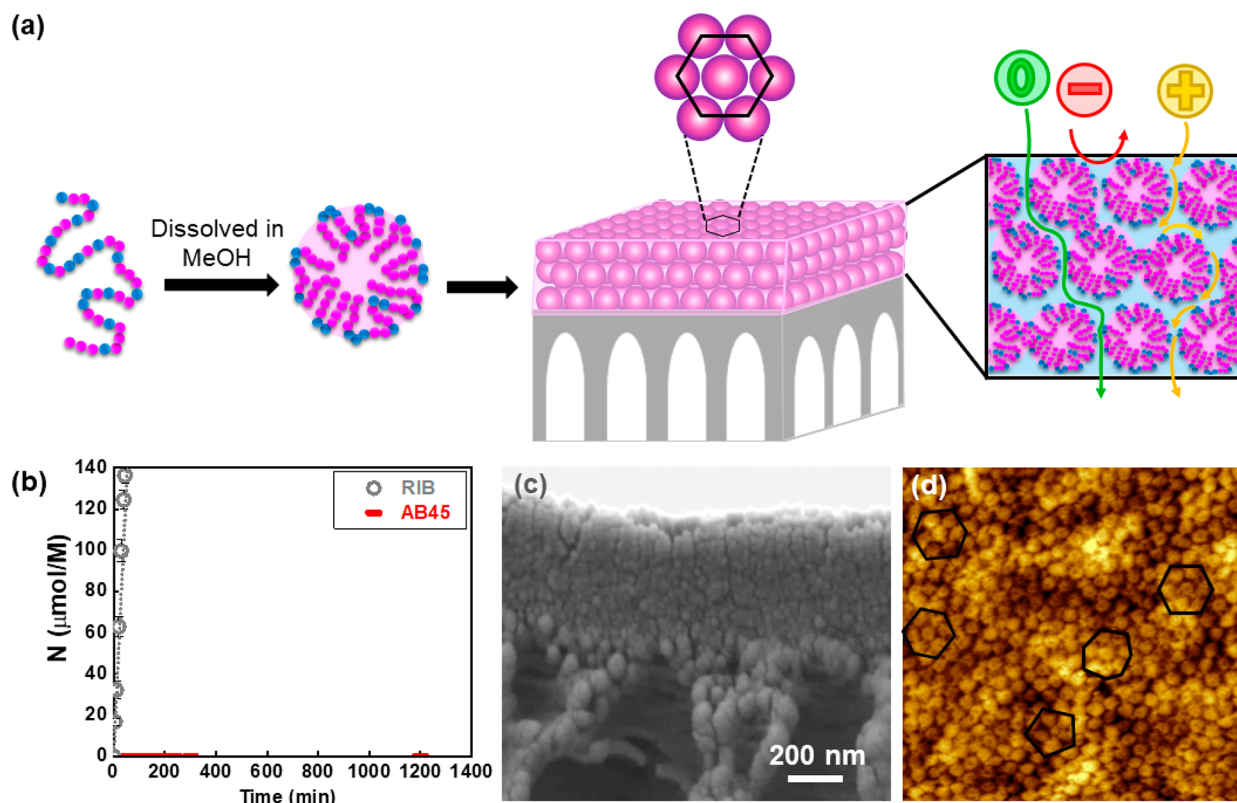


Figure 13. (a) Schematic illustration of the self-assembly of random copolymer micelles to create a packed array of polymer nanospheres, the interstices between which act as charged nanochannels 1–4 nm in diameter. (b) Permeation of neutral, riboflavin (RIB, gray) and anionic, acid blue 45 (AB45, red) through the membrane in competitive diffusion experiment, showing the complete blockage of anionic solute (N: moles of solute transferred normalized by feed concentration). (c) SEM cross-section and (d) AFM surface topography of the membrane, showing the packed micelle array. Reprinted with permission from ref 251. Copyright 2017 American Chemical Society.

1247 through BCP self-assembly, was described earlier (Figures 3).
 1248 This approach leads to membranes with evenly sized pores
 1249 typically in the 3–30 nm range, though some approaches can
 1250 further reduce this pore size. These membranes can be further
 1251 modified by tailoring the pore wall chemistry to impart
 1252 separation selectivity based on additional factors such as
 1253 charge. For example, isoporous membranes formed by SNIPS
 1254 using PS-*b*-P4VP have been further modified by the
 1255 quaternization of the P4VP block. This has led to the
 1256 formation of positively charged membranes that can effectively
 1257 separate proteins of similar size (bovine serum albumin and
 1258 globulin- γ) based on their charge with a selectivity of 87.²⁶ To
 1259 access a wider variety of pore wall chemistries, a triblock
 1260 terpolymer, polyisoprene-*b*-polystyrene-*b*-poly(*N,N*-dimethyl-
 1261 acrylamide) (PI-PS-PDMA), has been synthesized and
 1262 formed into membranes by SNIPS. The PDMA domains
 1263 lining the pore walls can be further converted to poly(acrylic
 1264 acid) by hydrolysis, yielding negatively charged pore walls⁵⁶
 1265 that can potentially be conjugated with a variety of moieties
 1266 using carbodiimide mediated coupling chemistry. Alternatively,
 1267 the addition of a very short functional (4 wt %), third block of
 1268 polypropylene sulfide to PS-*b*-P4VP can create covalent
 1269 binding sites for the functionalization of pore walls.²⁵²
 1270 Although these systems seem to have the potential to create
 1271 functional membranes with targeted selectivity, this has not yet
 1272 been studied in depth.

1273 **5.5.2. Microphase Separation of Comb-Shaped Copoly-
 1274 mers To Create Permeable Domains.** Copolymers with graft/
 1275 comb or random architectures can achieve smaller domain

1276 sizes than BCPs, potentially better enabling the separation of
 1277 small molecules. Often, these copolymers are initially designed
 1278 for size-based separation of organic compounds, as discussed in
 1279 an earlier section. An example of introducing new functionality
 1280 to such membranes utilizes self-assembling amphiphilic comb-
 1281 shaped copolymers with a polyacrylonitrile (PAN) backbone
 1282 and poly(ethylene glycol) (PEG) side-chains.⁷⁴ This copoly-
 1283 mer was synthesized by preparing a random copolymer of
 1284 acrylonitrile and PEG methacrylate, a macromonomer, and was
 1285 found to microphase separate to create \sim 1 nm bicontinuous
 1286 domains. The PEG-rich domains acted as effective nano-
 1287 channels for water permeation and enabled size-based
 1288 separation of organic dyes. To create charged nanochannels
 1289 using this system, a random terpolymer of acrylonitrile, PEG
 1290 methacrylate and glycidyl methacrylate (GMA), was synthe-
 1291 sized.⁷⁹ The terpolymer also microphase separates to form
 1292 PAN- and PEG-rich domains. The latter acts as effective pores
 1293 for water permeation. The reaction of GMA with a diamine
 1294 leads to the introduction of positively charged groups on the
 1295 pore walls. These functional groups can be further modified to
 1296 form negatively charged sulfonic acid groups. These membranes
 1297 exhibit salt rejection following Donnan exclusion theory.⁷⁹
 1298 Coarse-grain simulations of membrane performance under low
 1299 to moderate pressures and salt concentrations, showed that the
 1300 rejection of ions is largely governed by ion/pore wall
 1301 interactions. Ion selectivity can be further altered by
 1302 parameters such as charge density and spacer length of
 1303 moieties used to functionalize the membrane pore walls.²⁵³
 1304 Similar approaches to create functional nanochannels can likely

1305 be used with other copolymers that self-assemble to form
1306 interconnected pore networks.

1307 **5.5.3. Self-Assembly of Polymer Micelles.** Recently, we
1308 reported a simple and scalable method for manufacturing
1309 membranes with a thin selective layer consisting of a packed
1310 array of polymer nanospheres, creating a network of $\sim 1\text{--}3$ nm
1311 nanopores with carboxylate functional walls (Figure 13).²⁵¹
1312 This approach relies on the self-assembly of a random
1313 copolymer, poly(trifluoroethyl methacrylate-random-metha-
1314 crylic acid) (PTFEMA-*r*-PMAA), containing highly incompat-
1315 ible segments to spontaneously form ~ 20 nm micelles upon
1316 dissolving in methanol (Figure 13a).²⁵⁴ This solution is then
1317 coated onto a porous support, and after a brief evaporation
1318 time to direct the micelle self-assembly into a packed layer,
1319 immersed into water. The copolymer is insoluble in water, so
1320 this results in the quick precipitation of the micelles. Layer
1321 morphology is preserved due to the hydrophobicity and high
1322 glass transition temperature of the PTFEMA cores. The
1323 resultant membrane features a selective layer with a packed
1324 array of micelles (Figure 13c), arranged in a quasi-hexagonal
1325 close-packed array (Figure 13d). The interstices between the
1326 micelles serve as permeation pathways $\sim 1\text{--}4$ nm in diameter
1327 depending on micelle size, lined with carboxylate functional
1328 groups. In single solute permeation experiments, these
1329 membranes show a very high permeation selectivity of ~ 260
1330 between neutral and negatively charged molecules of similar
1331 size. In competitive diffusion experiments where both solutes
1332 are fed to the membrane simultaneously, the selectivity is
1333 enhanced further as the transport of the anionic molecules was
1334 completely blocked (Figure 13b). Similar trends were also
1335 observed in filtration experiments, where anionic solutes were
1336 rejected to a much higher degree than neutral ones of similar
1337 size. Unlike membranes prepared by template methods, these
1338 membranes also exhibited permeances comparable to
1339 commercial NF and tight UF membranes. This high degree
1340 of charge-based selectivity is likely the result of confining the
1341 flow into narrow channels, the high density of functional
1342 groups, and the tortuosity of the permeation pathway.
1343 Additionally, the carboxylic acid groups lining the pore walls
1344 can be used for functionalization through well-established
1345 conjugation chemistries for targeted separations. As such, this
1346 approach satisfies many key criteria for promising technologies
1347 for chemically selective membranes, including high flux, high
1348 selectivity, scalable manufacture, and functionalizability.

6. CHEMO-SELECTIVE MEMBRANES: SEPARATION OF 1349 ORGANIC MOLECULES BASED ON OTHER 1350 MOLECULAR CRITERIA

1351 Performing separations based on criteria other than solute size
1352 and charge is the true challenge for broadening the use of
1353 membranes to new applications. Only a relatively small
1354 number of studies have attempted to demonstrate selectivity
1355 between small organic molecules of similar size and charge;
1356 none have shown effective separation in a pressure-driven
1357 filtration system. Studies to date are all proof-of-concept
1358 demonstrations that focus on one molecular feature rather than
1359 separating solutes of commercial interest. Nonetheless, they
1360 demonstrate creative approaches that pave the way to the
1361 realization of such membranes by proposing new manufactur-
1362 ing schemes and exploring design features that yield the most
1363 promising results.

1364 **6.1. Hydrophobicity-Based Separations.** Hydrophobic
1365 interactions drive many important biological and colloidal self-

1366 assembly processes in water.^{255–257} For example, hydro-
1367 phobicity, quantified by total polar surface area (tPSA) of
1368 the molecule, has a strong influence on oral drug adsorption
1369 and its permeation through the small intestine and the blood-
1370 brain barrier.²⁵⁸ Many chemical reactions involve the
1371 introduction or removal of polar groups, differentiating
1372 reactants and products in terms of hydrophobicity. As such,
1373 developing membranes that can separate molecules based on
1374 their hydrophobicity is of interest. Some of the methods
1375 described above for preparing membranes with functional
1376 nanopores for charge-based separations have been modified to
1377 create membranes that can separate solutes of similar size and
1378 charge based on their hydrophobicity. All methods reported to
1379 date are template methods that result in membranes with 2–6
1380 nm cylindrical nanopores with a hydrophobic surface.
1381 Hydrophilic solutes are excluded from the pores, while
1382 hydrophobic molecules interact more strongly with the
1383 membrane, partition into the pores and permeate through
1384 faster.

1385 For example, electroless deposition of gold into the pores of
1386 TE or AAO membranes yield gold nanotubule membranes
1387 with nanopores down to ~ 1 nm in diameter that can be further
1388 functionalized through the formation of SAMs using functional
1389 thiols. This approach has been adapted to create membranes
1390 for separating small molecules based on their hydrophobicity
1391 by functionalizing the nanopores by the chemisorption of
1392 alkanethiols²⁵⁹ or perfluorinated thiols.¹⁸² Alkanethiol-modi-
1393 fied membranes showed 400 times faster permeation of
1394 toluene in comparison to pyridine in single solute diffusion
1395 experiments. The selectivity was decreased to 100 in a
1396 competitive diffusion experiment, still a very high selectivity
1397 and an excellent demonstration of the ability of this approach
1398 to create membranes with complex, customizable selectivity.
1399 The versatility of thiol chemistry allows the control of chemical
1400 interactions between solute and pore walls, so this method can
1401 also be expanded to other complex separations, as described
1402 below. Nonetheless, manufacturing issues and low porosity still
1403 limit the use of this approach for large scale separations.
1403

1404 An alternative approach for narrowing down AAO
1405 membrane pores involves atomic layer deposition (ALD) to
1406 create a thin, conformal coating layer within the pores. ALD
1407 involves sequential exposure of the AAO substrate to two
1408 precursors that react with each other, followed by purging to
1409 remove excess molecules. Membranes with hydrophobic pores
1410 have been fabricated by ALD of a thin silica (SiO_2) layer onto
1411 AAO membranes, followed by surface modification with a
1412 hydrophobic perfluorinated silane.¹⁸² This leads to membranes
1413 with a relatively low diffusion selectivity of 5.5 based on
1414 hydrophobicity. The brittleness of inorganic AAO substrates
1415 and the complex, high temperature coating process further
1416 limit the use of this approach for large scale manufacture of
1417 filtration membranes,¹⁷⁸ though ALD remains a promising
1418 approach for preparing gas separation and catalytic mem-
1419 branes.^{260–262}
1419

1420 Initiated chemical vapor deposition (iCVD) is an alternative
1421 method for narrowing down the pores of a TE membrane and
1422 controlling its surface chemistry. In this method, the TE
1423 membrane is placed on a chilled stage, in a reactor held at low
1424 vacuum. The monomer(s) and a thermally labile initiator are
1425 fed into the reactor as vapors. The initiator is decomposed by
1426 interaction with a hot filament and reacts with the monomer
1427 adsorbed on the surface. Pores can be narrowed down to about
1428 5 nm and coated with an additional polymer layer to control
1428

1429 pore functionality. Upon coating the pore walls with a
1430 fluorinated polymer, a diffusion selectivity of over 200 was
1431 achieved for two small, similarly sized organic molecules based
1432 on their hydrophobicity.¹⁷⁹ iCVD has better scale-up potential
1433 than ALD and electroless deposition, as it is a relatively shorter
1434 procedure and does not involve heating the template
1435 membrane to high temperatures. However, it still requires
1436 the use of a vacuum system and relatively long deposition
1437 times, particularly for achieving conformal coatings. These
1438 factors limit its use for large scale processing. Furthermore,
1439 functionalization is limited to only volatile monomers.

1440 Although these top-down approaches result in high
1441 separation selectivity, their large-scale application is limited
1442 due to the low porosity of resultant membranes and the
1443 difficulty of manufacturing procedures. Nonetheless, the high
1444 selectivities reported demonstrate the value of creating
1445 functional nanopores for separations based on hydrophobicity
1446 and other complex molecular features.

1447 **6.2. Enantioselective Membranes for Chiral Resolu-
1448 tion.** Many biochemicals are chiral, with each stereoisomer
1449 having different biological activity and toxicity. This makes the
1450 ability to separate stereoisomers of a chiral compound crucial
1451 in the production of pharmaceuticals, nutraceuticals, and
1452 agricultural chemicals.²⁶³ Conventional methods to obtain
1453 chiral resolution are crystallization, kinetic resolution (chem-
1454 ical/enzymatic catalysis) and chromatography.^{264,265} Enantio-
1455 selective membranes, which offer continuous and energy-
1456 efficient separation, can be fabricated either by intrinsically
1457 chiral polymers (e.g., peptides²⁶⁶ and polysaccharides includ-
1458 ing chitosan and sodium alginate²⁶⁷) or by immobilizing chiral
1459 selectors (e.g., cyclodextrins,²⁶⁸ proteins,²⁶⁹ DNA²⁷⁰) into the
1460 membrane. In this perspective, we focus on diffusion-
1461 enantioselective membranes, which preferentially transfer
1462 chiral isomer with higher affinity, as opposed to membranes
1463 that act as adsorbers to remove one enantiomer from the
1464 passing solution.²⁶³

1465 **6.2.1. Membranes Formed of Chiral Polymers.** One
1466 approach for preparing membranes with chiral selectivity
1467 involves forming a dense membrane selective layer from a
1468 chiral polymer. For example, hydrogel selective layers can be
1469 formed from water-soluble chiral polymers such as sodium
1470 alginate (SA) or chitosan (CS). These natural polymers can be
1471 solution cast onto a polyester film, dried and peeled off, and
1472 then immersed into an acetone solution containing gluta-
1473 raldehyde for cross-linking. A CS membrane prepared this way
1474 showed preferential transport of D- isomers of α -amino acids
1475 with an enantiomeric excess (ee; difference between the
1476 accumulated amount of D- and L- isomers in permeate) of up
1477 to 95% in pressure driven filtration experiments.²⁶⁷ These
1478 results imply that hydrogels with chiral groups may serve as
1479 effective membranes for enantioseparation even in the absence
1480 of complex nanostructures. However, most hydrogel mem-
1481 branes are relatively thick films with low flux. A major
1482 challenge is the scalable manufacture of TFC membranes with
1483 ultrathin hydrogel selective layers that would combine this
1484 selectivity with higher operating fluxes necessary for broader
1485 use. A recent method, Interfacially Initiated Free Radical
1486 Polymerization (IIFRP),²⁷¹ can potentially enable the
1487 formation of such membranes with high scalability and
1488 consistency. It can also potentially be adapted to integrate
1489 additional functionalities within the hydrogel selective layer,
1490 including but not limited to chiral selector moieties.

1491 **6.2.2. Membranes with Mobile Chiral Selector Moieties.** 1491
1492 Rather than forming a continuous selective layer, chiral 1492
1493 selectors can be trapped within membrane pores and serve 1493
1494 as carriers for facilitated transport. For example, apoenzyme, a 1494
1495 protein serving as a chiral selector, has been incorporated in 1495
1496 the nanopores of a TE membrane “plugged” by electro- 1496
1497 polymerized porous polypyrrole layers. The integration of 1497
1498 apoenzyme results in high enantioselectivity of up to 4.9 for a 1498
1499 chiral amino acid, phenylalanine, without causing irreversible 1499
1500 binding or unwanted chemical conversion of the solute.²⁶⁹ 1500
1501 While this approach still suffers from the low porosity inherent 1501
1502 to TE membranes and requires many manufacturing steps, it 1502
1503 also demonstrates the promise of creating a membrane with 1503
1504 mobile carriers for difficult separations. 1504

1505 **6.2.3. Nanopores Functionalized with Chiral Groups.** 1505
1506 Following the biomimetic approach inspired by porins and 1506
1507 other functional nanochannels, chiral moieties can be 1507
1508 integrated into nanopores to impart enantioselectivity to 1508
1509 membranes. Pores of UF membranes can be functionalized 1509
1510 with chiral groups using relatively simple methods, but the 1510
1511 short pore length and the large and polydisperse pore size 1511
1512 inherent to these membranes lead to low selectivity.^{272–274} 1512
1513 Instead, creating uniform, very small nanopores lined with 1513
1514 chiral functional groups is expected to yield higher selectivity. 1514
1515 This can be achieved utilizing methods described in earlier 1515
1516 sections, coupled with well-designed functionalization proce- 1516
1517 dures. For example, antibodies have been immobilized using 1517
1518 silane chemistry within the pores of AAO membranes to serve 1518
1519 as chiral selectors lining cylindrical nanopores.²⁷⁵ Antibodies 1519
1520 are known as the most specific molecular recognition proteins 1520
1521 due to their high binding constant. To chemically tune the 1521
1522 strength and reversibility of their interaction, dimethyl 1522
1523 sulfoxide was added to the racemic mixture of a chiral drug 1523
1524 fed to this membrane. A diffusion selectivity of 4.5 was 1524
1525 achieved in separating this mixture.²⁷⁶ In addition to other 1525
1526 limitations of templated approaches discussed earlier, these 1526
1527 membranes may not function well with complex feeds due to 1527
1528 the potential for nonspecific binding or protein degradation. 1528
1529 Nonetheless, this is one of the highest selectivities reported for 1529
1530 chiral resolution by a membrane. 1530

1531 In addition to templated nanotubes, colloidal silica NP opal 1531
1532 layers can also be functionalized to incorporate chiral selectors 1532
1533 by silane chemistry or to graft chiral polymer brushes that 1533
1534 partially fill the pores by surface-initiated ATRP (Figure 14). 1534 f14
1535 Similar to the studies on charge-based selectivity, most of this 1535
1536 work focused on opal layers covering electrodes as opposed to 1536
1537 free-standing membranes. By attaching chiral selectors such as 1537
1538 enantiopure molecules²⁷⁷ or thiocalixarene moieties²⁷⁸ and 1538
1539 controlling solvent polarity, permeation selectivities that range 1539
1540 between 2 and 4.5 can be achieved between optical isomers.²⁷⁹ 1540
1541 While grafting polymer brushes with chiral selector moieties 1541
1542 (e.g., polypeptides) onto the silica spheres can increase the 1542
1543 density of chiral binding sites within the pores, it would also 1543
1544 narrow them down. Films with grafted chiral polymers 1544
1545 exhibited comparable selectivities to those modified with a 1545
1546 chiral selector molecule, possibly because most of the chiral 1546
1547 sites on the grafted polymers were not accessible due to pore 1547
1548 narrowing.²⁸⁰ When thicker opal films were sintered to create 1548
1549 free-standing membranes, lower enantioselectivity was ob- 1549
1550 served due to the loss of functionalizable groups lining the 1550
1551 pores.²⁷⁸ Although films fabricated by self-assembled of silica 1551
1552 offer high chiral selectivity, making them into membranes 1552

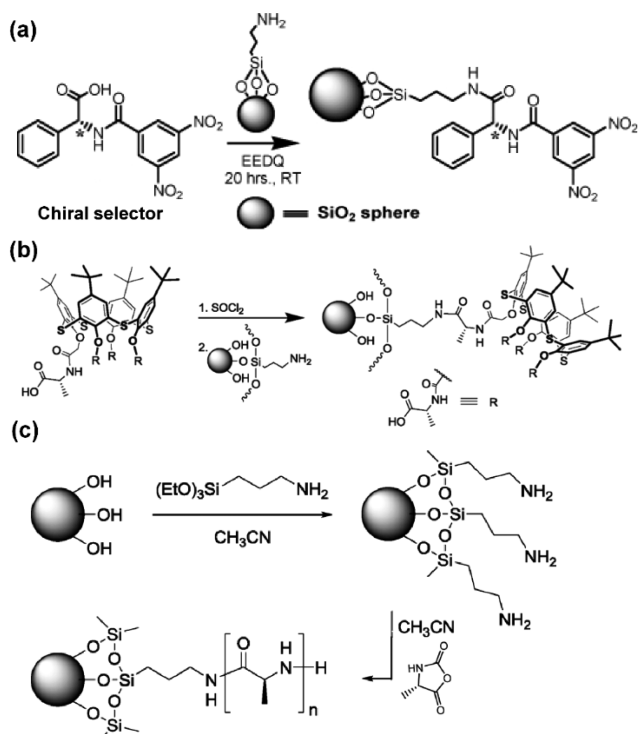


Figure 14. Modification of silica spheres by (a) immobilization of chiral selector moieties on the surface of spheres, (b) immobilization of chiral thiocalixarene, and (c) grafting poly(L-alanine) on the surface of silica spheres by surface-initiated ring-opening polymerization. Reprinted with permission from ref 278. Copyright 2014, John Wiley and Sons.

LBL deposition, and drop-casting.²⁸³ GO sheets contain 1561 oxygen containing functional groups (e.g., hydroxyl, epoxy, 1562 carbonyl, carboxyl) that offer potential for further functional- 1563 ization.²⁸⁴ To create enantioselective membranes, GO sheets 1564 were modified with chiral glutamic acid by carbodiimide 1565 chemistry. Membranes were then fabricated by the deposition 1566 of modified GO sheets onto a cellulose acetate (CA) or AAO 1567 support membrane by filtration, followed by the removal of 1568 water by storing in vacuum. These membranes exhibited lower 1569 rejection of dihydroxy-D-phenylalanine (D-DOPA) compared 1570 with the L-isomer in filtration experiments.²⁸⁵ To date, GO- 1571 based membranes have mostly been studied in size sieving, 1572 desalination, and gas-separation applications.²⁸⁴ GO-based 1573 membranes are at a relatively early stage of development and 1574 currently suffer from limited stability. Cross-linking the layer 1575 may help in improving stability but results in loss of functional 1576 groups. Nonetheless, the presence of very narrow permeation 1577 pathways and functionalizable pore entrances may enable the 1578 development of more selective membranes.¹⁵⁷⁹

6.3. Other Interactions. Although electrostatic-, hydro- 1580 phobic-, or stereospecific interactions have been utilized as the 1581 main separation mechanisms to date, other noncovalent 1582 interactions such as hydrogen bonding and $\pi-\pi$ interactions 1583 also affect membrane permeation selectivity.^{145,238,250,279,286,287} 1584 The same is also true for biological pores. For example, 1585 computational studies show that cation- π interactions play a 1586 key role in ion selectivity in potassium channels,²⁸⁷ along with 1587 electrostatic interactions.¹⁵⁰ Indeed, while researchers seek to 1588 focus on a particular, easily predicted interaction mechanism 1589 for designing separation membranes, solute-membrane 1590 interactions are complex, a sum of various forces affected not 1591 only by the pore and solute chemistry but also by the 1592 environment (e.g., solvent polarity) and nanoconfinement. As 1593 such, a better, more predictive understanding of these 1594 noncovalent interactions is needed to enable the rational 1595 design of new membranes with controlled selectivity.²⁷⁹¹⁵⁹⁶

Nonetheless, many studies including those listed above show 1597 that combining nanoscale confinement with specific solute- 1598 pore wall interactions is the biomimetic key to developing 1599 membranes featuring chemical-based selectivity. This phenom- 1600

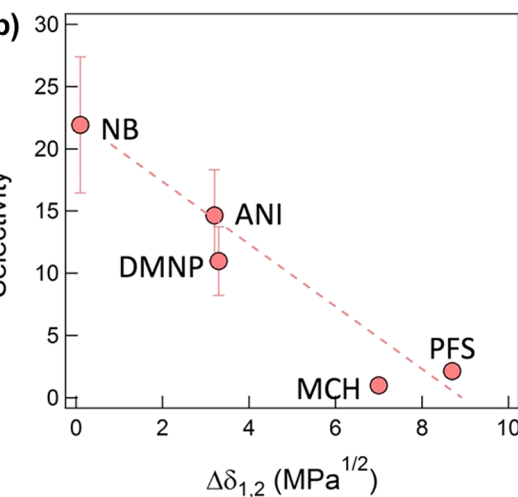


Figure 15. Permeation selectivity for small organic molecules, nitrobenzene (NB), methylcyclohexane (MCH), 4-methylphenol (MP), anisole (ANI), pentafluorostyrene (PFS), and dimethoxy naphthalene (DMNP), vs (a) molecular volume and (b) solubility parameter difference between solutes and PEGPEA, $\Delta\delta_{1,2}$, showing strong correlation between the membrane selectivity and solubility parameter difference. Reprinted with permission from ref 250. Copyright 2015 American Chemical Society.

1601 enon is demonstrated in a recent study comparing permeation
1602 in a homogeneous polymer membrane with permeation in
1603 confined, polymer-filled \sim 1 nm nanochannels, formed by the
1604 self-assembly of a comb-shaped copolymer (Figure 15).
1605 Permeation rates of organic molecules in isopropanol through
1606 a homogeneous, cross-linked film of poly(ethylene glycol
1607 phenyl ether acrylate) (PEGPEA) were directly correlated with
1608 solute size, indicating diffusivity-based selectivity (Figure 15a).
1609 The comb copolymer had a polyvinylidene fluoride (PVDF)
1610 backbone and PEGPEA side chains that microphase separated
1611 to form bicontinuous 1–3 nm nanodomains.²⁵⁰ Only PEGPEA
1612 was swollen in the solvent, isopropanol, thus confining
1613 permeation to only these domains. Interestingly, the
1614 permeation rates of different solutes were poorly correlated
1615 with size or polarity. Instead, they exhibited a strong
1616 correlation with the affinity of solutes to PEGPEA, quantified
1617 by solubility parameter differences (Figure 15b). The
1618 membrane showed a permeation selectivity of \sim 20 for small
1619 molecules of similar size. This study highlights the ability of
1620 nanoconfinement to emphasize solute–membrane interactions
1621 over size differences, significantly altering the basis of
1622 selectivity. It also shows that selectivity is driven by global
1623 measures of solute/membrane affinity as opposed to a single
1624 type of interaction (e.g., polarity, hydrogen bonding).

7. FUTURE OUTLOOK

1625 This perspective describes several approaches to creating
1626 membranes with improved, often more complex, selectivity.
1627 Many of these approaches are inspired, implicitly or explicitly,
1628 by biological systems that achieve extremely high selectivities
1629 while maintaining high permeability. This weaves a common
1630 thread among most of these successful approaches: creating
1631 nanoscale structures with controlled pore chemistry. The
1632 synthetic systems described here are not exact mimics of the
1633 highly complex biological pores with exquisite spatial control
1634 of chemical functionalities, so they do not have the same
1635 degree of selectivity and permeability of biological pores.
1636 Nonetheless, these studies are at the forefront of advanced
1637 materials that synergistically control nanoscale morphology
1638 and chemical features for an application with great potential
1639 impact in chemical, petrochemical, and pharmaceutical
1640 manufacturing. They represent innovative approaches to
1641 membrane manufacture that can overcome the limitations of
1642 existing membrane materials by utilizing modern techniques in
1643 chemistry, materials science, self-assembly, surface engineering,
1644 and biochemistry.

1645 A major challenge in the realization of these novel
1646 membrane materials for large scale use is the development of
1647 simple, scalable, and reproducible manufacturing methods that
1648 lead to highly controlled nanostructures and surface chem-
1649 istics. Many of the approaches described involve very
1650 complex, multistep manufacturing schemes. Several of them
1651 involve techniques that are well-established in lab settings yet
1652 hard to apply in the large-scale, continuous, roll-to-roll
1653 manufacturing lines used in membrane manufacture. Some of
1654 the most promising approaches also use raw materials that are,
1655 at least currently, difficult to acquire affordably in large enough
1656 quantities for scale-up. An important research and develop-
1657 ment need is the adaptation of successful approaches that show
1658 promise to improve scalability. These developments will be
1659 driven by innovations in large-scale, reliable manufacturing of
1660 nanoscale structures. We believe that soft matter self-assembly
1661 in particular will be a crucial tool in creating the functional

1662 nanostructures featured in this review. This is demonstrated by
1663 the ongoing commercialization efforts, focused heavily on
1664 technologies that feature self-assembly as part of the
1665 manufacturing scheme. For example, the manufacture of
1666 isoporous membranes prepared by SNIPS, which explicitly
1667 utilizes BCP self-assembly to create membranes with tightly
1668 controlled pore size and functionalizable pore chemistry, has
1669 been demonstrated in roll-to-roll and hollow fiber pilot
1670 systems.^{57,288,289} The scalability of the SNIPS process has led
1671 to ongoing commercialization efforts, including two start-up
1672 companies, Anfiro and Terapore, who are seeking to address
1673 challenges in water treatment and bioseparations, respectively.
1674 Self-assembly has been used to create aligned CNT
1675 membranes in both small and large scale. Mattershift, another
1676 start-up, is seeking to commercialize this approach. Isoporous,
1677 fouling resistant membranes formed by the self-assembly of
1678 zwitterionic random copolymers are currently being developed
1679 by another start-up, ZwitterCo. Each of these companies
1680 focuses on membranes that utilize advanced materials and soft
1681 matter self-assembly to overcome challenges yet rely on
1682 manufacturing methods that are well-established for roll-to-roll
1683 membrane manufacture such as coating or NIPS.
1683

1684 While a large portion of this perspective focuses on size- and
1685 charge-based separations, likely the biggest challenge remains
1686 the development of membranes that can separate organic
1687 molecules of similar size and charge but different chemical
1688 structure. To date, the studies in the literature are generally
1689 proof-of-concept demonstrations that show the ability to
1690 separate probe molecules based on a specific chemical feature
1691 (e.g., hydrophobicity). These are not true separation
1692 challenges faced by the chemical or pharmaceutical manu-
1693 facturing industries. Most pharmaceutical manufacturing
1694 processes are proprietary, and many are designed during the
1695 scale-up stage based on the capabilities of existing separation
1696 processes. Industry/academia partnerships can direct separa-
1697 tions research toward true industry challenges and lead to
1698 more impactful research.
1698

1699 Furthermore, it is rare to find realistic separation challenges
1700 that involve mixtures differentiated by only one prominent
1701 chemical feature. As membranes are developed with the goal of
1702 controlling chemical structure-based selectivity, solute–pore
1703 interactions need to be considered holistically. The membrane
1704 needs to be designed to control solute–pore wall interactions
1705 as a whole so as to impart selectivity. This requires
1706 fundamental studies that can enable the prediction and
1707 measurement of solute–surface interactions. Simulations and
1708 theoretical studies can provide key insights to the interaction of
1709 solutes with functional surfaces. Characterization techniques
1710 such as quartz crystal microbalance with dissipation, QCM-D,
1711 can provide important information on solute adsorption and
1712 desorption that can inform membrane design as well as our
1713 understanding of selectivity and transport mechanisms.
1713

1714 A significant need is the development of membrane models,
1715 both physical and theoretical, to understand the effect of
1716 nanoconfinement on transport. While many systems have been
1717 developed to create membranes with functional nanopores,
1718 fundamental studies of the effect of key parameters (pore size,
1719 interaction strength, reversibility of binding) on transport rate
1720 and selectivity are limited. This in part arises from challenges
1721 in measuring these key quantities. For example, it is very
1722 difficult to accurately determine pore sizes that are small
1723 enough to control small molecule separations, particularly in
1724 the wet state. The same is true for the measurement of
1724

1725 functional group densities within pores. Another challenge is
1726 the lack of detailed theoretical models that account for
1727 nanoconfinement, pore/solute interactions, tortuosity and
1728 interconnectedness of pores, and other features of real
1729 membranes designed for chemical separations. The solution-
1730 diffusion and pore-flow models do not explicitly account for
1731 these parameters. A handful of simple models have recently
1732 shone light on some of these effects and shown some
1733 significant features of biological and biomimetic pores.^{244,253}
1734 Such models will not only enhance our fundamental
1735 understanding of ion channels but also enable the rational
1736 design and engineering of functional membranes.

1737 In short, a key to the broader use of membranes in chemical,
1738 pharmaceutical, and petrochemical manufacturing is the
1739 development of membranes with controlled selectivity. This
1740 requires the design of membranes with highly controlled
1741 nanostructures and surface chemistries. Isoporous membranes
1742 with homogeneous pore size can not only serve as better size-
1743 selective filters but also serve as scaffolds for creating functional
1744 nanopores that enable complex separations. Membranes
1745 designed for charge-based separations are useful not only for
1746 purifying biochemicals but also for the creation of structures
1747 that mimic ion channels that can be further modified to adapt
1748 their selectivity. Membranes that separate based on criteria
1749 other than size and charge must operate on the basis of novel
1750 transport mechanisms that leverage membrane–solute inter-
1751 actions to differentiate between solutes. This requires the
1752 development of membranes that utilize state-of-the-art
1753 materials science. This burgeoning research area promises to
1754 transform chemical and pharmaceutical manufacturing if
1755 membranes with sufficient selectivity and flux can be
1756 manufactured through scalable methods, and highly custom-
1757 izable membrane systems enable the design of membranes
1758 targeted at each challenging separation. Insights gained from
1759 these membranes impact not only filters but also sensors, drug
1760 delivery, electrochemical systems, and other technologies
1761 where solute transport is crucial to performance.

1762 ■ AUTHOR INFORMATION

1763 Corresponding Author

1764 *(A.) E-mail: ayse.asatekin@tufts.edu.

1765 ORCID 

1766 Ilin Sadeghi: [0000-0002-3451-0709](https://orcid.org/0000-0002-3451-0709)

1767 Papatya Kaner: [0000-0002-6770-653X](https://orcid.org/0000-0002-6770-653X)

1768 Ayse Asatekin: [0000-0002-4704-1542](https://orcid.org/0000-0002-4704-1542)

1769 Notes

1770 The authors declare no competing financial interest.

1771 Biographies

1772 Dr. Ilin Sadeghi received her Bachelor's and Master's degrees in
1773 Chemical Engineering from Tehran Polytechnic (Amirkabir Uni-
1774 versity), Iran, in 2010 and 2012, respectively. During her Master's
1775 studies, she developed a new membrane surface modification
1776 technique, corona air plasma, to improve membrane fouling resistance
1777 for oil/water separation. She earned her Ph.D. in the Chemical and
1778 Biological Engineering Department at Tufts University in Prof.
1779 Asatekin's lab. During her PhD, she worked on novel approaches for
1780 manufacturing membranes with controlled selectivity. She developed
1781 chemoselective membranes for separation of small organic molecules
1782 by self-assembly of random copolymer micelles. Furthermore, she
1783 developed a new method for manufacturing ultrathin, multifunctional
1784 hydrogel selective layers. She also worked on superoleophilic

1785 electrospun membranes for oil/water separation by designing a
1786 surface-segregating copolymer.

1787 Dr. Papatya Kaner has received her Ph.D. in Chemical Engineering
1788 from Tufts University. She obtained her B.Sc. in Chemical
1789 Engineering from Istanbul Technical University (ITU), Turkey, in
1790 2009 and her M.Sc. in Chemical Engineering from Florida State
1791 University in 2012. Her M.Sc. studies focused on fundamental
1792 structure–property relationships that correlate polymer chemistry and
1793 architecture with polymer crystallization. She conducted her Ph.D.
1794 studies under the supervision of Prof. Ayse Asatekin. During her
1795 Ph.D., she developed stimuli-responsive and fouling resistant water
1796 filtration membranes by using custom-designed zwitterionic copoly-
1797 mers. In addition, she implemented comb-shaped, self-assembling
1798 zwitterionic copolymers to develop porous thin films with nanoscale,
1799 hierarchical morphology, and tunable pore size.

1800 Ayse Asatekin received B.S. degrees in Chemical Engineering and
1801 Chemistry from the Middle East Technical University (METU) in
1802 Turkey. She completed her Ph.D. in Chemical Engineering at
1803 Massachusetts Institute of Technology through the Program in
1804 Polymer Science and Technology, working on developing new fouling
1805 resistant membrane materials under Anne M. Mayes and Michael F.
1806 Rubner. She is a cofounder of Clean Membranes, Inc., a start-up
1807 initiated to commercialize this work. She completed her postdoctoral
1808 training with Karen K. Gleason at MIT and worked at Clean
1809 Membranes between 2011–2012. She is currently an assistant
1810 professor at Tufts University's Department of Chemical and
1811 Biological Engineering, where she leads a research group focused on
1812 utilizing polymer self-assembly for novel membrane materials for
1813 highly selective separations as well as water treatment. Her research
1814 interests also include surface engineering, multifunctional and
1815 responsive materials, polymer science, and energy storage.

1816 ■ ACKNOWLEDGMENTS

1817 We gratefully acknowledge financial support from Tufts
1818 University and the National Science Foundation (NSF)
1819 under Grant Nos. CBET-1703549 and CBET-1553661.

1820 ■ REFERENCES

- (1) Sholl, D. S.; Lively, R. P. Seven chemical separations to change the world. *Nature* **2016**, *532*, 435–437.
- (2) Cussler, E. L.; Dutta, B. K. On separation efficiency. *AIChE J.* **2012**, *58*, 3825–3831.
- (3) National Academy of Sciences. *Real Prospects for Energy Efficiency in the United States*; The National Academies Press: Washington, DC, 2010.
- (4) Werber, J. R.; Deshmukh, A.; Elimelech, M. The Critical Need for Increased Selectivity, Not Increased Water Permeability, for Desalination Membranes. *Environ. Sci. Technol. Lett.* **2016**, *3*, 112–120.
- (5) Koros, W. J.; Ma, Y. H.; Shimidzu, T. Terminology for membranes and membrane processes. *Pure Appl. Chem.* **1996**, *68*, 1479–1489.
- (6) Baker, R. W. *Membrane technology and applications*, 2nd ed.; J. Wiley: Chichester, New York, 2004.
- (7) Mehta, A.; Zydny, A. L. Permeability and selectivity analysis for ultrafiltration membranes. *J. Membr. Sci.* **2005**, *249*, 245–249.
- (8) Loeb, S.; Sourirajan, S. Sea Water Demineralization by Means of an Osmotic Membrane. *Saline Water Conversion—IIACS*; Advances in Chemistry Series; American Chemical Society: Washington, DC, 1963; Vol. 38.
- (9) Cadotte, J. E. Reverse osmosis membrane. U.S. Patent 3,926,798, December 1975.
- (10) Petersen, R. J. Composite Reverse-Osmosis and Nanofiltration Membranes. *J. Membr. Sci.* **1993**, *83*, 81–150.

1847 (11) Geise, G. M.; Park, H. B.; Sagle, A. C.; Freeman, B. D.;
1848 McGrath, J. E. Water permeability and water/salt selectivity tradeoff
1849 in polymers for desalination. *J. Membr. Sci.* **2011**, *369*, 130–138.

1850 (12) Bowen, W. R.; Welfoot, J. S. Modelling of membrane
1851 nanofiltration - pore size distribution effects. *Chem. Eng. Sci.* **2002**,
1852 *57*, 1393–1407.

1853 (13) Vandezande, P.; Gevers, L. E. M.; Vankelecom, I. F. J. Solvent
1854 resistant nanofiltration: separating on a molecular level. *Chem. Soc.*
1855 *Rev.* **2008**, *37*, 365–405.

1856 (14) Jue, M. L.; Koh, D. Y.; McCool, B. A.; Lively, R. P. Enabling
1857 Widespread Use of Microporous Materials for Challenging Organic
1858 Solvent Separations. *Chem. Mater.* **2017**, *29*, 9863–9876.

1859 (15) Sukma, F. M.; Culfaz-Emecen, P. Z. Cellulose membranes for
1860 organic solvent nanofiltration. *J. Membr. Sci.* **2018**, *545*, 329–336.

1861 (16) Marchetti, P.; Jimenez Solomon, M. F.; Szekely, G.; Livingston,
1862 A. G. Molecular Separation with Organic Solvent Nanofiltration: A
1863 Critical Review. *Chem. Rev.* **2014**, *114*, 10735–10806.

1864 (17) Priske, M.; Lazar, M.; Schnitzer, C.; Baumgarten, G. Recent
1865 Applications of Organic Solvent Nanofiltration. *Chem. Ing. Tech.*
1866 **2016**, *88*, 39–49.

1867 (18) Park, H. B.; Kamcev, J.; Robeson, L. M.; Elimelech, M.;
1868 Freeman, B. D. Maximizing the right stuff: The trade-off between
1869 membrane permeability and selectivity. *Science* **2017**, *356*, eaab0530.

1870 (19) Robeson, L. M. Correlation of Separation Factor Versus
1871 Permeability for Polymeric Membranes. *J. Membr. Sci.* **1991**, *62*, 165–
1872 185.

1873 (20) Zhang, H.; Geise, G. M. Modeling the water permeability and
1874 water/salt selectivity tradeoff in polymer membranes. *J. Membr. Sci.*
1875 **2016**, *520*, 790–800.

1876 (21) Robeson, L. M.; Hwu, H. H.; McGrath, J. E. Upper bound
1877 relationship for proton exchange membranes: Empirical relationship
1878 and relevance of phase separated blends. *J. Membr. Sci.* **2007**, *302*,
1879 70–77.

1880 (22) Abetz, V. Isoporous Block Copolymer Membranes. *Macromol.*
1881 *Rapid Commun.* **2015**, *36*, 10–22.

1882 (23) Lalia, B. S.; Kochkodan, V.; Hashaikeh, R.; Hilal, N. A Review
1883 on Membrane Fabrication: Structure, Properties and Performance
1884 Relationship. *Desalination* **2013**, *326*, 77–95.

1885 (24) Yang, S. Y.; Ryu, I.; Kim, H. Y.; Kim, J. K.; Jang, S. K.; Russell,
1886 T. P. Nanoporous Membranes with Ultrahigh Selectivity and Flux for
1887 the Filtration of Viruses. *Adv. Mater.* **2006**, *18*, 709–712.

1888 (25) Yang, S. Y.; Park, J.; Yoon, J.; Ree, M.; Jang, S. K.; Kim, J. K.
1889 Virus Filtration Membranes Prepared From Nanoporous Block
1890 Copolymers with Good Dimensional Stability under High Pressures
1891 and Excellent Solvent Resistance. *Adv. Funct. Mater.* **2008**, *18*, 1371–
1892 1377.

1893 (26) Qiu, X.; Yu, H.; Karunakaran, M.; Pradeep, N.; Nunes, S. P.;
1894 Peinemann, K. Selective Separation of Similarly Sized Proteins with
1895 Tunable Nanoporous Block Copolymer Membranes. *ACS Nano* **2013**,
1896 *7*, 768–776.

1897 (27) Chun, K.-Y.; Stroeve, P. Protein Transport in Nanoporous
1898 Membranes Modified with Self-Assembled Monolayers of Function-
1899 alized Thiols. *Langmuir* **2002**, *18*, 4653–4658.

1900 (28) Shah, T. N.; Foley, H. C.; Zydny, A. L. Development and
1901 Characterization of Nanoporous Carbon Membranes for Protein
1902 Ultrafiltration. *J. Membr. Sci.* **2007**, *295*, 40–49.

1903 (29) Ulbricht, M. Advanced Functional Polymer Membranes.
1904 *Polymer* **2006**, *47*, 2217–2262.

1905 (30) Lee, W.; Ji, R.; Gosele, U.; Nielsch, K. Fast fabrication of long-
1906 range ordered porous alumina membranes by hard anodization. *Nat.*
1907 *Mater.* **2006**, *5*, 741–747.

1908 (31) Li, M.; Douki, K.; Goto, K.; Li, X.; Coenjarts, C.; Smilgies, D.
1909 M.; Ober, C. K. Spatially Controlled Fabrication of Nanoporous
1910 Block Copolymers. *Chem. Mater.* **2004**, *16*, 3800–3808.

1911 (32) Werber, J. R.; Osuji, C. O.; Elimelech, M. Materials for Next-
1912 Generation Desalination and Water Purification Membranes. *Nat.*
1913 *Rev. Mater.* **2016**, *1*, 16018.

1914 (33) Han, K. P.; Xu, W. D.; Ruiz, A.; Ruchhoeft, P.; Chellam, S.
1915 Fabrication and characterization of polymeric microfiltration mem-
branes using aperture array lithography. *J. Membr. Sci.* **2005**, *249*, 1916
1917 193–206.

1918 (34) van Rijn, C. J. M.; Nijdam, W.; Kuiper, S.; Veldhuis, G. J.; van
1919 Wolferen, H.; Elwenspoek, M. Microsieves made with laser
1920 interference lithography for micro-filtration applications. *J. Micromech.*
1921 *Microeng.* **1999**, *9*, 170–172.

1922 (35) Korolkov, I.; Mashentseva, A.; Güven, O.; Gorin, Y.; Zdrovets, M.
1923 Protein Fouling of Modified Microporous PET track-etched
membranes. *Radiat. Phys. Chem.* **2018**, *151*, 141–148.

1924 (36) Whitesides, G. M.; Grzybowski, B. Self-assembly at all scales.
1925 *Science* **2002**, *295*, 2418–2421.

1926 (37) Kaner, P.; Bengani-Lutz, P.; Sadeghi, I.; Asatekin, A. Responsive
1927 filtration membranes by polymer self-assembly. *Technol.*
1928 **2016**, *4*, 217–228.

1929 (38) Asatekin, A.; Vannucci, C. Self-Assembled Polymer Nanostruc-
1930 tures for Liquid Filtration Membranes: A Review. *Nanosci. Nano-*
1931 *technol. Lett.* **2015**, *7*, 21–32.

1932 (39) Beveridge, T. J. Bacterial S-layers. *Curr. Opin. Struct. Biol.* **1994**,
1933 *4*, 204–212.

1934 (40) Beveridge, T. J.; Koval, S. F. *Advances in Bacterial Paracrystalline*
1935 *Surface Layers*; Plenum Press: New York, 1993.

1936 (41) Messner, P.; Sleytr, U. B. Crystalline bacterial cell-surface
1937 layers. *Adv. Microb. Physiol.* **1992**, *33*, 213–275.

1938 (42) Sleytr, U. B.; Messner, P.; Pum, D.; Sára, M. *Crystalline bacterial*
1939 *cell surface layers*; Springer: Berlin, Heidelberg, 2012.

1940 (43) Hovmöller, S.; Sjögren, A.; Wang, D. N. The Three-
1941 Dimensional Structure of Bacterial Surface Layers. In *Crystalline*
1942 *Bacterial Cell Surface Layers*; Sleytr, U. B., Messner, P., Pum, D., Sara, 1943
M., Eds.; Springer: Berlin, Heidelberg, 1988; Vol. 6, pp 60–64.

1944 (44) Hovmöller, S.; Sjögren, A.; Wang, D. N. The Structure of
1945 Crystalline Bacterial Surface Layers. *Prog. Biophys. Mol. Biol.* **1988**, *51*,
1946 131–163.

1947 (45) Sára, M.; Sleytr, U. B. Production and Characteristics of
1948 Ultrafiltration Membranes with Uniform Pores from Two-Dimen-
1949 sional Arrays of Proteins. *J. Membr. Sci.* **1987**, *33*, 27–49.

1950 (46) Küpcü, S.; Sára, M.; Sleytr, U. B. Chemical Modification of
1951 Crystalline Ultrafiltration Membranes and Immobilization of Macro-
1952 molecules. *J. Membr. Sci.* **1991**, *61*, 167–175.

1953 (47) Nunes, S. P.; Car, A. From Charge-Mosaic to Micelle Self-
1954 Assembly: Block Copolymer Membranes in the Last 40 Years. *Ind.*
1955 *Eng. Chem. Res.* **2013**, *52*, 993–1003.

1956 (48) Schacher, F. H.; Rupar, P. A.; Manners, I. Functional block
1957 copolymers: nanostructured materials with emerging applications.
1958 *Angew. Chem., Int. Ed.* **2012**, *51*, 7898–7921.

1959 (49) Park, C.; Yoon, J.; Thomas, E. L. Enabling nanotechnology with
1960 self assembled block copolymer patterns. *Polymer* **2003**, *44*, 6725–
1961 6760.

1962 (50) Rao, J.; De, S.; Khan, A. Synthesis and Self-Assembly of
1963 Dynamic Covalent Block Copolymers: Towards a General Route to
1964 Pore-Functionalized Membranes. *Chem. Commun.* **2012**, *48*, 3427–
1965 3429.

1966 (51) Bolton, J.; Bailey, T. S.; Rzayev, J. Large Pore Size Nanoporous
1967 Materials from the Self-Assembly of Asymmetric Bottlebrush Block
1968 Copolymers. *Nano Lett.* **2011**, *11*, 998–1001.

1969 (52) Jeong, U.; Ryu, D. Y.; Kim, J. K.; Kim, D. H.; Wu, X.; Russell,
1970 T. P. Precise Control of Nanopore Size in Thin Film Using Mixtures
1971 of Asymmetric Block Copolymer and Homopolymer. *Macromolecules*
1972 **2003**, *36*, 10126–10129.

1973 (53) Yu, H.; Qiu, X.; Nunes, S. P.; Peinemann, K. V. Self-Assembled
1974 Isoporous Block Copolymer Membranes with Tuned Pore Sizes.
1975 *Angew. Chem., Int. Ed.* **2014**, *53*, 10072–10076.

1976 (54) Gu, Y.; Wiesner, U. Tailoring Pore Size of Graded Mesoporous
1977 Block Copolymer Membranes: Moving from Ultrafiltration toward
1978 Nanofiltration. *Macromolecules* **2015**, *48*, 6153–6159.

1979 (55) Peinemann, K.-V.; Abetz, V.; Simon, P. F. Asymmetric
1980 Superstructure Formed in a Block Copolymer via Phase Separation.
1981 *Nat. Mater.* **2007**, *6*, 992.

1982 (56) Mulvenna, R. A.; Weidman, J. L.; Jing, B. X.; Pople, J. A.; Zhu,
1983 Y. X.; Boudouris, B. W.; Phillip, W. A. Tunable nanoporous
1984

1985 membranes with chemically-tailored pore walls from triblock polymer 1986 templates. *J. Membr. Sci.* **2014**, *470*, 246–256.

1987 (57) Zhang, Y. Z.; Sargent, J. L.; Boudouris, B. W.; Phillip, W. A. 1988 Nanoporous membranes generated from self-assembled block 1989 polymer precursors: Quo Vadis? *J. Appl. Polym. Sci.* **2015**, *132*, 41683.

1990 (58) Nunes, S. P. Block Copolymer Membranes for Aqueous 1991 Solution Applications. *Macromolecules* **2016**, *49*, 2905–2916.

1992 (59) Nunes, S. P.; Sougrat, R.; Hooghan, B.; Anjum, D. H.; Behzad, 1993 A. R.; Zhao, L.; Pradeep, N.; Pinnau, I.; Vainio, U.; Peinemann, K.-V. 1994 Ultraporous films with uniform nanochannels by block copolymer 1995 micelles assembly. *Macromolecules* **2010**, *43*, 8079–8085.

1996 (60) Nunes, S. P.; Karunakaran, M.; Pradeep, N.; Behzad, A. R.; 1997 Hooghan, B.; Sougrat, R.; He, H.; Peinemann, K.-V. From Micelle 1998 Supramolecular Assemblies in Selective Solvents to Isoporous 1999 Membranes. *Langmuir* **2011**, *27*, 10184–10190.

2000 (61) Marques, D. S.; Vainio, U.; Chaparro, N. M.; Calo, V. M.; 2001 Bezahd, A. R.; Pitera, J. W.; Peinemann, K. V.; Nunes, S. P. Self- 2002 assembly in casting solutions of block copolymer membranes. *Soft 2003 Matter* **2013**, *9*, 5557–5564.

2004 (62) Peinemann, K. V.; Abetz, V.; Simon, P. F. W. Asymmetric 2005 superstructure formed in a block copolymer via phase separation. *Nat. 2006 Mater.* **2007**, *6*, 992–996.

2007 (63) Gu, Y.; Dorin, R. M.; Wiesner, U. Asymmetric Organic– 2008 Inorganic Hybrid Membrane Formation via Block Copolymer– 2009 Nanoparticle Co-Assembly. *Nano Lett.* **2013**, *13*, 5323–5328.

2010 (64) Nunes, S. P.; Behzad, A. R.; Hooghan, B.; Sougrat, R.; 2011 Karunakaran, M.; Pradeep, N.; Vainio, U.; Peinemann, K.-V. 2012 Switchable pH-responsive polymeric membranes prepared via block 2013 copolymer micelle assembly. *ACS Nano* **2011**, *5*, 3516–3522.

2014 (65) Madhavan, P.; Peinemann, K.-V.; Nunes, S. P. Complexation– 2015 Tailored Morphology of Asymmetric Block Copolymer Membranes. 2016 *ACS Appl. Mater. Interfaces* **2013**, *5*, 7152–7159.

2017 (66) Madhavan, P.; Sougrat, R.; Behzad, A. R.; Peinemann, K.-V.; 2018 Nunes, S. P. Ionic Liquids as Self-Assembly Guide for the Formation 2019 of Nanostructured Block Copolymer Membranes. *J. Membr. Sci.* **2015**, 2020 *492*, 568–577.

2021 (67) Phillip, W. A.; Dorin, R. M.; Werner, J. r.; Hoek, E. M.; 2022 Wiesner, U.; Elimelech, M. Tuning Structure and Properties of 2023 Graded Triblock Terpolymer-Based Mesoporous and Hybrid Films. 2024 *Nano Lett.* **2011**, *11*, 2892–2900.

2025 (68) Clodt, J. I.; Rangou, S.; Schröder, A.; Buhr, K.; Hahn, J.; Jung, 2026 A.; Filiz, V.; Abetz, V. Carbohydrates as Additives for the Formation 2027 of Isoporous PS-*b*-P4VP Diblock Copolymer Membranes. *Macromol. 2028 Rapid Commun.* **2013**, *34*, 190–194.

2029 (69) Gallei, M.; Rangou, S.; Filiz, V.; Buhr, K.; Bolmer, S.; Abetz, C.; 2030 Abetz, V. The Influence of Magnesium Acetate on the Structure 2031 Formation of Polystyrene-block-poly (4-vinylpyridine)-Based Inter- 2032 gral-Asymmetric Membranes. *Macromol. Chem. Phys.* **2013**, *214*, 2033 1037–1046.

2034 (70) Park, S.; Lee, D. H.; Xu, J.; Kim, B.; Hong, S. W.; Jeong, U.; Xu, 2035 T.; Russell, T. P. Macroscopic 10-Terabit-per-Square-Inch Arrays 2036 from Block Copolymers with Lateral Order. *Science* **2009**, *323*, 1030– 2037 1033.

2038 (71) Yu, H.; Qiu, X.; Moreno, N.; Ma, Z.; Calo, V. M.; Nunes, S. P.; 2039 Peinemann, K. V. Self-Assembled Asymmetric Block Copolymer 2040 Membranes: Bridging the Gap from Ultra-to Nanofiltration. *Angew. 2041 Chem., Int. Ed.* **2015**, *54*, 13937–13941.

2042 (72) Zhang, Y.; Mulvenna, R. A.; Qu, S.; Boudouris, B. W.; Phillip, 2043 W. A. Block Polymer Membranes Functionalized with Nanoconfined 2044 Polyelectrolyte Brushes Achieve Sub-Nanometer Selectivity. *ACS 2045 Macro Lett.* **2017**, *6*, 726–732.

2046 (73) Asatekin, A.; Menniti, A.; Kang, S.; Elimelech, M.; Morgenroth, 2047 E.; Mayes, A. M. Antifouling Nanofiltration Membranes for 2048 Membrane Bioreactors from Self-Assembling Graft Copolymers. *J. 2049 Membr. Sci.* **2006**, *285*, 81–89.

2050 (74) Asatekin, A.; Olivetti, E. A.; Mayes, A. M. Fouling resistant, 2051 high flux nanofiltration membranes from polyacrylonitrile-graft- 2052 poly(ethylene oxide). *J. Membr. Sci.* **2009**, *332*, 6–12.

(75) Akthakul, A.; Salinero, R. F.; Mayes, A. M. Antifouling polymer 2053 membranes with subnanometer size selectivity. *Macromolecules* **2004**, 2054 37, 7663–7668.

(76) Asatekin, A.; Mayes, A. M. Responsive Pore Size Properties of 2056 Composite NF Membranes Based on PVDF Graft Copolymers. *Sep. 2057 Sci. Technol.* **2009**, *44*, 3330–3345.

(77) Shinozaki, A.; Jasnow, D.; Balazs, A. C. Microphase Separation 2059 in Comb Copolymers. *Macromolecules* **1994**, *27*, 2496–2502.

(78) Foster, D. P.; Jasnow, D.; Balazs, A. C. Macrophase and 2061 Microphase Separation in Random Comb Copolymers. *Macro- 2062 molecules* **1995**, *28*, 3450–3462.

(79) Qu, S.; Dilenschneider, T.; Phillip, W. A. Preparation of 2064 chemically-tailored copolymer membranes with tunable ion transport 2065 properties. *ACS Appl. Mater. Interfaces* **2015**, *7*, 19746–19754.

(80) Lovell, N. G. *Control of size and charge selectivity in amphiphilic 2067 graft copolymer nanofiltration membranes*. Ph.D. Thesis, Massachusetts 2068 Institute of Technology, 2010.

(81) Bengani, P.; Kou, Y.; Asatekin, A. Zwitterionic copolymer self- 2070 assembly for fouling resistant, high flux membranes with size-based 2071 small molecule selectivity. *J. Membr. Sci.* **2015**, *493*, 755–765.

(82) Bengani-Lutz, P.; Converse, E.; Cebe, P.; Asatekin, A. Self- 2073 Assembling Zwitterionic Copolymers as Membrane Selective Layers 2074 with Excellent Fouling Resistance: Effect of Zwitterion Chemistry. 2075 *ACS Appl. Mater. Interfaces* **2017**, *9*, 20859–20872.

(83) Bengani-Lutz, P.; Zaf, R. D.; Culfa-Zemecen, P. Z.; Asatekin, A. 2077 Extremely fouling resistant zwitterionic copolymer membranes with 2078 similar to 1 nm pore size for treating municipal, oily and textile 2079 wastewater streams. *J. Membr. Sci.* **2017**, *543*, 184–194.

(84) Carter, B. M.; Wiesner, B. R.; Hatakeyama, E. S.; Barton, J. 2081 L.; Noble, R. D.; Gin, D. L. Glycerol-Based Bicontinuous Cubic 2082 Lyotropic Liquid Crystal Monomer System for the Fabrication of 2083 Thin-Film Membranes with Uniform Nanopores. *Chem. Mater.* **2012**, 2084 *24*, 4005–4007.

(85) Carter, B. M.; Wiesner, B. R.; Noble, R. D.; Gin, D. L. Thin- 2086 Film Composite Bicontinuous Cubic Lyotropic Liquid Crystal 2087 Polymer Membranes: Effects of Anion-Exchange on Water Filtration 2088 Performance. *J. Membr. Sci.* **2014**, *455*, 143–151.

(86) Gin, D. L.; Gu, W.; Pindzola, B. A.; Zhou, W. J. Polymerized 2090 Lyotropic Liquid Crystal Assemblies for Materials Applications. *Acc. 2091 Chem. Res.* **2001**, *34*, 973–980.

(87) Zhou, M.; Kidd, T. J.; Noble, R. D.; Gin, D. L. Supported 2093 Lyotropic Liquid-Crystal Polymer Membranes: Promising Materials 2094 for Molecular Size-Selective Aqueous Nanofiltration. *Adv. Mater.* **2095 2005**, *17*, 1850.

(88) Zhou, M.; Nemade, P. R.; Lu, X.; Zeng, X.; Hatakeyama, E. S.; 2097 Noble, R. D.; Gin, D. L. New Type of Membrane Material for Water 2098 Desalination Based on a Cross-Linked Bicontinuous Cubic Lyotropic 2099 Liquid Crystal Assembly. *J. Am. Chem. Soc.* **2007**, *129*, 9574–9575.

(89) Gin, D. L.; Bara, J. E.; Noble, R. D.; Elliott, B. J. Polymerized 2101 lyotropic liquid crystal assemblies for membrane applications. *Macromol. Rapid Commun.* **2008**, *29*, 367–389.

(90) Hatakeyama, E. S.; Gabriel, C. J.; Wiesner, B. R.; Lohr, J. L.; 2104 Zhou, M.; Noble, R. D.; Gin, D. L. Water Filtration Performance of a 2105 Lyotropic Liquid Crystal Polymer Membrane with Uniform, Sub-1- 2106 nm Pores. *J. Membr. Sci.* **2011**, *366*, 62–72.

(91) Kato, T. From Nanostructured Liquid Crystals to Polymer- 2108 Based Electrolytes. *Angew. Chem., Int. Ed.* **2010**, *49*, 7847–7848.

(92) Kuringen, P. C. H.; Schenning, A. P. H. J.; Broer, D. J. Liquid 2110 Crystal Polymer Membranes. In *Encyclopedia of Membranes*; Drioli, E., 2111 Giorno, L., Eds.; Springer: Berlin, Heidelberg, 2016.

(93) Mukai, T.; Yoshio, M.; Kato, T.; Yoshizawa, M.; Ohno, H. 2113 Anisotropic Ion Conduction in a Unique Smectic Phase of Self- 2114 Assembled Amphiphilic Ionic Liquids. *Chem. Commun.* **2005**, 1333– 2115 1335.

(94) Yoshio, M.; Mukai, T.; Kanie, K.; Yoshizawa, M.; Ohno, H.; 2117 Kato, T. Layered Ionic Liquids: Anisotropic Ion Conduction in New 2118 Self-Organized Liquid-Crystalline Materials. *Adv. Mater.* **2002**, *14*, 2119 351–354.

2121 (95) Ichikawa, T.; Yoshio, M.; Hamasaki, A.; Taguchi, S.; Liu, F.;
2122 Zeng, X.-b.; Ungar, G.; Ohno, H.; Kato, T. Induction of
2123 Thermotropic Bicontinuous Cubic Phases in Liquid-Crystalline
2124 Ammonium and Phosphonium Salts. *J. Am. Chem. Soc.* **2012**, *134*,
2125 2634–2643.

2126 (96) Soberats, B.; Yoshio, M.; Ichikawa, T.; Taguchi, S.; Ohno, H.;
2127 Kato, T. 3D Anhydrous Proton-Transporting Nanochannels Formed
2128 by Self-Assembly of Liquid Crystals Composed of a Sulfobetaine and
2129 a Sulfonic Acid. *J. Am. Chem. Soc.* **2013**, *135*, 15286–15289.

2130 (97) Frise, A. E.; Ichikawa, T.; Yoshio, M.; Ohno, H.; Dvinskikh, S.
2131 V.; Kato, T.; Furo, I. Ion conductive behaviour in a confined
2132 nanostructure: NMR observation of self-diffusion in a liquid-
2133 crystalline bicontinuous cubic phase. *Chem. Commun.* **2010**, *46*,
2134 728–730.

2135 (98) Ichikawa, T.; Yoshio, M.; Hamasaki, A.; Mukai, T.; Ohno, H.;
2136 Kato, T. Self-organization of room-temperature ionic liquids
2137 exhibiting liquid-crystalline bicontinuous cubic phases: Formation of
2138 nano-ion channel networks. *J. Am. Chem. Soc.* **2007**, *129*, 10662–
2139 10663.

2140 (99) Henmi, M.; Nakatsuji, K.; Ichikawa, T.; Tomioka, H.;
2141 Sakamoto, T.; Yoshio, M.; Kato, T. Self-Organized Liquid-Crystalline
2142 Nanostructured Membranes for Water Treatment: Selective Per-
2143 meation of Ions. *Adv. Mater.* **2012**, *24*, 2238–2241.

2144 (100) Hatakeyama, E. S.; Gabriel, C. J.; Wiesnauer, B. R.; Lohr, J.
2145 L.; Zhou, M. J.; Noble, R. D.; Gin, D. L. Water filtration performance
2146 of a lyotropic liquid crystal polymer membrane with uniform, sub-1-
2147 nm pores. *J. Membr. Sci.* **2011**, *366*, 62–72.

2148 (101) Dischinger, S. M.; Rosenblum, J.; Noble, R. D.; Gin, D. L.;
2149 Linden, K. G. Application of a lyotropic liquid crystal nanofiltration
2150 membrane for hydraulic fracturing flowback water: Selectivity and
2151 implications for treatment. *J. Membr. Sci.* **2017**, *543*, 319–327.

2152 (102) Lu, X. Y.; Nguyen, V.; Zeng, X. H.; Elliott, B. J.; Gin, D. L.
2153 Selective rejection of a water-soluble nerve agent stimulant using a
2154 nanoporous lyotropic liquid crystal-butyl rubber vapor barrier
2155 material: Evidence for a molecular size-discrimination mechanism. *J.*
2156 *Membr. Sci.* **2008**, *318*, 397–404.

2157 (103) Hsieh, Y. P.; Hofmann, M.; Farhat, H.; Barros, E. B.; Kalbac,
2158 M.; Kong, J.; Liang, C. T.; Chen, Y. F.; Dresselhaus, M. S. Chiral angle
2159 dependence of resonance window widths in $(2n+m)$ families of
2160 single-walled carbon nanotubes. *Appl. Phys. Lett.* **2010**, *96*, 103118.

2161 (104) Gin, D. L.; Lu, X. Y.; Nemade, P. R.; Pecinovsky, C. S.; Xu, Y.
2162 J.; Zhou, M. J. Recent advances in the design of polymerizable
2163 lyotropic liquid-crystal assemblies for heterogeneous catalysis and
2164 selective separations. *Adv. Funct. Mater.* **2006**, *16*, 865–878.

2165 (105) Shen, Y. X.; Saboe, P. O.; Sines, I. T.; Erbakan, M.; Kumar, M.
2166 Biomimetic membranes: A review. *J. Membr. Sci.* **2014**, *454*, 359–381.

2167 (106) Benavides, S.; Qu, S. Y.; Gao, F.; Phillip, W. A. Polymeric Ion
2168 Pumps: Using an Oscillating Stimulus To Drive Solute Transport in
2169 Reactive Membranes. *Langmuir* **2018**, *34*, 4503–4514.

2170 (107) Friedman, M. H. *Principles and models of biological transport*,
2171 2nd ed.; Springer: New York, NY, 2008; p xvii, 508 p.

2172 (108) Baker, R. W. Future directions of membrane gas separation
2173 technology. *Ind. Eng. Chem. Res.* **2002**, *41*, 1393–1411.

2174 (109) Visser, H. C.; Reinhoudt, D. N.; Dejong, F. Carrier-Mediated
2175 Transport through Liquid Membranes. *Chem. Soc. Rev.* **1994**, *23*, 75–
2176 81.

2177 (110) Miedema, H. Ion-Selective Biomimetic Membranes. In
2178 *Biomimetic Membranes for Sensor and Separation Applications*; Hélix-
2179 Nielsen, C., Ed.; Springer, Dordrecht, 2012; pp 63–86.

2180 (111) Lim, R. Y. H.; Aebi, U.; Fahrenkrog, B. Towards reconciling
2181 structure and function in the nuclear pore complex. *Histochem. Cell*
2182 *Biol.* **2008**, *129*, 105–116.

2183 (112) Koebnik, R.; Locher, K. P.; Van Gelder, P. Structure and
2184 function of bacterial outer membrane proteins: barrels in a nutshell.
2185 *Mol. Microbiol.* **2000**, *37*, 239–253.

2186 (113) Zeth, K.; Thein, M. Porins in prokaryotes and eukaryotes:
2187 common themes and variations. *Biochem. J.* **2010**, *431*, 13–22.

2188 (114) Schirmer, T. General and specific porins from bacterial outer
2189 membranes. *J. Struct. Biol.* **1998**, *121*, 101–109.

2190 (115) Kumar, M.; Payne, M. M.; Poust, S. K.; Zilles, J. L. Polymer-
2191 Based Biomimetic Membranes for Desalination. In *Biomimetic* **2191**
2192 *Membranes for Sensor and Separation Applications*; Hélix-Nielsen, C.,
2193 Ed.; Springer Netherlands: Dordrecht, 2012; pp 43–62.

2194 (116) Kumar, M.; Grzelakowski, M.; Zilles, J.; Clark, M.; Meier, W.
2195 Highly permeable polymeric membranes based on the incorporation
2196 of the functional water channel protein Aquaporin Z. *Proc. Natl. Acad.* **2196**
2197 *Sci. U. S. A.* **2007**, *104*, 20719–20724.

2198 (117) Giwa, A.; Hasan, S. W.; Yousuf, A.; Chakraborty, S.; Johnson,
2199 D. J.; Hilal, N. Biomimetic membranes: A critical review of recent
2200 progress. *Desalination* **2017**, *420*, 403–424.

2201 (118) Shen, Y. X.; Si, W.; Erbakan, M.; Decker, K.; De Zorzi, R.;
2202 Saboe, P. O.; Kang, Y. J.; Majd, S.; Butler, P. J.; Walz, T.; Aksimentiev,
2203 A.; Hou, J. L.; Kumar, M. Highly permeable artificial water channels
2204 that can self-assemble into two-dimensional arrays. *Proc. Natl. Acad.* **2204**
2205 *Sci. U. S. A.* **2015**, *112*, 9810–9815.

2206 (119) Licsandru, E.; Kocsis, I.; Shen, Y. X.; Murail, S.; Legrand, Y.;
2207 van der Lee, A.; Tsai, D.; Baaden, M.; Kumar, M.; Barboiu, M.
2208 Salt-Excluding Artificial Water Channels Exhibiting Enhanced Dipolar
2209 Water and Proton Translocation. *J. Am. Chem. Soc.* **2016**, *138*, 5403–
2210 5409.

2211 (120) Shen, Y. X.; Song, W. C.; Barden, D. R.; Ren, T. W.; Lang, C.;
2212 Feroz, H.; Henderson, C. B.; Saboe, P. O.; Tsai, D.; Yan, H. J.; Butler,
2213 P. J.; Bazan, G. C.; Phillip, W. A.; Hickey, R. J.; Cremer, P. S.;
2214 Vashisth, H.; Kumar, M. Achieving high permeability and enhanced
2215 selectivity for Angstrom-scale separations using artificial water channel
2216 membranes. *Nat. Commun.* **2018**, *9*, 2294.

2217 (121) Werber, J. R.; Elimelech, M. Permselectivity limits of
2218 biomimetic desalination membranes. *Sci. Adv.* **2018**, *4*, eaar8266.

2219 (122) Barboiu, M.; Gilles, A. From Natural to Bioassisted and
2220 Biomimetic Artificial Water Channel Systems. *Acc. Chem. Res.* **2013**, *46*,
2221 2814–2823.

2222 (123) Barboiu, M. Artificial Water Channels. *Angew. Chem., Int. Ed.* **2012**, *51*,
2223 11674–11676.

2224 (124) Stillwell, W. Chapter 19 - Membrane Transport. In *An*
2225 *Introduction to Biological Membranes*, 2nd ed.; Stillwell, W., Ed.;
2226 Elsevier: 2016; pp 423–451.

2227 (125) Herrington, J.; Arey, B. J. Conformational Mechanisms of
2228 Signaling Bias of Ion Channels. In *Biased Signaling in Physiology,
2229 Pharmacology and Therapeutics*; Arey, B. J., Ed.; Academic Press: San
2230 Diego, 2014; pp 173–207.

2231 (126) Lim, R. Y. H.; Fahrenkrog, B.; Koser, J.; Schwarz-Herion, K.;
2232 Deng, J.; Aebi, U. Nanomechanical basis of selective gating by the
2233 nuclear pore complex. *Science* **2007**, *318*, 640–643.

2234 (127) Shannon, M. A.; Bohn, P. W.; Elimelech, M.; Georgiadis, J. G.;
2235 Marinas, B. J.; Mayes, A. M. Science and technology for water
2236 purification in the coming decades. *Nature* **2008**, *452*, 301–310.

2237 (128) Daiguji, H. Ion transport in nanofluidic channels. *Chem. Soc.* **2010**, *39*,
2238 901–911.

2239 (129) Martin, C. R.; Kohli, P. The emerging field of nanotube
2240 biotechnology. *Nat. Rev. Drug Discovery* **2003**, *2*, 29–37.

2241 (130) Gyurcsanyi, R. E. Chemically-modified nanopores for sensing.
2242 *TrAC, Trends Anal. Chem.* **2008**, *27*, 627–639.

2243 (131) Hong, S. U.; Bruening, M. L. Separation of amino acid
2244 mixtures using multilayer polyelectrolyte nanofiltration membranes. *J.*
2245 *Membr. Sci.* **2006**, *280*, 1–5.

2246 (132) Ku, J. R.; Lai, S. M.; Ileri, N.; Ramirez, P.; Mafe, S.; Stroeve, P.
2247 pH and ionic strength effects on amino acid transport through Au-
2248 nanotube membranes charged with self-assembled monolayers. *J.*
2249 *Phys. Chem. C* **2007**, *111*, 2965–2973.

2250 (133) Shim, Y. K.; Chellam, S. Steric and electrostatic interactions
2251 govern nanofiltration of amino acids. *Biotechnol. Bioeng.* **2007**, *98*,
2252 451–461.

2253 (134) Wang, K. Y.; Chung, T. S. The characterization of flat
2254 composite nanofiltration membranes and their applications in the
2255 separation of Cephalexin. *J. Membr. Sci.* **2005**, *247*, 37–50.

2256 (135) Wang, K. Y.; Xiao, Y. C.; Chung, T. S. Chemically modified
2257 polybenzimidazole nanofiltration membrane for the separation of
2258 electrolytes and cephalexin. *Chem. Eng. Sci.* **2006**, *61*, 5807–5817.

2259 (136) Walsh, G. Biopharmaceutical benchmarks 2006. *Nat. Biotechnol.* **2006**, *24*, 769–U5.

2260 (137) Geise, G. M.; Freeman, B. D.; Paul, D. R. Sodium chloride diffusion in sulfonated polymers for membrane applications. *J. Membr. Sci.* **2013**, *427*, 186–196.

2261 (138) Zhang, H.; Geise, G. M. Modeling the water permeability and water/salt selectivity tradeoff in polymer membranes. *J. Membr. Sci.* **2016**, *520*, 790–800.

2262 (139) Donnan, F. G. The theory of membrane equilibria. *Chem. Rev.* **1924**, *1*, 73–90.

2263 (140) Schaepl, J.; Van der Bruggen, B.; Vandecasteele, C.; Wilms, D. Influence of ion size and charge in nanofiltration. *Sep. Purif. Technol.* **1998**, *14*, 155–162.

2264 (141) Baker, J. S.; Dudley, L. Y. Biofouling in membrane systems - A review. *Desalination* **1998**, *118*, 81–89.

2265 (142) Goosen, M. F. A.; Sablani, S. S.; Al-Hinai, H.; Al-Obeidani, S.; Al-Belushi, R.; Jackson, D. Fouling of reverse osmosis and ultrafiltration membranes: A critical review. *Sep. Sci. Technol.* **2005**, *39*, 2261–2297.

2266 (143) Sadeghi, I.; Aroujalian, A.; Raisi, A.; Dabir, B.; Fathizadeh, M. Surface modification of polyethersulfone ultrafiltration membranes by corona air plasma for separation of oil/water emulsions. *J. Membr. Sci.* **2013**, *430*, 24–36.

2267 (144) Verliefde, A. R. D.; Cornelissen, E. R.; Heijman, S. G. J.; Verberk, J. Q. J. C.; Amy, G. L.; Van der Bruggen, B.; van Dijk, J. C. The role of electrostatic interactions on the rejection of organic solutes in aqueous solutions with nanofiltration. *J. Membr. Sci.* **2008**, *322*, 52–66.

2268 (145) Shen, M.; Keten, S.; Lueptow, R. M. Rejection mechanisms for contaminants in polyamide reverse osmosis membranes. *J. Membr. Sci.* **2016**, *509*, 36–47.

2269 (146) Nghiem, L. D.; Schafer, A. I.; Elimelech, M. Pharmaceutical retention mechanisms by nanofiltration membranes. *Environ. Sci. Technol.* **2005**, *39*, 7698–7705.

2270 (147) Braeken, L.; Ramaekers, R.; Zhang, Y.; Maes, G.; Van der Bruggen, B.; Vandecasteele, C. Influence of hydrophobicity on retention in nanofiltration of aqueous solutions containing organic compounds. *J. Membr. Sci.* **2005**, *252*, 195–203.

2271 (148) Van der Bruggen, B.; Schaepl, J.; Wilms, D.; Vandecasteele, C. Influence of molecular size, polarity and charge on the retention of organic molecules by nanofiltration. *J. Membr. Sci.* **1999**, *156*, 29–41.

2272 (149) Szymczyk, A.; Fievet, P. Investigating transport properties of nanofiltration membranes by means of a steric, electric and dielectric exclusion model. *J. Membr. Sci.* **2005**, *252*, 77–88.

2273 (150) Noskov, S. Y.; Berneche, S.; Roux, B. Control of ion selectivity in potassium channels by electrostatic and dynamic properties of carbonyl ligands. *Nature* **2004**, *431*, 830–834.

2274 (151) Bruening, M. L.; Dotzauer, D. M.; Jain, P.; Ouyang, L.; Baker, G. L. Creation of functional membranes using polyelectrolyte multilayers and polymer brushes. *Langmuir* **2008**, *24*, 7663–7673.

2275 (152) Hollman, A. M.; Bhattacharyya, D. Pore assembled multilayers of charged polypeptides in microporous membranes for ion separation. *Langmuir* **2004**, *20*, 5418–5424.

2276 (153) Armstrong, J. A.; Bernal, E. E. L.; Yaroshchuk, A.; Bruening, M. L. Separation of Ions Using Polyelectrolyte-Modified Nanoporous Track-Etched Membranes. *Langmuir* **2013**, *29*, 10287–10296.

2277 (154) Lazzara, T. D.; Lau, K. H. A.; Abou-Kandil, A. I.; Caminade, A. M.; Majoral, J. P.; Knoll, W. Polyelectrolyte Layer-by-Layer Deposition in Cylindrical Nanopores. *ACS Nano* **2010**, *4*, 3909–3920.

2278 (155) Ali, M.; Yameen, B.; Cervera, J.; Ramirez, P.; Neumann, R.; Ensinger, W.; Knoll, W.; Azzaroni, O. Layer-by-Layer Assembly of Polyelectrolytes into Ionic Current Rectifying Solid-State Nanopores: Insights from Theory and Experiment. *J. Am. Chem. Soc.* **2010**, *132*, 8338–8348.

2279 (156) Decher, G. Fuzzy nanoassemblies: Toward layered polymeric multicomposites. *Science* **1997**, *277*, 1232–1237.

2280 (157) Liang, Z. J.; Susha, A. S.; Yu, A. M.; Caruso, F. Nanotubes prepared by layer-by-layer coating of porous membrane templates. *Adv. Mater.* **2003**, *15*, 1849–1853.

2281 (158) Ai, S. F.; Lu, G.; He, Q.; Li, J. B. Highly flexible polyelectrolyte nanotubes. *J. Am. Chem. Soc.* **2003**, *125*, 11140–11141.

2282 (159) Rajesh, S.; Yan, Y.; Chang, H. C.; Gao, H. F.; Phillip, W. A. Mixed Mosaic Membranes Prepared by Layer-by-Layer Assembly for Ionic Separations. *ACS Nano* **2014**, *8*, 12338–12345.

2283 (160) Fujimoto, T.; Ohkoshi, K.; Miyaki, Y.; Nagasawa, M. A New Charge-Mosaic Membrane from a Multiblock Copolymer. *Science* **1984**, *224*, 74–76.

2284 (161) Weinstein, J. N.; Caplan, S. R. Charge-Mosaic Membranes - Enhanced Permeability and Negative Osmosis with a Symmetrical Salt. *Science* **1968**, *161*, 70–72.

2285 (162) Chen, Y. L.; Cui, Y. M.; Jia, Y. S.; Zhan, K.; Zhang, H.; Chen, G. X.; Yang, Y. D.; Wu, M.; Ni, H. M. Preparation of Charged Mosaic Membrane of Sodium Polystyrene Sulfonate and Poly(4-vinyl pyridine) by Conjugate Electrospinning. *J. Appl. Polym. Sci.* **2014**, *131*, 40716.

2286 (163) Low, Z. X.; Chua, Y. T.; Ray, B. M.; Mattia, D.; Metcalfe, I. S.; Patterson, D. A. Perspective on 3D printing of separation membranes and comparison to related unconventional fabrication techniques. *J. Membr. Sci.* **2017**, *523*, 596–613.

2287 (164) Qu, S. Y.; Shi, Y.; Benavides, S.; Hunter, A.; Gao, H. F.; Phillip, W. A. Copolymer Nanofilters with Charge-Patterned Domains for Enhanced Electrolyte Transport. *Chem. Mater.* **2017**, *29*, 762–772.

2288 (165) Gao, P.; Hunter, A.; Summe, M. J.; Phillip, W. A. A Method for the Efficient Fabrication of Multifunctional Mosaic Membranes by Inkjet Printing. *ACS Appl. Mater. Interfaces* **2016**, *8*, 19772–19779.

2289 (166) Savariar, E. N.; Krishnamoorthy, K.; Thayumanavan, S. Molecular discrimination inside polymer nanotubules. *Nat. Nano- technol.* **2008**, *3*, 112–117.

2290 (167) Savariar, E. N.; Sochat, M. M.; Klaikherd, A.; Thayumanavan, S. Functional group density and recognition in polymer nanotubes. *Angew. Chem., Int. Ed.* **2009**, *48*, 110–114.

2291 (168) Nishizawa, M.; Menon, V. P.; Martin, C. R. Metal nanotube membranes with electrochemically switchable ion-transport selectivity. *Science* **1995**, *268*, 700–702.

2292 (169) Jirage, K. B.; Hulteen, J. C.; Martin, C. R. Nanotubule-based molecular-filtration membranes. *Science* **1997**, *278*, 655–658.

2293 (170) Jirage, K. B.; Hulteen, J. C.; Martin, C. R. Effect of thiol chemisorption on the transport properties of gold nanotube membranes. *Anal. Chem.* **1999**, *71*, 4913–4918.

2294 (171) Kang, M. S.; Martin, C. R. Investigations of potential-dependent fluxes of ionic permeates in gold nanotube membranes prepared via the template method. *Langmuir* **2001**, *17*, 2753–2759.

2295 (172) Martin, C. R.; Nishizawa, M.; Jirage, K.; Kang, M. S.; Lee, S. B. Controlling ion-transport selectivity in gold nanotube membranes. *Adv. Mater.* **2001**, *13*, 1351–1362.

2296 (173) Lee, S. B.; Martin, C. R. pH-switchable, ion-selective gold nanotube membrane based on chemisorbed cysteine. *Anal. Chem.* **2001**, *73*, 768–775.

2297 (174) Martin, C. R.; Nishizawa, M.; Jirage, K.; Kang, M. R. Investigations of the transport properties of gold nanotube membranes. *J. Phys. Chem. B* **2001**, *105*, 1925–1934.

2298 (175) Love, J. C.; Estroff, L. A.; Kriebel, J. K.; Nuzzo, R. G.; Whitesides, G. M. Self-assembled monolayers of thiolates on metals as a form of nanotechnology. *Chem. Rev.* **2005**, *105*, 1103–1169.

2299 (176) Baker, R. W. *Membrane technology and applications*; McGraw-Hill: New York, 2000.

2300 (177) Velleman, L.; Triani, G.; Evans, P. J.; Shapter, J. G.; Losic, D. Structural and chemical modification of porous alumina membranes. *Microporous Mesoporous Mater.* **2009**, *126*, 87–94.

2301 (178) Li, F. B.; Li, L.; Liao, X. Z.; Wang, Y. Precise pore size tuning and surface modifications of polymeric membranes using the atomic layer deposition technique. *J. Membr. Sci.* **2011**, *385*, 1–9.

2302 (179) Asatekin, A.; Gleason, K. K. Polymeric nanopore membranes for hydrophobicity-based separations by conformal initiated chemical vapor deposition. *Nano Lett.* **2011**, *11*, 677–686.

2395 (180) Parthasarathy, R. V.; Martin, C. R. Synthesis of Polymeric
2396 Microcapsule Arrays and Their Use for Enzyme Immobilization.
2397 *Nature* **1994**, *369*, 298–301.

2398 (181) Lepoitevin, M.; Ma, T. J.; Bechelany, M.; Janot, J. M.; Balme,
2399 S. Functionalization of single solid state nanopores to mimic
2400 biological ion channels: A review. *Adv. Colloid Interface Sci.* **2017**,
2401 *250*, 195–213.

2402 (182) Velleman, L.; Shapter, J. G.; Losic, D. Gold nanotube
2403 membranes functionalised with fluorinated thiols for selective
2404 molecular transport. *J. Membr. Sci.* **2009**, *328*, 121–126.

2405 (183) Lopez-Lorente, A. I.; Simonet, B. M.; Valcarcel, M. The
2406 Potential of Carbon Nanotube Membranes for Analytical Separations.
2407 *Anal. Chem.* **2010**, *82*, 5399–5407.

2408 (184) Corry, B. Designing carbon nanotube membranes for efficient
2409 water desalination. *J. Phys. Chem. B* **2008**, *112*, 1427–1434.

2410 (185) Skouidas, A. I.; Ackerman, D. M.; Johnson, J. K.; Sholl, D. S.
2411 Rapid transport of gases in carbon nanotubes. *Phys. Rev. Lett.* **2002**,
2412 *89*, 185901.

2413 (186) Chen, H. B.; Sholl, D. S. Rapid diffusion of CH₄/H₂
2414 mixtures in single-wall carbon nanotubes. *J. Am. Chem. Soc.* **2004**,
2415 *126*, 7778–7779.

2416 (187) Lagerwall, J.; Scialia, G.; Haluska, M.; Dettlaff-Weglowska,
2417 U.; Roth, S.; Giesselmann, F. Nanotube alignment using lyotropic
2418 liquid crystals. *Adv. Mater.* **2007**, *19*, 359–364.

2419 (188) Casavant, M. J.; Walters, D. A.; Schmidt, J. J.; Smalley, R. E.
2420 Neat macroscopic membranes of aligned carbon nanotubes. *J. Appl.*
2421 *Phys.* **2003**, *93*, 2153–2156.

2422 (189) Fischer, J. E.; Zhou, W.; Vavro, J.; Llaguno, M. C.; Guthy, C.;
2423 Haggenueller, R.; Casavant, M. J.; Walters, D. E.; Smalley, R. E.
2424 Magnetically aligned single wall carbon nanotube films: Preferred
2425 orientation and anisotropic transport properties. *J. Appl. Phys.* **2003**,
2426 *93*, 2157–2163.

2427 (190) Vigolo, B.; Penicaud, A.; Coulon, C.; Sauder, C.; Pailler, R.;
2428 Journet, C.; Bernier, P.; Poulin, P. Macroscopic fibers and ribbons of
2429 oriented carbon nanotubes. *Science* **2000**, *290*, 1331–1334.

2430 (191) Jin, L.; Bower, C.; Zhou, O. Alignment of carbon nanotubes in
2431 a polymer matrix by mechanical stretching. *Appl. Phys. Lett.* **1998**, *73*,
2432 1197–1199.

2433 (192) Fagan, J. A.; Simpson, J. R.; Landi, B. J.; Richter, L. J.;
2434 Mandelbaum, I.; Bajpai, V.; Ho, D. L.; Raffaelle, R.; Walker, A. R. H.;
2435 Bauer, B. J.; Hobbie, E. K. Dielectric response of aligned
2436 semiconducting single-wall nanotubes. *Phys. Rev. Lett.* **2007**, *98*,
2437 147402.

2438 (193) Kim, S.; Jinschek, J. R.; Chen, H.; Sholl, D. S.; Marand, E.
2439 Scalable fabrication of carbon nanotube/polymer nanocomposite
2440 membranes for high flux gas transport. *Nano Lett.* **2007**, *7*, 2806–
2441 2811.

2442 (194) McGinnis, R. L.; Reimund, K.; Ren, J.; Xia, L. L.; Chowdhury,
2443 M. R.; Sun, X. H.; Abril, M.; Moon, J. D.; Merrick, M. M.; Park, J.;
2444 Stevens, K. A.; McCutcheon, J. R.; Freeman, B. D. Large-scale
2445 polymeric carbon nanotube membranes with sub-1.27-nm pores. *Sci.*
2446 *Adv.* **2018**, *4*, e1700938.

2447 (195) Che, G. L.; Lakshmi, B. B.; Fisher, E. R.; Martin, C. R. Carbon
2448 nanotubule membranes for electrochemical energy storage and
2449 production. *Nature* **1998**, *393*, 346–349.

2450 (196) Kyotani, T.; Tsai, L. F.; Tomita, A. Formation of Ultrafine
2451 Carbon Tubes by Using an Anodic Aluminum-Oxide Film as a
2452 Template. *Chem. Mater.* **1995**, *7*, 1427–1428.

2453 (197) Hinds, B. J.; Chopra, N.; Rantell, T.; Andrews, R.; Gavalas, V.;
2454 Bachas, L. G. Aligned multiwalled carbon nanotube membranes.
2455 *Science* **2004**, *303*, 62–65.

2456 (198) Holt, J. K.; Noy, A.; Huser, T.; Eaglesham, D.; Bakajin, O.
2457 Fabrication of a carbon nanotube-embedded silicon nitride membrane
2458 for studies of nanometer-scale mass transport. *Nano Lett.* **2004**, *4*,
2459 2245–2250.

2460 (199) Fornasiero, F.; Park, H. G.; Holt, J. K.; Stadermann, M.;
2461 Grigoropoulos, C. P.; Noy, A.; Bakajin, O. Ion exclusion by sub-2-nm
2462 carbon nanotube pores. *Proc. Natl. Acad. Sci. U. S. A.* **2008**, *105*,
2463 17250–17255.

200 (200) Alvarez, M. M.; Aizenberg, J.; Analoui, M.; Andrews, A. M.;
2464 Bisker, G.; Boyden, E. S.; Kamm, R. D.; Karp, J. M.; Mooney, D. J.;
2465 Oklu, R.; Peer, D.; Stolzoff, M.; Strano, M. S.; Trujillo-de Santiago, G.;
2466 Webster, T. J.; Weiss, P. S.; Khademhosseini, A. Emerging Trends
2467 in Micro- and Nanoscale Technologies in Medicine: From Basic
2468 Discoveries to Translation. *ACS Nano* **2017**, *11*, 5195–5214.

201 (201) Zhang, J. Q.; Landry, M. P.; Barone, P. W.; Kim, J. H.; Lin, S.;
2470 C.; Ulissi, Z. W.; Lin, D. H.; Mu, B.; Boghossian, A. A.; Hilmer, A. J.;
2471 Rwei, A.; Hinckley, A. C.; Kruss, S.; Shandell, M. A.; Nair, N.; Blake,
2472 S.; Sen, F.; Sen, S.; Croy, R. G.; Li, D. Y.; Yum, K.; Ahn, J. H.; Jin, H.;
2473 Heller, D. A.; Essigmann, J. M.; Blankschtein, D.; Strano, M. S.
2474 Molecular recognition using corona phase complexes made of
2475 synthetic polymers adsorbed on carbon nanotubes. *Nat. Nanotechnol.*
2476 **2013**, *8*, 959–968.

202 (202) Fornasiero, F.; In, J. B.; Kim, S.; Park, H. G.; Wang, Y.;
2477 Grigoropoulos, C. P.; Noy, A.; Bakajin, O. pH-Tunable Ion Selectivity
in Carbon Nanotube Pores. *Langmuir* **2010**, *26*, 14848–14853.

203 (203) Majumder, M.; Chopra, N.; Hinds, B. J. Effect of tip
2481 functionalization on transport through vertically oriented carbon
2482 nanotube membranes. *J. Am. Chem. Soc.* **2005**, *127*, 9062–9070.

204 (204) Majumder, M.; Keis, K.; Zhan, X.; Meadows, C.; Cole, J.;
2484 Hinds, B. J. Enhanced electrostatic modulation of ionic diffusion
2485 through carbon nanotube membranes by diazonium grafting
2486 chemistry. *J. Membr. Sci.* **2008**, *316*, 89–96.

205 (205) Majumder, M.; Corry, B. Anomalous decline of water
2488 transport in covalently modified carbon nanotube membranes.
2489 *Chem. Commun.* **2011**, *47*, 7683–7685.

206 (206) Majumder, M.; Chopra, N.; Hinds, B. J. Mass Transport
2491 through Carbon Nanotube Membranes in Three Different Regimes:
2492 Ionic Diffusion and Gas and Liquid Flow. *ACS Nano* **2011**, *5*, 3867–
2493 3877.

207 (207) Corry, B. Water and ion transport through functionalised
2495 carbon nanotubes: implications for desalination technology. *Energy*
2496 *Environ. Sci.* **2011**, *4*, 751–759.

208 (208) Hughes, Z. E.; Shearer, C. J.; Shapter, J.; Gale, J. D. Simulation
2498 of Water Transport Through Functionalized Single-Walled Carbon
2499 Nanotubes (SWCNTs). *J. Phys. Chem. C* **2012**, *116*, 24943–24953.

209 (209) Hata, K.; Futaba, D. N.; Mizuno, K.; Namai, T.; Yumura, M.;
2501 Iijima, S. Water-Assisted Highly Efficient Synthesis of Impurity-Free
2502 Single-Walled Carbon Nanotubes. *Science* **2004**, *306*, 1362–1364.

210 (210) Murakami, Y.; Chiashi, S.; Miyauchi, Y.; Hu, M. H.; Ogura,
2504 M.; Okubo, T.; Maruyama, S. Growth of vertically aligned single-
2505 walled carbon nanotube films on quartz substrates and their optical
2506 anisotropy. *Chem. Phys. Lett.* **2004**, *385*, 298–303.

211 (211) Maruyama, S.; Einarsson, E.; Murakami, Y.; Edamura, T.
2508 Growth process of vertically aligned single-walled carbon nanotubes.
2509 *Chem. Phys. Lett.* **2005**, *403*, 320–323.

212 (212) De Volder, M. F. L.; Tawfick, S. H.; Baughman, R. H.; Hart,
2511 A. J. Carbon Nanotubes: Present and Future Commercial
2512 Applications. *Science* **2013**, *339*, 535–539.

213 (213) Holt, J. K.; Park, H. G.; Wang, Y.; Stadermann, M.; Artykhin,
2514 A. B.; Grigoropoulos, C. P.; Noy, A.; Bakajin, O. Fast mass transport
2515 through sub-2-nanometer carbon nanotubes. *Science* **2006**, *312*,
2516 1034–1037.

214 (214) Shimizu, T.; Masuda, M.; Minamikawa, H. Supramolecular
2518 nanotube architectures based on amphiphilic molecules. *Chem. Rev.*
2519 **2005**, *105*, 1401–1443.

215 (215) Percec, V.; Dulcey, A. E.; Balagurusamy, V. S. K.; Miura, Y.;
2521 Smidrkal, J.; Peterca, M.; Nummelin, S.; Edlund, U.; Hudson, S. D.;
2522 Heiney, P. A.; Duan, H.; Magonov, S. N.; Vinogradov, S. A. Self-
2523 assembly of amphiphilic dendritic dipeptides into helical pores. *Nature*
2524 **2004**, *430*, 764–768.

216 (216) Hartgerink, J. D.; Granza, J. R.; Milligan, R. A.; Ghadiri, M. R.
2526 Self-assembling peptide nanotubes. *J. Am. Chem. Soc.* **1996**, *118*, 43–
2527 50.

217 (217) Davis, J. T.; Spada, G. P. Supramolecular architectures
2529 generated by self-assembly of guanosine derivatives. *Chem. Soc. Rev.*
2530 **2007**, *36*, 296–313.

2532 (218) Zang, L.; Che, Y. K.; Moore, J. S. One-Dimensional Self-
2533 Assembly of Planar pi-Conjugated Molecules: Adaptable Building
2534 Blocks for Organic Nanodevices. *Acc. Chem. Res.* **2008**, *41*, 1596–
2535 1608.

2536 (219) Sakai, N.; Kamikawa, Y.; Nishii, M.; Matsuoka, T.; Kato, T.;
2537 Matile, S. Dendritic folate rosettes as ion channels in lipid bilayers. *J.
2538 Am. Chem. Soc.* **2006**, *128*, 2218–2219.

2539 (220) Pedersen, C. J. Cyclic Polyethers and Their Complexes with
2540 Metal Salts. *J. Am. Chem. Soc.* **1967**, *89*, 2495–2496.

2541 (221) Beginn, U.; Zipp, G.; Möller, M. Self-organization of liquid
2542 crystalline 3,4,5-tris[(11-methacryloyl-undecyl-1-oxy)-4-benzyloxy]-
2543 benzoates in low-shrinkage methacrylate mixtures. *J. Polym. Sci.,
2544 Part A: Polym. Chem.* **2000**, *38*, 631–640.

2545 (222) Beginn, U.; Zipp, G.; Möller, M. Functional membranes
2546 containing ion-selective matrix-fixed supramolecular channels. *Adv.
2547 Mater.* **2000**, *12*, 510–513.

2548 (223) Beginn, U.; Zipp, G.; Mourran, A.; Walther, P.; Möller, M.
2549 Membranes Containing Oriented Supramolecular Transport Chan-
2550 nels. *Adv. Mater.* **2000**, *12*, 513–516.

2551 (224) Brea, R. J.; Castedo, L.; Granja, J. R. Large-diameter self-
2552 assembled dimers of alpha,gamma-cyclic peptides, with the nano-
2553 tubular solid-state structure of cyclo-[(L-Leu-D-N-Me-gamma-Acp)-
2554 (4-)] 4CHCl(2)COOH. *Chem. Commun.* **2007**, 3267–3269.

2555 (225) Ghadiri, M. R.; Granja, J. R.; Buehler, L. K. Artificial
2556 Transmembrane Ion Channels from Self-Assembling Peptide Nano-
2557 tubes. *Nature* **1994**, *369*, 301–304.

2558 (226) Helsel, A. J.; Brown, A. L.; Yamato, K.; Feng, W.; Yuan, L. H.;
2559 Clements, A. J.; Harding, S. V.; Szabo, G.; Shao, Z. F.; Gong, B.
2560 Highly Conducting Transmembrane Pores Formed by Aromatic
2561 Oligoamide Macrocycles. *J. Am. Chem. Soc.* **2008**, *130*, 15784–15785.

2562 (227) Wei, X. X.; Zhang, G. Q.; Shen, Y.; Zhong, Y. L.; Liu, R.;
2563 Yang, N.; Al-mkhaizim, F. Y.; Kline, M. A.; He, L.; Li, M. F.; Lu, Z. L.;
2564 Shao, Z. F.; Gong, B. Persistent Organic Nanopores Amenable to
2565 Structural and Functional Tuning. *J. Am. Chem. Soc.* **2016**, *138*,
2566 2749–2754.

2567 (228) Ishida, H.; Qi, Z.; Sokabe, M.; Donowaki, K.; Inoue, Y.
2568 Molecular design and synthesis of artificial ion channels based on
2569 cyclic peptides containing unnatural amino acids. *J. Org. Chem.* **2001**,
2570 *66*, 2978–2989.

2571 (229) Parra, R. D.; Furukawa, M.; Gong, B.; Zeng, X. C. Energetics
2572 and cooperativity in three-center hydrogen bonding interactions. I.
2573 Diacetamide-X dimers (X = HCN, CH₃OH). *J. Chem. Phys.* **2001**,
2574 *115*, 6030–6035.

2575 (230) Parra, R. D.; Gong, B.; Zeng, X. C. Energetics and
2576 cooperativity in three-center hydrogen bonding interactions. II.
2577 Intramolecular hydrogen bonding systems. *J. Chem. Phys.* **2001**,
2578 *115*, 6036–6041.

2579 (231) Xu, T.; Zhao, N. N.; Ren, F.; Hourani, R.; Lee, M. T.; Shu, J.
2580 Y.; Mao, S.; Helms, B. A. Subnanometer Porous Thin Films by the
2581 Co-assembly of Nanotube Subunits and Block Copolymers. *ACS
2582 Nano* **2011**, *5*, 1376–1384.

2583 (232) Zhang, C.; Xu, T. Co-assembly of cyclic peptide nanotubes
2584 and block copolymers in thin films: controlling the kinetic pathway.
2585 *Nanoscale* **2015**, *7*, 15117–15121.

2586 (233) Bhave, R. *Inorganic Membrane Synthesis Characteristics and
2587 Applications*, 1st ed.; Van Nostrand Reinhold: New York, 1991.

2588 (234) Gong, B.; Shao, Z. F. Self-Assembling Organic Nanotubes
2589 with Precisely Defined, Sub-nanometer Pores: Formation and Mass
2590 Transport Characteristics. *Acc. Chem. Res.* **2013**, *46*, 2856–2866.

2591 (235) Newton, M. R.; Bohaty, A. K.; Zhang, Y. H.; White, H. S.;
2592 Zharov, I. pH- and ionic strength-controlled cation permselectivity in
2593 amine-modified nanoporous opal films. *Langmuir* **2006**, *22*, 4429–
2594 4432.

2595 (236) Newton, M. R.; Bohaty, A. K.; White, H. S.; Zharov, I.
2596 Chemically modified opals as thin permselective nanoporous
2597 membranes. *J. Am. Chem. Soc.* **2005**, *127*, 7268–7269.

2598 (237) Iki, N.; Kumagai, H.; Morohashi, N.; Ejima, K.; Hasegawa, M.;
2599 Miyanari, S.; Miyano, S. Selective oxidation of thiocalix[4]arenes to
the sulfinyl- and sulfonylcalix[4]arenes and their coordination ability
2600 to metal ions. *Tetrahedron Lett.* **1998**, *39*, 7559–7562.

2601 (238) Molland, A.; Ibragimova, D.; Antipin, I. S.; Konovalov, A. I.;
2602 Stoikov, I.; Zharov, I. Molecular transport in thiocalix[4]arene-
2603 modified nanoporous colloidal films. *Microporous Mesoporous Mater.* **2604**
2605 **2010**, *131*, 378–384.

2606 (239) Schepelina, O.; Zharov, I. Poly(2-(dimethylamino)ethyl
2607 methacrylate)-Modified Nanoporous Colloidal Films with pH and
2608 Ion Response. *Langmuir* **2008**, *24*, 14188–14194.

2609 (240) Schepelina, O.; Zharov, I. Polymer-modified opal nanopores.
2610 *Langmuir* **2006**, *22*, 10523–10527.

2611 (241) Bohaty, A. K.; Smith, J. J.; Zharov, I. Free-Standing Silica
2612 Colloidal Nanoporous Membranes. *Langmuir* **2009**, *25*, 3096–3101.

2613 (242) Schepelina, O.; Poth, N.; Zharov, I. pH-Responsive Nano-
2614 porous Silica Colloidal Membranes. *Adv. Funct. Mater.* **2010**, *20*,
2615 1962–1969.

2616 (243) Ignacio-de Leon, P. A. A.; Zharov, I. SiO₂@Au Core-Shell
2617 Nanospheres Self-Assemble To Form Colloidal Crystals That Can Be
2618 Sintered and Surface Modified To Produce pH-Controlled Mem-
2619 branes. *Langmuir* **2013**, *29*, 3749–3756.

2620 (244) Zilman, A.; Di Talia, S.; Jovanovic-Talisman, T.; Chait, B. T.;
2621 Rout, M. P.; Magnasco, M. O. Enhancement of transport selectivity
2622 through nano-channels by non-specific competition. *PLoS Comput.
2623 Biol.* **2010**, *6*, e1000804.

2624 (245) Park, M. H.; Ofir, Y.; Samanta, B.; Rotello, V. M. Robust and
2625 Responsive Dendrimer-Gold Nanoparticle Nanocomposites via
2626 Dithiocarbamate Crosslinking. *Adv. Mater.* **2009**, *21*, 2323–2327.

2627 (246) Park, M.; Subramani, C.; Rana, S.; Rotello, V. M. 2628 Chemoselective nanoporous membranes via chemically directed
2629 assembly of nanoparticles and dendrimers. *Adv. Mater.* **2012**, *24*,
2630 5862–5866.

2631 (247) Nunes, S. P.; Car, A. From Charge-Mosaic to Micelle Self-
2632 Assembly: Block Copolymer Membranes in the Last 40 Years. *Ind.
2633 Eng. Chem. Res.* **2013**, *52*, 993–1003.

2634 (248) Yu, H. Z.; Qiu, X. Y.; Moreno, N.; Ma, Z. W.; Calo, V. M.;
2635 Nunes, S. P.; Peinemann, K. V. Self-Assembled Asymmetric Block
2636 Copolymer Membranes: Bridging the Gap from Ultra- to Nano-
2637 filtration. *Angew. Chem., Int. Ed.* **2015**, *54*, 13937–13941.

2638 (249) Akthakul, A.; Hochbaum, A. I.; Stellacci, F.; Mayes, A. M. Size
2639 fractionation of metal nanoparticles by membrane filtration. *Adv.
2640 Mater.* **2005**, *17*, 532–535.

2641 (250) Vannucci, C.; Taniguchi, I.; Asatekin, A. Nanoconfinement
2642 and chemical structure effects on permeation selectivity of self-
2643 assembling graft copolymers. *ACS Macro Lett.* **2015**, *4*, 872–878.

2644 (251) Sadeghi, I.; Kronenberg, J.; Asatekin, A. Selective transport
2645 through membranes with charged nanochannels formed by scalable
2646 self-assembly of random copolymer micelles. *ACS Nano* **2018**, *12*,
2647 95–108.

2648 (252) Zhang, Q.; Gu, Y. B.; Li, Y. M.; Beauchage, P. A.; Kao, T.;
2649 Wiesner, U. Dynamically Responsive Multifunctional Asymmetric
2650 Triblock Terpolymer Membranes with Intrinsic Binding Sites for
2651 Covalent Molecule Attachment. *Chem. Mater.* **2016**, *28*, 3870–3876.

2652 (253) Rathee, V. S.; Qu, S. Y.; Phillip, W. A.; Whitmer, J. K. A
2653 coarse-grained thermodynamic model for the predictive engineering
2654 of valence-selective membranes. *Mol. Syst. Des. Eng.* **2016**, *1*, 301–
2655 312.

2656 (254) Sadeghi, I.; Asatekin, A. Spontaneous self-assembly and
2657 micellization of random copolymers in organic solvents. *Macromol.
2658 Chem. Phys.* **2017**, *218*, 1700226.

2659 (255) Israelachvili, J.; Wennerstrom, H. Role of hydration and water
2660 structure in biological and colloidal interactions. *Nature* **1996**, *379*,
2661 219–225.

2662 (256) Hillyer, M. B.; Gibb, B. C. Molecular Shape and the
2663 Hydrophobic Effect. *Annu. Rev. Phys. Chem.* **2016**, *67*, 307–329.

2664 (257) Chandler, D. Interfaces and the driving force of hydrophobic
2665 assembly. *Nature* **2005**, *437*, 640–647.

2666 (258) Kelder, J.; Grootenhuis, P. D. J.; Bayada, D. M.; Delbressine,
2667 L. P. C.; Ploemen, J. P. Polar molecular surface as a dominating
2668

2668 determinant for oral absorption and brain penetration of drugs.
2669 *Pharm. Res.* **1999**, *16*, 1514–1519.

2670 (259) Hulteen, J. C.; Jirage, K. B.; Martin, C. R. Introducing
2671 chemical transport selectivity into gold nanotubule membranes. *J. Am.*
2672 *Chem. Soc.* **1998**, *120*, 6603–6604.

2673 (260) Clavel, G.; Marichy, C.; Pinna, N. Sol-Gel Chemistry and
2674 Atomic Layer Deposition. In *Atomic Layer Deposition of Nano-*
2675 *structured Materials*; Pinna, N., Knez, M., Eds.; Wiley-VCH:
2676 Weinheim, 2012; pp 61–82.

2677 (261) Ott, A. W.; Klaus, J. W.; Johnson, J. M.; George, S. M.;
2678 McCarley, K. C.; Way, J. D. Modification of porous alumina
2679 membranes using Al₂O₃ atomic layer controlled deposition. *Chem.*
2680 *Mater.* **1997**, *9*, 707–714.

2681 (262) Pellin, M. J.; Stair, P. C.; Xiong, G.; Elam, J. W.; Birrell, J.;
2682 Curtiss, L.; George, S. M.; Han, C. Y.; Iton, L.; Kung, H.; Kung, M.;
2683 Wang, H. H. Mesoporous catalytic membranes: Synthetic control of
2684 pore size and wall composition. *Catal. Lett.* **2005**, *102*, 127–130.

2685 (263) Higuchi, A.; Tamai, M.; Ko, Y. A.; Tagawa, Y. I.; Wu, Y. H.;
2686 Freeman, B. D.; Bing, J. T.; Chang, Y.; Ling, Q. D. Polymeric
2687 Membranes for Chiral Separation of Pharmaceuticals and Chemicals.
2688 *Polym. Rev.* **2010**, *50*, 113–143.

2689 (264) Crosby, J. Synthesis of Optically-Active Compounds - a Large-
2690 Scale Perspective. *Tetrahedron* **1991**, *47*, 4789–4846.

2691 (265) Lochmuller, C. H.; Souter, R. W. Chromatographic
2692 Resolution of Enantiomers - Selective Review. *J. Chromatogr. A*
2693 **1975**, *113*, 283–302.

2694 (266) Lee, N. H.; Frank, C. W. Separation of chiral molecules using
2695 polypeptide-modified poly(vinylidene fluoride) membranes. *Polymer*
2696 **2002**, *43*, 6255–6262.

2697 (267) Kim, J. H.; Kim, J. H.; Jegal, J.; Lee, K. H. Optical resolution
2698 of alpha-amino acids through enantioselective polymeric membranes
2699 based on polysaccharides. *J. Membr. Sci.* **2003**, *213*, 273–283.

2700 (268) Wang, H. D.; Chu, L. Y.; Song, H.; Yang, J. P.; Xie, R.; Yang,
2701 M. Preparation and enantiomer separation characteristics of chitosan/
2702 beta-cyclodextrin composite membranes. *J. Membr. Sci.* **2007**, *297*,
2703 262–270.

2704 (269) Lakshmi, B. B.; Martin, C. R. Enantioseparation using
2705 apoenzymes immobilized in a porous polymeric membrane. *Nature*
2706 **1997**, *388*, 758–760.

2707 (270) Higuchi, A.; Furuta, K.; Yomogita, H.; Yoon, B. O.; Hara, M.;
2708 Maniwa, S.; Saitoh, M. Optical resolution of amino acid by
2709 ultrafiltration through immobilized DNA membranes. *Desalination*
2710 **2002**, *148*, 155–157.

2711 (271) Sadeghi, I.; Yi, H.; Asatekin, A. A method for manufacturing
2712 membranes with ultrathin hydrogel selective layers for protein
2713 purification: Interfacially Initiated Free Radical Polymerization
2714 (IIFRP). *Chem. Mater.* **2018**, *30*, 1265–1276.

2715 (272) Higuchi, A.; Yomogita, H.; Yoon, B. O.; Kojima, T.; Hara, M.;
2716 Maniwa, S.; Saitoh, M. Optical resolution of amino acid by
2717 ultrafiltration using recognition sites of DNA. *J. Membr. Sci.* **2002**,
2718 *205*, 203–212.

2719 (273) Randon, J.; Garnier, F.; Rocca, J. L.; Maisterrena, B.
2720 Optimization of the enantiomeric separation of tryptophan analogs
2721 by membrane processes. *J. Membr. Sci.* **2000**, *175*, 111–117.

2722 (274) Matsuoka, Y.; Kanda, N.; Lee, Y. M.; Higuchi, A. Chiral
2723 separation of phenylalanine in ultrafiltration through DNA-immobi-
2724 lized chitosan membranes. *J. Membr. Sci.* **2006**, *280*, 116–123.

2725 (275) Lakshmi, B. B.; Patrissi, C. J.; Martin, C. R. Sol-gel template
2726 synthesis of semiconductor oxide micro- and nanostructures. *Chem.*
2727 *Mater.* **1997**, *9*, 2544–2550.

2728 (276) Lee, S. B.; Mitchell, D. T.; Trofin, L.; Nevanen, T. K.;
2729 Soderlund, H.; Martin, C. R. Antibody-based bio-nanotube
2730 membranes for enantiomeric drug separations. *Science* **2002**, *296*,
2731 2198–2200.

2732 (277) Cichelli, J.; Zharov, I. Chiral permselectivity in surface-
2733 modified nanoporous opal films. *J. Am. Chem. Soc.* **2006**, *128*, 8130–
2734 8131.

278 (278) Ignacio-de Leon, P. A.; Abelow, A. E.; Cichelli, J. A.; Zhukov, A.;
2735 Stoikov, I. I.; Zharov, I. Silica Colloidal Membranes with
2736 Enantioselective Permeability. *Isr. J. Chem.* **2014**, *54*, 767–773.

2737 (279) Cichelli, J.; Zharov, I. Chiral permselectivity in nanoporous
2738 opal films surface-modified with chiral selector moieties. *J. Mater.*
2739 *Chem.* **2007**, *17*, 1870–1875.

2740 (280) Ignacio-de Leon, P. A.; Cichelli, J. A.; Abelow, A. E.; Zharov, I. Pore-Filled
2741 Nanoporous Silica Colloidal Films with Enantioselective
2742 Permeability. *Z. Anorg. Allg. Chem.* **2014**, *640*, 649–654.

2743 (281) Joshi, R. K.; Carbone, P.; Wang, F. C.; Kravets, V. G.; Su, Y.;
2744 Grigorjeva, I. V.; Wu, H. A.; Geim, A. K.; Nair, R. R. Precise and
2745 Ultrafast Molecular Sieving Through Graphene Oxide Membranes.
2746 *Science* **2014**, *343*, 752–754.

2747 (282) Zhou, K. G.; Vasu, K. S.; Cherian, C. T.; Neek-Amal, M.;
2748 Zhang, J. C.; Ghorbanfekr-Kalashami, H.; Huang, K.; Marshall, O. P.;
2749 Kravets, V. G.; Abraham, J.; Su, Y.; Grigorenko, A. N.; Pratt, A.; Geim,
2750 A. K.; Peeters, F. M.; Novoselov, K. S.; Nair, R. R. Electrically
2751 controlled water permeation through graphene oxide membranes.
2752 *Nature* **2018**, *559*, 236–240.

2753 (283) Fathizadeh, M.; Xu, W. W. L.; Zhou, F. L.; Yoon, Y.; Yu, M. Graphene
2754 Oxide: A Novel 2-Dimensional Material in Membrane
2755 Separation for Water Purification. *Adv. Mater. Interfaces* **2017**, *4*,
2756 1600918.

2757 (284) Zhou, F. L.; Fathizadeh, M.; Yu, M. Single- to Few-Layered,
2758 Graphene-Based Separation Membranes. *Annu. Rev. Chem. Biomol.*
2759 *Eng.* **2018**, *9*, 17–39.

2760 (285) Meng, C. C.; Sheng, Y. J.; Chen, Q. B.; Tan, H. L.; Liu, H. L. Exceptional
2761 chiral separation of amino acid modified graphene oxide
2762 membranes with high-flux. *J. Membr. Sci.* **2017**, *526*, 25–31.

2763 (286) Nghiem, L. D.; Schafer, A. I.; Waite, T. D. Adsorptive
2764 interactions between membranes and trace contaminants. *Desalination*
2765 **2002**, *147*, 269–274.

2766 (287) Kumpf, R. A.; Dougherty, D. A. A Mechanism for Ion
2767 Selectivity in Potassium Channels - Computational Studies of Cation-
2768 Pi Interactions. *Science* **1993**, *261*, 1708–1710.

2769 (288) Hilke, R.; Pradeep, N.; Madhavan, P.; Vainio, U.; Behzad, A.;
2770 R.; Sougrat, R.; Nunes, S. P.; Peinemann, K. V. Block Copolymer
2771 Hollow Fiber Membranes with Catalytic Activity and pH-Response.
2772 *ACS Appl. Mater. Interfaces* **2013**, *5*, 7001–7006.

2773 (289) Nunes, S. P.; Behzad, A. R.; Peinemann, K. V. Self-assembled
2774 block copolymer membranes: From basic research to large-scale
2775 manufacturing. *J. Mater. Res.* **2013**, *28*, 2661–2665.